Standardized Process for Filed Estimation of Unconfined Compressive Strength Using Leeb Hardness

by

Yassir Asiri

Submitted in partial fulfilment of the requirements
for the degree of Master of Applied Science

at

Dalhousie University
Halifax, Nova Scotia
February 2017

TABLE OF CONTENTS

LIST OF TABLES

LIST OF FIGURES

ABSTRACT

An investigation of the statistical relationship between Leeb Hardness ("D" type) values (HLD) and unconfined compressive strength values (UCS) for different rock types was conducted. The Leeb hardness test (LHT) procedure was evaluated by investigating the sample size effect on HLD values and the optimum number of impacts that are required to get a reasonable measure of the hardness of the rock specimen. For improving the UCS-HLD correlation, the laboratory testing was carried out on rock specimens and combined with other literature values to develop a database with a total of 311 UCS and HLD results. Statistical analysis was carried out on the database. The predictions of the results of correlation analysis from the tests are presented. A reasonable correlation was found to exist between HLD and UCS. The findings from these evaluations will improve the UCS prediction and the LHT procedure

List of Abbreviations and Symbols

A_0	Initial area of the specimen
D_0	Initial diameter of the specimen
DF	Degree of freedom
E	Young's modulus
E_R	Energy consumed due to frictional effects
g	Gravitational constant
h_i & hr	Impact and rebound height
HL	Leeb hardness value
HLD	Hardness value of impact device D
L & Lr	Length of a spring before and after impact action
L_0	Initial length of the specimen
LHT	Leeb hardness test
m	Mass of impact body
ME	Margin of error
Mgs	Potential gravitational energy
MSE	Mean square of the error
N	Total number of rebound readings
n	Sample size
r	Range
S	Standard error of the regression
SSE	Sum of squared errors of prediction
UCS	Unconfined compressive strength
v_r	Rebound velocity
v_i	Impact velocity

V	Coefficient of variation
W	Total deformation
W_{E1}	Deformation of Elastic
W_{p1}	Deformation of Plastic
$\bar{X}$	Sample mean
μ	Population mean
λ	Transformation parameter
σ	Real standard deviation
σ_c	Ultimate compressive stress.
σ_{pr1}, σ_{pr2}, σ_{pr3}	Principal stresses
ε	Strain

ACKNOWLEDGEMENTS

I would like to sincerely acknowledge Dr. Andrew Corkum and Dr. Hany El Naggar because without them the completion of this work would not be possible. I also thank them for all of their effort to make this thesis what it looks like now. Their guidance, support, and advice have encouraged me to undertake the research topic "standardized process for field estimation of Unconfined Compressive Strength (UCS) using Leeb Hardness". I am really grateful to them. I also would like to thank my loving family, mom, my brothers, and especially my wife and kids for their moral support, care and patience through the duration of my time in Canada. Also, I would like to give thanks to Jesse Keane, a technician in the Department of Civil & Resource Engineering at Dalhousie University, who assisted me in the laboratory during the experimental tests. Special thanks also are due for the Saudi Arabian Cultural Bureau in Canada who supported me financially.

CHAPTER 1 INTRODUCTION

1.1 Overview

In rock engineering projects such as slope stability analysis, the design of underground spaces, drilling, and rock blasting, an engineer requires knowledge of the rock strength. Laboratory samples are idealized representations of the intact component of complex rock masses and provide an essential starting point to determine rock mass behavior. The Unconfined Compressive Strength (UCS) is one of the most important measures of intact rock strength (Hoek & Martin, 2014). However, UCS tests can be time consuming to preform. The Leeb Hardness Test (LHT) can be used to estimate the UCS quickly in the field or laboratory environment to provide more samples and a preliminary estimation of rock strength.

The UCS is a typical and convenient measure of rock strength, which is one of the common parameters used in the Geotechnical Engineering field. It is a stress state where σ_{pr1} is the axial stress and there is zero confining stress ($\sigma_{pr2} = \sigma_{pr3} = 0$), and it is widely understood as an index which gives a first approximation of the range of issues that are likely to be encountered in a variety of engineering problems including roof support, pillar design, and excavation techniques (Hoek, 1977).

The UCS of rock is a very important parameter for rock classification, rock engineering design, and numerical modeling. In addition, for most coal mine design problems, a reasonable approximation of the UCS is sufficient; this is due in part to the high variability of UCS measurements in coal rock units. This property is essential for judgment about a rock's suitability for various construction purposes. However, determining rock UCS is relatively time consuming and expensive for many projects. Consequently, the use of a portable, fast and cost effective index test that can reasonably estimate UCS is desirable.
Other index field tests, such as the Schmidt Hammer (R) and the field estimation methods outlined by the ISRM (2007) are commonly used with some acknowledged limitations.

Hack (1997) mentioned that the field estimation methods outlined by the ISRM (2007), although useful, are "obviously partly subjective."

The Leeb Hardness Test (LHT), as a means to predict UCS is the focus of this thesis. The LHT sometimes referred to as the "Equotip" is a quick, inexpensive, non-destructive, repeatable, and convenient test, and is therefore particularly valuable at preliminary project stages.

The LHT method was introduced in 1975 by Dietmar Leeb at Proceq SA (Kompatscher, 2004). The LHT is a portable hardness tester originally developed for measuring the strength of metallic materials. In rock mechanics, the first application of the LHT was done by Hack et al (1993), followed by Verwaal and Mulder (1993) and Asef (1995). Recently, it has been applied to various rocks for testing their hardness (e.g. Aoki and Matsukura, 2007; Viles et al., 2011). It has also been correlated with rock UCS according to Kawasaki et al. (2002) and Aoki and Matsukura (2007). Moreover, it is used to assess the effects of weathering on hardness values of rock (Kawasaki and Kaneko, 2004; Aoki and Matsukura, 2007; Viles et al., 2011). The LHT can be used in laboratory or in the field at any angle to the rock surface (Viles et al. 2011), since the instrument uses automatic compensation for impact direction (see the Chapter 2 for more details). The LHT is similar to the popular Schmidt hammer test, but because of its lower energy it is suitable for a wider range of rock types (i.e. hardness) compared with the Schmidt Hammer test (Aoki and Matsukura 2007).

1.2 The Aim of This Study (Objectives)

One main objective of this thesis is to investigate the statistical relationship between the LHT values (test value referred to as HLD for the standard type D test) and UCS for a wide range of rock types and larger database. For this reason, laboratory testing was carried out on specimens of different rock types and combined with other literature values to develop a database with a total of 311 test results.

The additional objective of this study was the LHT methodology that was also evaluated (sample size and the number of Leeb readings that comprise an average test result). No well-established standard methodology exists for LHT testing of rock specimens. Issues such as specimen size and the number of readings (impacts) averaged per "test" result were investigated. Statistical analysis was carried out on the UCS-HLD database and the results of correlation analysis from tests are presented. Reasonable correlations between HLD and UCS for different rock types were developed and their accuracy was assessed. It is expected that the LHT can be particularly useful for field estimation of UCS and offer a significant improvement over the field estimation methods such as the Schmidt Hammer test and the field estimation methods outlined by the ISRM (2007). Also, part of this study was to develop an equation that relates HLD to UCS that is simple, practical and accurate enough to apply in the field. Although the empirical rock strength predicted from the LHT results contains some level of uncertainty, the results are of significant value as a preliminary estimate of UCS.

1.3 Thesis outline

The thesis is divided into five chapters. Chapter 2 presents a literature review that includes a discussion of the direct and indirect methods for the estimation of rock UCS strength, a comparison between LHT and the Schmidt Hammer test, and a summary of previous studies in relation to the HLD – UCS correlation for rock.

Chapter 3 describes the methodology used to conduct the LHT and UCS tests, and discusses the laboratory testing performed as part of this thesis. The discussion includes specimen preparation, tests performed, and testing methods. The main focus of this chapter is the study of LHT methodology.

Chapter 4 presents the relations developed from the testing and summarized test results. Simple relationships are developed between UCS and HLD, and advanced relations are also developed for UCS for different rock types.

Chapter 5 contains a discussion of analysis. Included in this chapter is a discussion of the required statistical measurements conducted on the database to determine how well the Regression line fits the data, such as values called R-Squared (R^2), and Standard Error of the regression (S). In addition, the database is analyzed on the basis of rock types (sedimentary, metamorphic and igneous) in subsection and the plot of UCS-HLD correlations are presented. Classifying the HLD values based on analyzing the presented study database was also including in this chapter before the section of the comparison between HLD and Schmidt Hammer. The final section in this chapter presents a published conference paper studying the LHT for sandstone specimens (see Appendix A).

Chapter 6 presents the conclusions and recommendations for future work for other researchers who may wish to investigate the effects of sample size on HLD value.

CHAPTER 2 LITERATURE REVIEW

This chapter presents a review of the direct and indirect methods for the determination and estimation of rock UCS. The first section discusses the UCS and Point Load Test (PLT). The second section reviews the ISRM Field Methods for determination of rock strength. The third section overviews the rebound techniques for rock strength determination, which is included in the subsections "Operating principal of the rebound tester" and "Processes of impact and rebound," where the concepts are defined and related to the methods of the hardness test. Later in the chapter, the Schmidt Hammer test and LHT are discussed individually. The former section (LHT) is divided in two subsections, one discussing its design and operation, and the other defining and describing the hardness value HLD. A comparison between the LHT and the Schmidt Hammer test is discussed in the following section. Finally, the chapter summarizes previous studies in relation to the HLD – UCS correlation for rocks.

2.1 Conventional Laboratory Methods for Rock Strength Estimation

2.1.1 Unconfined Compressive Strength (UCS) Test

The UCS is an important input parameter in rock engineering. It is commonly used in engineering to determine the strength properties of a rock, soil, or other material; however, it is not simple to perform properly and results can vary as test conditions are varied. Specimens should be prepared and tested according to the American Society for Testing and Materials (ASTM, 1986a) standard D4543-08 or the International Society for Rock Mechanics (ISRM, 1981), using rock cores as cylindrical test specimens.

The test specimen should be a rock cylinder of length-to-diameter ratio in the range of 2–2.5 with flat, smooth, and parallel ends, cut perpendicularly to the cylinder axis. Test

procedures are provided in ASTM D-7012 standard. Typically, a UCS test is performed on a universal testing machine UTM. This machine designed with different capacities such as: 1000 kN or 2000 kN, and applies uniaxial load at a constant strain rate on specimens by applying an increasing load to a cylindrical sample, until the sample fails. During the tests, typically a load cell or a pair of strain gauges measure applied load and deformation. Both cell and strain gauges are wired to a logging system to record. Computers are used to continuously log the stress-strain, and the failure stress will be considered as the UCS of specimens. Major deformation of the sample or fracture of the rock generally defines the peak stress level achieved. Failures can range from benign compression to explosion of the sample. UCS is often measured in MPa, which can be calculated from the following equation in its basic definition:

$$\sigma = \frac{F}{A} \qquad [2 - 1]$$

F is the force recorded by the load frame in Newton, and A is the area of the cylindrical surface in m^2.

2.1.2 Point Load Test

The Point Load Test (PLT) is an accepted rock mechanics testing procedure and is an attractive alternative to the UCS used for the calculation of rock strength. It is used to obtain the strength classification ($\boldsymbol{I_{s(50)}}$) of a rock material as well as the strength anisotropy ($\boldsymbol{I_{a(50)}}$) (Bell, 2013). PLT has been used in geotechnical analysis for over thirty years (ISRM, 1985). The rock specimen can be in any form from core specimens, cut blocks, to irregular lumps resulting in very little or no preparation at sometimes. Portable PLT equipment provides to the UCS with a correlation factor at a lower cost, making it more feasible to use in the field. Early studies (Bieniawski, 1975; Broch and Franklin, 1972) were conducted on hard, strong rocks, and found that the relationship between UCS and the point load strength could be expressed as:

$$UCS = (K)\, I_{s(50)} \qquad [2 - 2]$$

In this equation, K is the "conversion factor." Subsequent studies found that K=24 was not as universal as had been hoped, and that instead there appeared to be a broad range of conversion factors. It was found that the K value varied depending on the rock type with a range of 15 to 50 (Akram & Bakar, 2016). Consequently, it is safer to directly use $\boldsymbol{I_{s(50)}}$, as reporting the UCS without the K value when using an inappropriate K value can result in up to 100% error (ISRM, 1985). The shape of the sample used greatly affects the accuracy of the results. However, the relationship above is used in many of today's projects, replacing the standard UCS test.

Broch and Franklin (1972) reported less distribution of PLT strength test results, making it advantageous compared to standard UCS test results. While Bieniawski (1975) reported the opposite, Cargill and Shakoor (1990) concluded the same coefficient of variation (V) for both tests. UCS tests showed a V of 3.1-17.1% with an average of 9.2% for different types or rock. PLT showed a V of 4.1-24.8% with an average of 11.6%. The distribution of points was observed to be lower at low-medium strength values and to increase as corresponding values increase. Accordingly, they concluded that empirical equations are better for low to medium values, as the equations become less reliable for higher strength values.

There are many studies proposing relationships between $Is_{(50)}$ and UCS (Hawkins 1998; Hawkins and Olver 1986; Romana 1999; Palchik and Hatzor 2004; Thuro and Plinninger, 2005). Tsiambaos and Sabatakakis (2004) reported that there are multiple factors, such as composition and texture of rocks, that affect the UCS and $Is_{(50)}$ correlation and stated that for soft to hard rock different conversion factors are required.

2.2 ISRM Field Method for UCS Strength Determination

The ISRM suggested method for field estimation of UCS has been useful in rock engineering practice. Rock hardness can be determined by Schmidt Hammer test, UCS, the ISRM method or LHT. Table 2.1 shows the ISRM method to estimate rock strength by hammer blows or breaking by hand as grades 'R'. It is used in rock mechanics to classify rock strength in the field (Burnett, 1975).

Table 2.1 ISRM Suggested Method of UCS

Grade	Term	UCS (MPa)	Field estimation method
R0	Extremely weak	0.25 – 1	Indented by thumbnail
R1	Very weak	1 – 5	Crumbles under firm blows with point of a geological hammer, can be peeled by a pocket knife
R2	Weak	5 – 25	Can be peeled with a pocket knife with difficulty, shallow indentation made by firm blow with point of a geological hammer
R3	Medium strong	25 – 50	Cannot be scraped or peeled with a pocket knife, specimen can be fractured with a single blow from a geological hammer
R4	Strong	50 – 100	Specimen requires more than one blow of a geological hammer to fracture it
R5	Very strong	100 – 250	Specimen requires many blows of a geological hammer to fracture it
R6	Extremely strong	>250	Specimen can only be chipped with a geological hammer

This method was based on the results of many different researchers to avoid any bias, by taking a large number of assessments of rock strength on the same rock. Results for this method are "obviously partly subjective" (Hack, 1996). It is standardized with a British code (BS 5930, 1981). However, its lack of accuracy and reliability for estimating the strength of intact rock is its limitation, and makes it highly inaccurate.

2.3 Rebound Techniques for Rock Strength Determination

This section overviews the rebound techniques for rock strength determination, which is included in subsections "Operating principal of the rebound tester" and "Processes of impact and rebound," where the concepts are defined and related to the methods of a hardness test. The process of measurement is divided into three main phases; the Striking phase, the Impact phase and the Rebound phase. The residual energy has two components: the kinetic energy component and the potential energy component, which are discussed in individual subsections. The Schmidt Hammer test and LHT were discussed individually. The LHT is discussed, its design and operation, and the other defining and describing the hardness value 'HLD'.

2.3.1 Operating Principle of the Rebound Tester

In order to understand the operating principle of the rebound tester, the processes of impact and rebound should be defined in hardness tests.

2.3.1.1 Processes of Impact and Rebound

Typically, in performing rock hardness tests, the response of the rock material to the impact is recorded by measuring the change in residual energy before and after rebounding. The process is divided into three main phases (Leeb, 1986): The Striking phase, the Impact phase and the Rebound phase.

The Striking phase is the first phase; the impact body's potential energy is converted into kinetic energy, either by free fall or via a spring system mechanism, and the impact tip hits the rock sample at a specified impact velocity.

The second phase is the Impact phase; this phase is divided into two sub-phases, a Compression phase and a Recovery phase. In the Compression phase, the impact body depresses the test material (rock), and deforms it either plastically or elastically or both. As

a result, the impact body deforms plastically with some energy lost as heat. The compression phase comes to an end once the test body reaches full stop. The moment of maximum compression is known when velocity reaches a value of zero. In the Recovery phase, due to elasticity forces, the two bodies move apart, as the testing body fully recovers its elasticity. However, the test material partially recovers depending on how much energy it has accumulated. The recovery phase is considered to be complete once the testing body is accelerated to a rebound velocity as it leaves the test material.

The third main phase is the Rebound phase. In this phase, the present residual kinetic energy of the testing body is converted into potential energy, which is controlled by the height of the rebound. The impact and rebound energy equations are as follow:

$$\text{Impact} \qquad mgh_i = \frac{1}{2}mv_i^2 \qquad [2\text{-}3]$$

$$\text{Rebound} \qquad mgh_R = \frac{1}{2}mv_R^2 \qquad [2\text{-}4]$$

Where:

m = impact body mass

g = gravitational constant

h_i, h_R= height of impact and rebound

v_i, v_r = velocity of impact and rebound

mgh_R= potential energy component

$\frac{1}{2}$mv_R^2 = kinetic energy component

In LHT, hardness is defined as the ratio between impact and rebound velocity (v_i / v_r) multiplied by 1000 (Leeb, 1986). The UCS of a rock is one of the key parameters affecting the hardness (Price, 1991). Also, the elasticity modulus (Figure 2.1) has an effect on the harness value; by using two specimens with the same compressive strength but with a

different modulus of elasticity, different rebound values will be exhibited (M. Kompatscher, 2004).

$$W = W_{e1} + W_{p1} = W_{e2} + W_{p2} \quad [2\text{-}5]$$

In which:

W = Total deformation work

E = Young's modulus

$W_{e1\&2}$, $W_{p1\&2}$ = Deformation of Elastic and Plastic

Residual energy is controlled by two effects: the yielding effect and the spring effect. Yielding only affects the residual energy by decreasing it, unlike the spring, which can either increase or decrease its value. As a result, it is recommended that testing specimens are to be of a sufficient mass to eliminate both effects (Leeb, 1978).

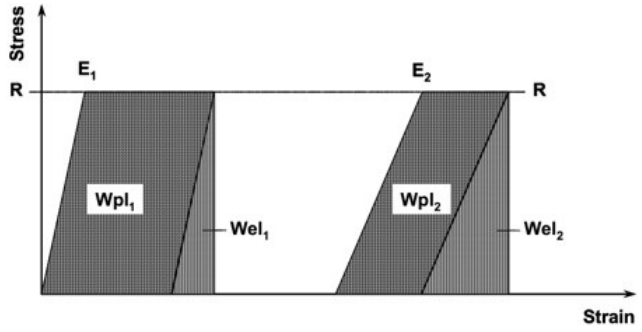

Figure 2.1 Two specimens with the same compressive strength but with a different modulus of elasticity (After D. Leeb, 1979).

2.3.1.2 Residual Energy Measurement:

The residual energy can be measured by either the kinetic energy component or the potential energy component. However, there are some constraints limiting the use of one over the other, and they are as follows:

- The Potential energy method: The rebound height (h_R) controls the residual energy, limiting the measurement of some of the ranges, and thereby affecting the reliability of the rebound values. The free fall system is only restricted to horizontally placed materials with low impact energy, limiting it to medium-high strength material (e.g. Schmidt Hammer). The forces of friction and gravity come into effect, especially when a spring action instrument is being used.
- The Kinetic energy method: The forces of friction and gravity do not come into effect, making this method more accurate than the Potential energy method. The direction in which the test is carried out is not a limiting factor. The test should be carried out in a rapid manner to avoid interference of any of the results (Asef, 1995).

2.3.1.3 Kinetic Energy Measurement:

In this method, the LHT is the only tool known to the author that can be used. It measures both the impact and rebound energy based on the kinetic component. This is achieved as the device measures v_i and v_r, impact and rebound velocities, respectively, just before the impact body strikes the sample material and immediately after. The ratio of the impact velocity to the rebound velocity is then calculated and is later used to determine the hardness value. The energy equations can be expressed as follows:

Residual energy prior to impact

$$½\, cs^2 \pm mgs + E = ½\, mv_A^2 \qquad [2-6]$$

Residual energy after impact

$$½\, mv_R^2 = ½\, cs_R^2 \pm mgs_R + E_R \qquad [2-7]$$

Where:

m = impact body mass

v_i = impact velocity

v_r = rebound velocity

c = spring constant

g = gravitational constant

E_R= energy consumed due to frictional effects along rebound track

E = energy component consumed by the frictional effects along the entire spring track

½ mv_R^2 = kinetic energy at rebound starting

½ cs^2 = potential residual energy of the spring system

½ mv_A^2 = impact body kinetic energy immediately before impact

mgs_R= energy of potential residual gravitational

cs_R^2 = spring system potential energy

mgs = energy of potential gravitational

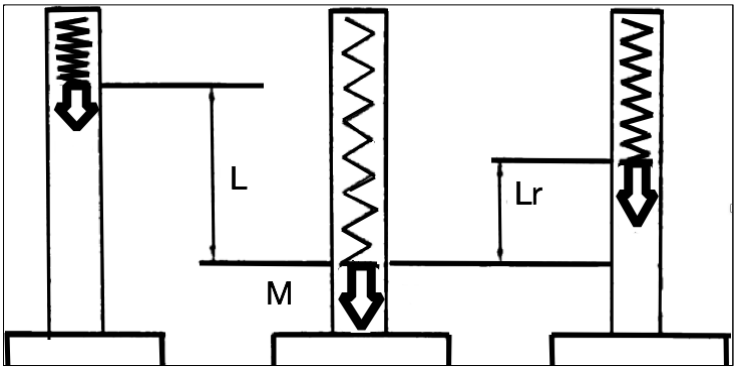

Figure 2.2 Leeb hardness measures both the impact and rebound energy based on the kinetic component. L and Lr are the length of a spring before and after impact action (After D. Leeb, 1979).

2.3.2 Schmidt Hammer Rebound Test

The Rebound Hammer has been around since the late 1940s and today is a commonly used method for estimating the compressive strength of in-place concrete and rock. Ernst Schmidt first developed the device in 1948. The device measures the hardness of concrete surfaces using the rebound principle. The device is often referred to as a 'Swiss Hammer',

it is a standard test (ASTM D5873-05, 2005). In 1965, Miller determined that the Rebound Hammer could correlate rock UCS using non-destructive test (NDT) methods. For its mobility, it is used to measure specimens directly in the field, and in the lab for core specimens starting at NX size (Edge length ≥ 60 mm). However, the rock-mass sample must be free of any localized discontinuity, and it has to be smooth and flat for the area below the plunger (ISRM, 1978). Since its discovery as a tool to measure rock strength, researchers have been attempting to come up with the best recording techniques, associated empirical formulas and the possibility of obtaining the modulus of elasticity. In 1980, Pool and Farmer examined different techniques of hardness recording; 10 impacts are to be performed at every point, and the peak rebound value is recorded, as well as an average of all recorded rebound values at every point, five rebound values from single impacts of closely spaced points are separately recorded, and then the average of the highest 3 is calculated. Within an area with spacing of at least 25mm, 15 rebound values are recorded; the highest 10 values are averaged within an area of 100 mm^2, where 10 rebound values are recorded. All values are averaged after the elimination of ±5 cut-off values (Proceq, 1977). An average of 9-25 single impact rebound values are used to calculate the average, standard deviation, range, and the variation. Using a plunger diameter as a spacer, 20 rebound values are recorded from single impacts, and the highest 10 values are averaged after eliminating any values taken from cracked rock-specimens.

Hucka's methods (Hucka, 1965) were the accepted technique for recording, unlike all others that were based on the single impact method on different areas. Pool and Farmer carried out further field experiments by conducting an intensive testing program in a shallow coal mine in order to conclude the best recording technique. The team was split into two groups; the first group carried out tests on three series of rocks. In the first 2 series, testing was carried out 10 times at the same point; however, it was done 15 times in the third series. Tests were carried out on a closely packed grid (200 mm^2, 4×4 grid). The second group performed tests by carrying out 16 impacts, each at a one-meter interval. Statistical analysis showed a normal distribution of: rebound values were consistent, with slight variations in the first 3-4 impacts. Hence, they concluded that 5 successive impacts are to be carried out before they obtain the peak value.

Sachpazis (1990) used the Schmidt Hammer test to determine the UCS and Young's modulus of carbonate rocks in Greece. He reported linear correlations as the best choices for rebound values, and putting UCS against Young's modulus, he obtained the following coefficient of determinations (R^2) of 0.7764 and 0.8151; r = 0.881 and 0.903 respectively.

For application to assess the degree of rock weathering. Sjoberg and Broadbent (1991) used the Schmidt Hammer test to estimate the alteration and degree of rock weathering. McCarrol (1991) has reported a strong negative correlation between rebound values and the degree of weathering.

From the previous experiments, it is confirmed that the Schmidt hammer is an applicable tool to be used to predict rock-mass properties. However, it cannot provide one empirical equation with the desired accuracy for all different rock-types. Kolaiti and Papadopoulus (1993) noticed that the correction of the hammer direction is unnecessary for all cases. Inaccuracies during measurement of material response and intrinsic inaccuracy of rebound methods occur due to the interference of effected factors.

2.3.3 Leeb Hardness Tester

The Leeb hardness tester is a fairly new measuring hardness device. Recently, it has been applied to various rocks for testing their hardness (Aoki and Matsukura, 2007; Viles et al., 2011), and it can also be correlated with rock UCS according to Kawasaki et al. (2002) and Aoki and Matsukura (2007). Moreover, it is used to assess the weathering effects on hardness values (Kawasaki and Kaneko, 2004; Aoki and Matsukura, 2007; Viles et al., 2011). The LHT can be used in laboratory or the field at any angle (Viles et al. 2011), since the instrument uses automatic compensation for direction of impact (Yilmaz, 2012). It is suitable for applications to cover a wider range of rock hardness compared with the Schmidt hammer (Aoki and Matsukura 2007).

2.3.3.1 Design and Operation

The LHT is made of two main components: the impact device and the electronic indicator device. The body of the impact device is made from tungsten carbide and is placed against the surface of the material. The electronic indicator device is to measure the impact and rebound velocities, v_i and v_r respectively. The v_i and v_r are measured by voltage U in which the U is generated in a transmitter from the movement of the permanent magnet through the coil inside the guide tube of the impact body (Figure 2.3).

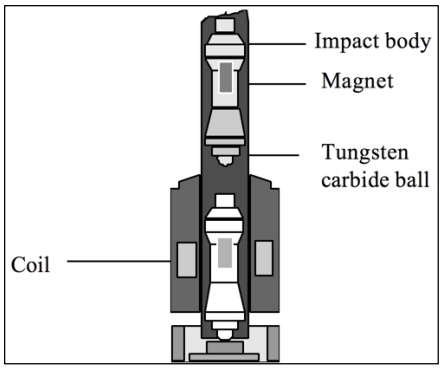

Figure 2.3 Cross - section of Leeb hardness Tester (Frank et al, 2002).

By this contactless manner, the U is then recorded as a function of time and is considered to reach its maximum when the impact body is 1 mm away from the surface that is to be tested (Figure 2.4). The hardness value 'HL' is essentially calculated by multiplying the v_i to v_r ratio by a thousand (Leeb, 1979), see Figure 2.4.

$$\mathrm{HLD} = 1000 \times \left(v_i \, / v_r\right) \qquad [2-8]$$

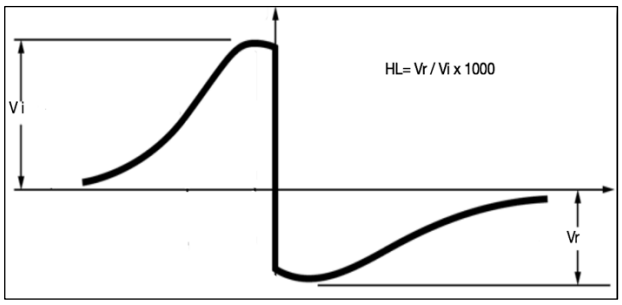

Figure 2.4 Standard voltage signals generated during the impact and rebound actions of Leeb hardness test (Frank et al, 2002).

The operator using the tool should ensure that the rock-mass specimens are of enough weight, eliminating the effect of yielding or spring on the residual energy discussed in its section. Proceq SA further invented different probe types and impact devices. The main differences between all the devices resides in the weight of the impact body and the impact energy. In this research, only one probe type was used (D).

2.3.3.2 Hardness Value 'HLD' Definition

In the LHT, the rock hardness is known as the material response to an impacting device. The theory behind the method is based upon the dynamic impact principle; the height of the rebound of a small tungsten carbide ball (diameter of 3 mm) is applied on a material surface. The test result depends on the elasticity of the surface and energy loss by plastic deformation, all related to the mechanical strength of a material (Aoki and Matsukura, 2008). The ball rebounds faster from a harder specimen than it does from a softer one. The impact ball is shot against the material surface and when the ball rebounds through the coil, it induces a current in the coil. The measured voltage of this electric current is proportional to the rebound velocity.

The hardness value is the ratio of rebound velocity to impact velocity (unitless), which is quoted in the Leeb hardness unit HL (Leeb hardness), also known as an L-value. Some papers have used different terms; for example, Meulenkamp and Grima (1999) used the "RHN" term to express rebound hardness number, while Aoki and Matsukura (2007) used

the L-value term for a single impact "Ls". The HLD denotes testing with the D device, which can be described as:

$$\mathrm{HLD} = \frac{\mathrm{V\ rebound}}{\mathrm{V\ impact}} \mathrm{X1000} \qquad [2-9]$$

In this study, the LHT ("D" type) was used to predict the UCS for core specimens. There is still no established testing procedure for using the LHT to predict UCS on rocks. Therefore, the single impact method (12 impacts) on the core specimens (Daniels et al., 2012) is used on core specimens. The maximum and minimum reading is excluded, and the average of the 10 remaining readings are used. The averaged Leeb hardness readings are correlated with the UCS-test. The results show that the LHT can be particularly useful for estimating the UCS with some level of uncertainty. Moreover, to get a reasonable measure of the "Statistically representative" hardness of a sample rock, the LHT methodology was examined by quantifying sample size and the number of Leeb readings (CHAPTER 4).

2.4 Comparison between the Leeb Hardness Test and the Schmidt Hammer Test

Both the LHT and Schmidt hammer are rebound-measuring devices. The Schmidt hammer follows traditional static tests where the test is uniformly loaded, while the LHT follows dynamic testing methods that apply an impulsive load. The Schmidt hammer is the traditional method that is based on clear physical indentation; it measures the distance of rebound after a plunger hits the material surface. In contrast, the LHT (Figure 5) is a lighter, smaller and non-destructive device that leaves a little damage with an indentation of just ~0.5 mm, which allows for an advantageous measurement for a thin layer. LHT is also faster: the duration of the test is only seconds.

Figure 2.5 Leeb Hardness Tester. The light weight and compact size of the device make it convenient for fieldwork.

Thus, for practical purposes, the speed, size and weight of the LHT make it easier to deal with in the field.

The Schmidt Hammer test has certain limitations in its application. It is not applicable to extremely weak rocks, nonhomogeneous rocks like conglomerates, and Breccia. Because it has high impact energy, its result is influenced by the layer characteristics beneath the tested surface. This makes using the Schmidt Hammer to measure soft rocks more difficult than using the LHT. Viles et al (2011) pointed out that the impact energy of the LHT-D type is nearly 1/200 of the Schmidt Hammer Tester N-type, and 1/66 of the Schmidt Hammer L-type. By using LHT, which is more sensitive, less damage is caused to the tested surface. As a result, the LHT has the ability to measure soft and thin material due to its lower impact energy, which is not possible with the Schmidt Hammer (Aoki and Matsukura, 2007a). Hack and Huisman (2002) reported that the material to a fairly large depth behind the tested surface influences the Schmidt hammer values. As a result, if a discontinuity or flow exists within the influence zone, the Schmidt hammer values could be affected. They suggested that the LHT and other rebound impact devices might make for a more suitable measurement in such a situation.

Furthermore, moisture can influence Schmidt Hammer test results, but does not significantly influence the LHT readings. Aoki and Matsukura (2007) examined this by preforming the tests on a sample when wet and when dry. Haramy and DeMarco (1985) reported that the Schmidt hammer is affected by water content of the surface in addition to the roughness of the surface area, rock strength, cleavage and pores as well. The LHT device is sensitive to surface conditions, so it cannot be used successfully on friable or rough surfaces of rocks.

The LHT has the ability to repeat the impact test on the same sample, and even on the same spot without breaking the sample, which is not always possible with the Schmidt hammer (Aoki and Matsukura, 2007a). This allows the LHT to be used on small specimens or on those of limited thickness. In the laboratory, both devices require the specimens to be well clamped in order to avoid any movement. The Schmidt hammer is less sensitive to localized conditions at the impact location, making readings more consistent and representative of the average rock properties. The LHT is more precise (i.e. covers a smaller area), and therefore is affected by local mineralogy and geometry. Doing multiple Leeb readings and averaging them for a single "test" reading can alleviate this pitfall. LHT has certain advantages, such as the smaller diameter of its tip (3 mm), which allows for greater accuracy of its measurement. Another advantage is the device's automatic correction of the angle (Yilmaz, 2012), which minimizes the variations in measurements produced by the gravity force. In addition, the LHT can be used in either the laboratory or the field because of its portability, simplicity, low cost, speed and non-destructiveness (as shown in Figure 2.6). Also, it positions at any angle on either a straight or curved surface, while the Schmidt hammer's direction is restricted.

Figure 2.6 Leeb hardness tester vs. Schmidt hammer

2.5 Previous Studies on Leeb Hardness Tester (LHT)

LHT has been used widely to estimate the rock UCS by several authors (Table 2.2). Verwaal and Mulder (1993) at the Delft University of Technology examined the possibility of predicting the UCS from HLD value. They reported results on a UCS versus HLD relationship, as well as on the influence of the surface roughness on the LHT measurement. They also observed that the sample thickness has slight effect on the LHT measurement. They used limestone core specimens of three different types: 15 cm long with diameters of 3, 6, and 10 cm. The HLD values were taken as the average of ten radial impacts. It was noticed that the hardness tests performed on 3 cm diameter cores provided HLD lower than those of the 6 and 10 cm diameter. Consequently, it was concluded that the LHT may not give appropriate hardness values with cores smaller than 5.4 cm in diameter. They ended with a simple equation for estimating UCS from the measurements of LHT.

Additionally, Hack et al. (1993) used both LHT and ball rebound tests to describe the UCS of the discontinuity plane for mixed lithologies of various rock type specimens. They studied the effect of unit weight on the hardness values of both devices. They reported that the results have an inverse relation. Furthermore, no relationship between Young's modulus and hardness rebound values was found.

Table 2.2 Proposed correlation equations for UCS and Rebound hardness values (RHN)

Source	Leeb - UCS Equation	R^2	Tested rock	Number of sample
Verwaal and Mulder (1993)	UCS= 8 X 10^{-6} RHN $^{2.5}$	0.77	mix	28
Meulenkamp (1997)	UCS=1.21E-11 RHN$^{3.8}$	-	-	-
Meulenkamp and Grima (1999)	UCS=0.25RHN+28.14density-.75porosity-15.47grainsize-21.55rocktype	-	mix	194
Grima and Babuska (1999)	UCS=0.386RHN+39.268Density-1.307Porosity- 246.804	-	mix	226
Meulenkamp and Grima (1999)	UCS=1.75 E-9 RHN $^{3.8}$	0.806	mix	194
Verwaal and Mulder (2000)	UCS= 3.38E-9 RHN $^{2.974}$	-	mix	28
Kawasaki et al (2002)	UCS=1.49+0.248RHN	0.578	sandstone	5
Kawasaki et al (2002)	UCS=64.6+0.122RHN	0.339	hornfels	5
Kawasaki et al (2002)	UCS=156+0.309RHN	0.818	shale	11
Kawasaki et al (2002)	UCS=271-0.38RHN	0.356	granite	3
Kawasaki et al (2002)	UCS=538+0.939 RHN	0.811	sandstone	8
Aoki and Matsukura (2008)	UCS= 0.079 e $^{-0.039\ n}$ RHN $^{1.1}$	0.88	mix	
Yilmaz (2013)	UCS= 4.5847 ESH-142.22	0.674	carbonate	18
Lee et al (2014)	UCS= 2.3007 e $^{0.0057RHN}$	0.8235	shale	24

Source	Leeb - UCS Equation	R^2	Tested rock	Number of sample
Lee et al (2014)	UCS= 2.1454 e $^{0.0058\ RHN}$	0.8093.	shale	24
Lee et al (2014)	UCS= 3.7727 e $^{0.005\ RHN}$	0.7799	shale	24

* Equotip Shore hardness (ESH), RHN= rebound hardness number (Equotip)

Table 2.3 Description of rock specimens from previous studies using the Leeb hardness tester (LHT)

Author	Rock type	Sample size	Condition
Verwaal and Mulder, 1993	limestone, granite, sandstone and man-mad gypsum	Core, 30mm Dia 60 mm L	Intact
Hack et al, 1993	granite, limestone, sandstone	Cubic, 20cm side	Weathered
Meulenkamp and Grima, 1999	lime, granite, sandstone, dolostone and granodiorite	NF*	Intact
Aoki and Matsukura, 2008	tuff, sandstone, granite, andesite, gabbro and lime	Prism50x50x70m	Intact
Viles et al, 2011	sandstone, lime, basalt and dolerite	30 × 30cm	Weathered
Daniels et al, 2012	sandstone	NF*	Intact
Yilmaz, 2013	carbonate rocks	Cubic, 7cm side-length	Intact
Coombes et al, 2013	limestone, granite & concert	Block, 100x40x40mm	Weathered
Lee et al, 2014	laminated shale	Slab, 10 cm Dia, 6.8cm Length	Laminated

* NF is information not found

The surface roughness of a rock sample had an influence on the hardness values because the rougher surface has more asperities that could be crushed under the rebound hardness test, leading to a loss of rebound energy. Other influences that a rough surface may have on the hardness test is that the ball inside the device tube may not turn back

perpendicularly and could touch the tube sides (friction), resulting in the reduced height of the ball rebound. Therefore, they suggested that, before conducting the rebound hardness testing, the surface should be reasonably smooth – e.g. simple grinding and sawing processes are satisfactory enough to get a smooth surface. Furthermore, the hardness values are affected more by the asperity crushing and sample surface in the case of soft rocks. In the case of the hard rocks, the hardness values are affected more by the parameters of elasticity. Hack and colleagues (1993) attempted to uncover a relationship between the UCS and the rebound value, to estimate the mechanical strength of the rock surface along a discontinuity using the Verwaal and Mulder equation.

Asef (1994) used 55 block specimens from 14 different rock types, mostly sedimentary. He attempted to develop an empirical method relating UCS, Young's modulus and LHT by using three (3) types of Equotip (D with ball, D without ball, and C). He reported that dryness, density, surface roughness and size, and impact body and shape affected the Equotip values. He used different impact methods; for example, one such method is where 10 impacts on different spots are measured (the results present a stronger correlation). He applied the same method on untreated smooth surfaces of block specimens. He used a 40 mm core diameter for strong rocks and 50 mm for weak rocks. He used the STRATGRAPHICS software to calculate S, σ and V for LHT values. The results for uniform rocks show a low σ, and anisotropic specimens with irregular roughness had the highest variation. Linear, multiplicative and exponential correlations were reported; the multiplicative results displayed strongest correlation. Asef (1994) concluded that the values of Leeb that had not been processed for highest and lowest readings showed the highest variance.

In the following year, Asef (1995) studied four types of rocks (very strong, strong, weak and very weak). For stronger rocks the HLD values show no significant change related to the length of specimens, however, for medium to weak rocks his study reports that the size of specimens can influence the Leeb values, the LHT values are decreased with the decrease in the sample size, the sample length should be at least 6-9 cm long to avoid the size effect, and the higher strength values of rock specimens tend to be more scattered.

Meulenkamp and Grima (1999) used a neural network to predict the UCS from HLD and several other rock characteristics (porosity, density, grain size and rock type) as input. However, this is a complex approach and required many input parameters, each of which added complexity and additional uncertainty to the method. This removed the "simplicity" of the test and it restricted their approach to the availability and quality of the secondary inputs. Moreover, the proposed equation includes many variables, which in turn is not practical in field estimation. Finally, to the author's knowledge, the neural network algorithm details were not published and made readily available.

Okawa et al. (1999) tested the effects of the measurement conditions on the rebound value and concluded that the rebound value depends partially on specimen support (i.e., physical constraint). In addition, multiple tests on the exact same location tend to increase the local density, thus HLD increases with additional impacts at a given point. The roughness of the testing surface has no clear influence on the test result of rebound value.

Kawasaki and colleagues (2002), studying unweathered rocks, proposed that the UCS could be estimated from LHT values by using the Leeb test to establish the strength of rocks in the field. They also established the effects of the test conditions, including the roughness and size of the sample and the impact direction, and used cylindrical specimens of rock types including sandstone, shale, granite, hornfels and schist, collected from different locations in Japan. They reported that the specimen thickness has slight influence on the LHT measurement in specimens more than 50 mm thick. In 2007, Aoki and Matsukura used the type "D" hardness tester to study rock hardness from nine

locations, eight in Japan and one in Indonesia. They proposed an equation relating UCS to HLD and porosity:

$$UCS = \ 0.079e^{-0.039n}\, HLD^{1.1} \qquad [2\text{-}10]$$

Where "n" is the porosity and "HLD" is the Leeb hardness value.

The LHT has been used to study the degree of weathering. Aoki and Matsukura (2008) investigated the degree of weathering by examining the difference between the repeated impact method and the single impact method. Another specific weathering assessment of the LHT in terms of rock surfaces is when Viles et al. (2011) compared mean hardness values at fifteen different sites determined by four testing devices including Equotip, piccolo, silver Schmidt (silvers) and classic Schmidt (classics). They studied their hardness before and after applying carborundum to see the impact of carborundum pretreatment on the results. Moreover, they conducted comparisons for all four devices divided by the rocks having differences in wetness/dryness of its surface area, surface hardness, boulder size influence, edge effects, and operator variance. They concluded that each device has its strengths and weaknesses depending on the purpose of collecting the hardness values. The LHT has been shown in their study to be insensitive to block size for the range of sizes in their study. They studied the sample size effect on the HLD values, on sandstone block from Oribi Vulture site that have volumes that ranged between under 200 cm^3 to nearly 20000 cm^3 and 30 hardness values were taken with the Equotip device. They concluded that there is no relationship between the sample size and the HLD values.

More recently, Daniels et al. (2012) studied the strength of sandstone. They indicated that the original Verwaal and Mulder (1993) correlation could overestimate the rock strength of weak sandstone. Yilmaz (2013) considered only one rock group (carbonate rocks) to determine the suitability of different rebound testing procedures with the LHT for UCS estimations and came up with different regression models. He used a new testing methodology, hybrid dynamic hardness (HDH), which depends on a combination of the surface rebound hardness and compaction ratio (the ratio between HLD and the peak hardness value earned after ten repeated impacts at the same spot) of a rock material. He pointed out that the predicted UCS is more accurate when density is available, which means that density is also could be correlated to intact strength. Moreover, he reported that there is no clear evidence of size effect on the hardness values. He experimentally studied the effect of sample size on the HLD values by using the EHT on 18 different types of rock specimens. Cubic specimens with 7 cm sides were tested

combined with other cubic specimens with 5, 9, 11, 13, and 15 cm sides. All specimens were grounded with 220 sand paper and dried for 24 hours. The hardness tests were performed with 20 single impacts and then got averaged. He attributed the variations in the HLD values to the in-homogeneities existing in the fabric of rock, rather than the size of the specimen and the dissipation of impact energy to "the randomly distributed voids underneath the tested surfaces" (Yilmaz, 2013). He recommended that there is a need for more studies on other rock types with different geometries to investigate the sample size effect.

In the case of layered rocks, Lee et al. (2014) applied LHT in order to estimate the UCS of laminated shale formations. They updated the calibration equation using 62 points from Meulenkamp (1997), Meulenkamp and Grima (1999) and Verwaal and Mulder (2000). In addition, Lee et al. (2014) investigated the effect of sample thickness by studying relationship between density and thickness on a reference test block (a dense material of steel with a dimension of 9.14 cm in diameter and 5.84 cm in thickness). The measurements were taken using the Equotip Hardness Tester. The HLD measured from the block is consistent since it is an isotropic and homogeneous continuum material. Lee and colleagues (2014) used aluminum (Al) 6061-T6 specimens to examine the effect of sample length on HLD with specimens that have identical density (2.70 g/cm3). Their Al specimens have exactly the same diameter of 3.81 cm and six different lengths as following 2.54, 5.08, 7.62, 10.16, 12.7, and 15.24 cm, respectively. They found that the HLD increases as sample length increases, until the tested material reaches a minimum length to obtain consistent HLD. It is noted that the HLD of the

specimens increased in a non-linear form until 12.7 cm. The study proposed that this value is the minimum length of the Al sample for valid measurement of HLD based on its density. The study also examined the thickness effect of shale cores with 10.16 cm in diameter for both sections: 3.38 cm slab and 6.78 cm of butt sections. For each core section, the impact direction is perpendicular to the cut face. The measurements were repeated at the same depth, but on different spots on the sample. For each depth, the mean

value was recorded. It was concluded that the HLD of the 2/3 butt section is higher than the 1/3 slab section.

Figure 2.7 shows the HLD and UCS proposed correlations of previous studies that were conducted using LHT. Some proposed correlations were selected over others because some papers imbedded their datapoints inside other paper's curve, e.g. Lee at al (2014), and Aoki and Matsukura (2007) used the correlation curve of Verwaal and Mulder (1993).

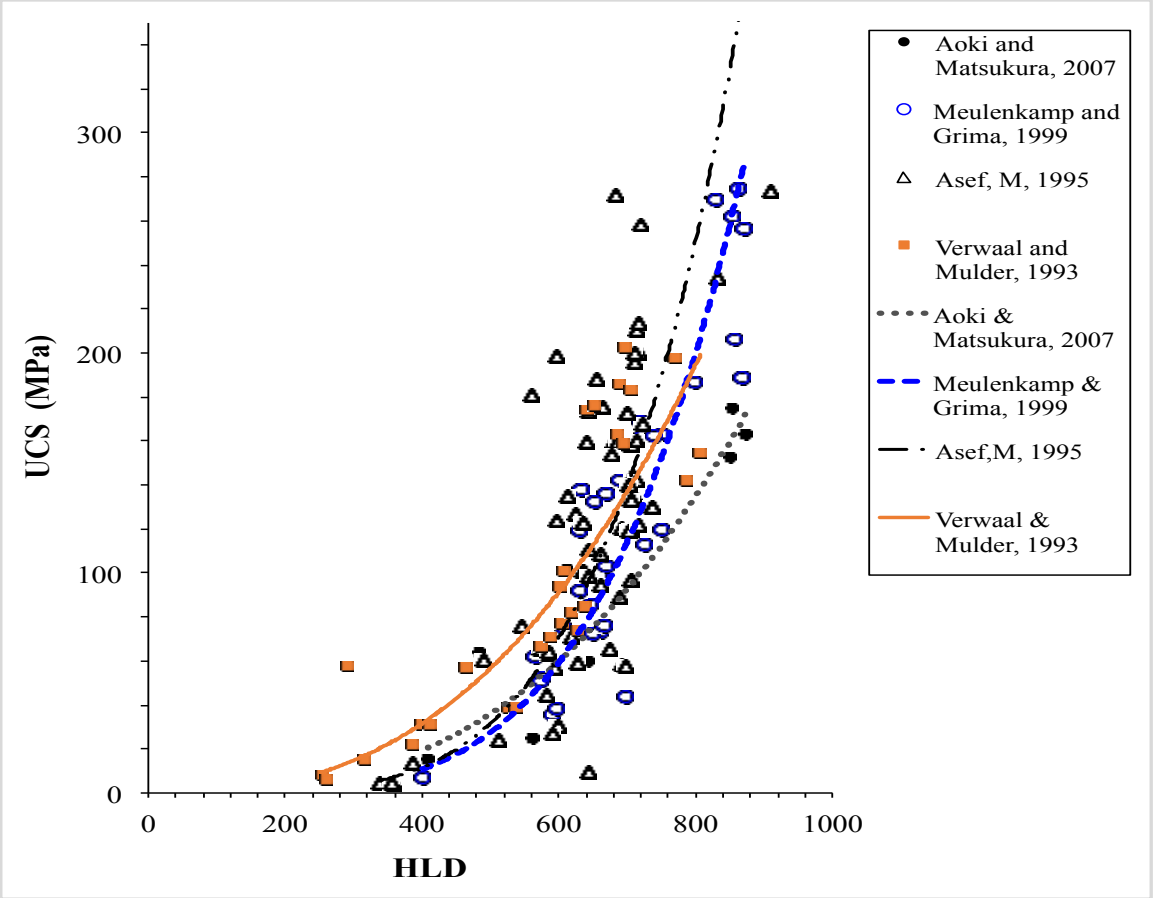

Figure 2.7 HLD and UCS proposed correlation of previous studies (Verwaal & Mulder, 1993; Asef, 1995; Aoki & Matsukura, 2007; Meulenkamp & Grima, 1999)

CHAPTER 3 STUDY METHODOLOGY

This chapter describes the test methodology that has been used to achieve the main goal of this study, which is to develop a relationship between UCS and HLD values. The chapter begins by discussing lab testing methodology which includes collecting, UCS tests on specimens, how they were prepared based on the ASTM recommendations, and LHT on core and cubic specimens. Following that is a discussion of analysis methods, which includes an evaluation of Leeb test methodology. Two methods have been used to evaluate the LHT: the first is to evaluate the number of impacts, and the second is to evaluate the sample size. The final section in this chapter is Leeb – UCS correlation. Statistical analysis (Regression, T-Test, F-Test, residual) has been used to develop the relationship between the mean value of hardness tests and their corresponding rock strengths.

This study used LHT ("D" type) series TH170, to measure the non-destructive hardness values of rock specimens to relate them to the UCS values to investigate and develop an appropriate relationship between the two mechanical properties of rock specimens. The TH170 accuracy varies with respect to different testers and scales of hardness; however, it is able to compare and convert these values into several types of hardness, and the accuracy of measuring was commonly taken as ±0.5% (see the instruction manual of the TH 170). The LHT is a portable hardness tester developed for measuring the hardness of rock materials. It is very convenient and easy to use in the laboratory as well as in the field. This was the first stage in developing a robust relationship linking HLD to UCS, which is described in the subsequent chapters of this study. The manufacturer's manual specified that the minimum weight of the test piece should be 0.05-2 kg and the roughness of the surface equal to or less than 1.6 micrometer for accurate hardness test results and the testing method described in this chapter confirmed all these recommendations.

3.1 Lab Testing Methodology

This section contains a discussion of the lab test methodology which was used in this research. Included in this section are the locations the specimens were taken from, how they were collected, and the number of specimens obtained. This section also includes a discussion of the UCS test methodology used in the study, including sample preparation. Finally, LHT testing methodology for core and cubic specimens is discussed.

3.1.1 Collection

In this study, significant laboratory work was carried out in cooperation with other researchers on collected specimens from the mining industry partners and from local quarries. Therefore, the database was obtained from diverse sources; university lab specimens were combined with other literature to build a database with a total of 336 points to use in this research. The specimens that were obtained for the test results in our lab originate in diverse Quarries throughout Nova Scotia.

3.1.1.1 Previously Published

There are two methods used to obtain from previously published work. The first method is to obtain them directly from the published tables. The second way is to digitize them from an image of a graph that presents the points. The first way to get from the tables is a direct way, but it is impossible to obtain the existing on the image of the graph without using a special software that has the ability to pick the values of those on the image of the graphs. For that reason, 'Graph Click' software was used as a graph digitizer software, which allows researchers to automatically regain the original (x, y) from the graphs. In other words, if one has a graph as an image, but not the corresponding, the only way to get the trajectory of a graph is the graph digitizer software or by hand. Graph Click is one of the best ways to deal with that kind of issue. By clicking on the image of the plot, the obtained coordinates of the points can be directly exported into Microsoft Excel or any other similar

application. This software has many features including image modification, an unlimited undo function, handling with two ordinate axes, covering for different scales such as linear, logarithmic or inverse scales, and the use of several sets in the same document.

3.1.1.2 Quarries

A number of the points that were used in this study were collected from the test results on specimens brought in May 2015 from quarries located in Nova Scotia. Sandstone rocks with intruding organic matter dots and classic olive grey colour were collected from Wallace Quarries Ltd, which is located at Wallace, Nova Scotia, Canada. The site is approximately 163 km from Halifax, Nova Scotia, Canada. Wallace sandstone is known as one of the most durable sandstones in the world and it has been quarried for the last 150 years.

Dolostone blocks were brought from Halifax Stone LTD, Middle Musquodoboit, NS, Canada. The site is approximately 67 km from Halifax, NS, Canada. The weathered porous limestone blocks were brought from Mosher Limestone Company LTD, Upper Musquodoboit, NS. The site is approximately 90 km from Halifax, NS, Canada.

Schist rocks were brought from a mine in eastern Canada: three Quartz Sericite Schist core specimens, (two of them show a foliation of 45° to the core axis and one has a 40° foliation to the core axis), five Quartz Chlorite Schist core specimens, (two with a foliation angle of 45° to the core axis, two with a 40° angle, and one with a 30° angle) and two core specimens of Mafic Dyke. The mine is located in Newfoundland. The site is approximately 1000 km from Halifax, NS. All schist rocks (soft rock) are foliated and host stringer pyrite. Some of the foliated schist core specimens are damaged a bit from blasting and have natural fractures.

Coal Sandstone (a micro defected gray sandstone with coal bands) was obtained from the Stellarton Surface Coal Mine, which is an open pit coal mine located at 1 Westville, Nova

Scotia, Canada. It is owned and operated by Pioneer Coal Limited. The site is approximately 150 km from Halifax, NS, Canada. Greywacke is from the Lower Ordovician Meguma Group. Slate (Metamorphic Rock), which is formed when fine-grained sedimentary rock (shale) is exposed to high pressure deep beneath the surface of the earth, is characterized by the way it breaks, along closely spaced parallel fractures (U.S. Geological Survey). A granite block, 35 cm x 25 cm x 15 cm, approximately, was picked up from Langes Rock Farm Ltd, Maplewood, Nova Scotia. The site is approximately 120 km from Halifax, NS, Canada.

Within the framework of this study, rock blocks were cored and inspected for the existence of any macro-defects so that standard specimens with no cracks and fractures would be used. It is well known that porosity and anisotropy (schistosity and foliation) are the mechanical parameters affecting the mechanical properties (HLD, UCS, etc.) of the rock specimens. This study attempted to avoid the effecting of these parameters by picking the specimens that show no high porosity and performing the tests with considering of foliation plans.

All specimens were marked, labeled, and the specimen geometry was checked prior to the lab tests to minimize any error during the experiments. For the UCS tests and hardness tests, the specimens were labeled as the following (S.S) for sandstone (C) for Coal (mine) sandstone, (L) for limestone, (D) for dolostone, (G) for granite, (W) for greywacke, (SH) for schist with horizontal foliation to axial load, (SV) for schist with vertical foliation to axial load.

(a) Schist

(b) Dolostone

(c) Greywacke

(d) Granite

(e) Wallace Sandstone

(f) Granite

Figure 3.1 (a, b, c, d, e and f) Block specimens of various rock types that were used in this study from mining operations Eastern Canada.

3.1.2 UCS Testing

In this study, our core specimens, with 54 mm diameter and 113 - 121 mm height, were prepared from a block from different rock types (granite, schist, limestone, marble, dolostone and sandstone), which were obtained from different mining operations in Eastern Canada (see quarries section). All UCS tests were carried out in the Dalhousie University laboratory, Halifax, Nova Scotia, Canada. In this study, the core specimens were prepared for the UCS tests, and are as follows: three Quartz Sericite Schist, two of which show foliation of 45° to core axis and one with 40° to core axis; 5 Quartz Chlorite

Schist, two with a foliation angle of 45° to the core axis, and the other two with a 40° angle, and one with a 30° angle, and 2 core specimens of Mafic Dyke. In addition, two sandstone core specimens, three limestone core specimens, three Greywacke core specimens, three dolostone core specimens, four Granite core specimens, 12 Schist core specimens with horizontal foliation, sex Schist core specimens with vertical foliation, three Coal sandstone core specimens, and 6 Slate core specimens (Metamorphic Rock) were used. Four months, from May 2015- August 2015, were spent on UCS tests, from the first day the specimens arrived at our lab until we finished all UCS tests. Table 3 provides details of the used core specimens.

Table 3 The core specimens that were prepared for the UCS tests in present study

Number of sample	Lithology	Foliation to core axis
3	quartz sericite schist	1-> 40°;2-> 45°
5	quartz chlorite schist	1-> 30°;2-> 40°;2-> 45°
2	mafic dyke	unfoliated
2	sandstone	unfoliated
3	limestone	unfoliated
3	greywacke	unfoliated
3	dolostone	unfoliated
4	granite	unfoliated
12	schist	90°
6	schist	0°
3	coal sandstone	90°

After that, a compression-testing machine of about 2000 kN (200-tonne) capacity with a loading rate of 0.3 - 0.5 mm/min was applied for UCS tests with a duration of 7 – 13 minutes in average (see section 2.1.1)

3.1.2.1 Specimen Preparation (Core Sample Processes: Drilling, Cutting, Grinding and Levelness evaluation)

Preparing the specimens for UCS testing occurred in the following steps according to ASTM standard (ASTM. D4543-08, 2008):

1/ The desired rock sample was placed on the platform (Figure 3.2). Handles at the back of the platform can be loosened to raise, lower, and rotate the platform (Figure 3.3).

Figure 3.2 Drilling machine (Photo courtesy of J Perrier-Daigle).

2/ The height of the platform was set so that the bit can drill through the whole sample.

3/ Using the wheel at the top right of the machine shown in Figure 3.3 (b), the drill was lowered and a small amount of force was applied to the rock.

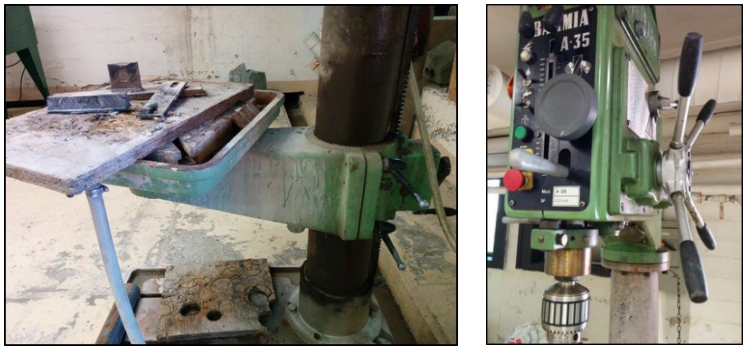

(a) (b)

Figure 3.3 Close up of drill platform (a) and drill handles (b) (Photo courtesy of J Perrier-Daigle).

4/ The drill bit was lifted off the rock, and the green button was pushed to start the drill.

5/ The water valve was partially opened, and drilling manually, the drill was slowly lowered into the rock sample. Applying very little force, a pilot hole was drilled into the rock approximately ¾ of the drill bit tip deep.

6/ After the pilot hole was drilled and the drill bit was determined to not shake, the gray lever was pushed to activate the automatic feeder, and then the water valve was fully opened.

7/ The drill was monitored regularly to make sure that the bit was not shaking and the rock was stable. Once the drill bit reached the end of the rock sample, the drill was turned off.

Some rock types were relatively weak, and fractured during drilling, leaving unusable core specimens. These rocks were examined for discontinuities, fractures, or joints in the rock. Furthermore, some rocks had dominant structural orientations such as schist, and it is

necessary to make sure that one is drilling in the proper orientation, avoiding any fractures in the rock specimen that may result in cracked or weakened specimens.

Care was taken during drilling near the edge of a rock or next to another drill hole. Drilling a hole approximately 1 cm away from another hole may cause the drill to tear the supporting wall between the two holes.

Figure 3.4 Blade rock saw machine (Photo courtesy of J Perrier-Daigle).

In the cutting stage, after drilling the sample, the core still had rough ends. These ends cut in order to test the specimens with an even load distribution. Since the rock needed to be cut, this was done with the wet blade saw machine shown in Figure 3.4. The machine uses a diamond-encrusted blade that moves at a set rate while constantly being lubricated.

Figure 3.5. Close up of vice controls inside the wet blade saw machine ("Photo courtesy of J Perrier-Daigle).

The core was placed in the vice, and another sample was placed beside core specimens that were shorter than the length of the vice to prevent any vibrations while cutting. The vice was tightened using the knob shown in the center of Figure 3.5. Using the wheel on the right, the vice slid, allowing the blade to cut the sample to the desired length, and the top hatch of the machine was lowered when the sample was ready.

Figure 3.6 Speed settings for the saw (Photo courtesy of J Perrier-Daigle).

The mechanism shown in Figure 3.6 was used to adjust the speed at which the sample was cut; Figure 3.6 shows the slowest possible setting. During the process, the specimens were checked regularly. Once the sample was cut, the sample was turned over and the process was repeated to cut the other side.

The saw sometime left a small chip at the end of the sample. This happens when the force from any hanging rock or from the blade is too strong. To prevent such chipping, the specimens were orientated so that any dominant structure resisted the force of the blade and did not chip off. Another way to prevent chipping was to remove as little height off the sample as possible.

Figure 3.7 Grinding machine (Photo courtesy of J Perrier-Daigle).

Figure 3.8 Cross feeding wheels and adjusting switches (Photo courtesy of J Perrier-Daigle).

After a sample was cut, the end surfaces needed to be ground to provide the most even load distribution possible. For this we used the grinder machine shown in Figure 3.7.

Figure 3.9 Adjusting switches of the grinding machine (Photo courtesy of J Perrier-Daigle).

Figure 3.10 Top right panel of the grinding machine (Photo courtesy of J Perrier-Daigle).

The grinding machine was properly adjusted and then the ends of the sample were marked with a marker, so as to cover most of the surface area. The sample was placed in one of the

four slots of the v-clamp. Figures 3.8 and 3.9 show the grinding switches that adjusted the area that was ground. Once the spindle was set at the appropriate height and was not touching the sample, the grinding began. The top right panel was turned on (Figure 3.10), the increment (in inches) was selected, and then, by adjusting its keys, the grinder started to descend. This should generally be around 13 μm.

3.1.2.2 UCS Test Preparation

The following are the steps followed in preparation for performing UCS testing on the specimens:

Step 1: Sanding

Sanding the specimens creates a relatively flat surface so the strain gauge can rest evenly on each sample. Sanding likewise provides a smoother area for the gauge to bond to.

Step 2: Strain gauges' application

The second step of preparing a core for UCS testing is to apply strain gauges to some of the specimens; this is the most sensitive part of the UCS test preparation.

3.1.2.3 Specimen Specification

After the previous steps, the core sample was ready for testing. Several vital pieces of information were noted before breaking the specimens for the UCS test. It is necessary to have information such as such as the height, diameter, weight, etc. of the sample written down before it is broken. Before performing the UCS test, each sample was examined thoroughly for any dominant structures, flaws, or inclusions, and the observations were written down and photographed; pictures were also taken of each core sample before and after testing.

3.1.2.4 Management

After breaking the sample, the was prepared using a template excel file in order to receive fast output. Figure 3.11 shows a general stress-strain curve. When dealing with rocks, especially compact rocks like sandstone, the yield stress and the ultimate stress will be very similar or the same, since the rock will most likely explode instead of deforming. Stress, the y-axis, is always measured in MPa. The vertical displacement was given by the strain gauge measurements, and the strain can be calculated using this equation:

$$\epsilon = \frac{\Delta L}{L} \qquad [3\text{-}1]$$

Where ΔL is the vertical displacement measured from the load frame, and L is the length of the sample.

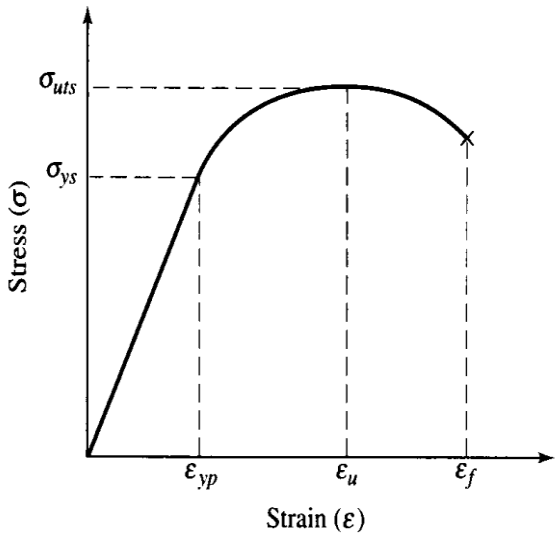

Figure 3.11 Generic stress-strain curve

For Young's Modulus calculation, the value at 50% of the maximum stress was determined. The slope of a tangent line created at that point gave the modulus. The problem with this

method was that there were many points off, which created a zigzag pattern, and calculating the modulus from one single point would give an inaccurate value. Instead, a more practical way of calculating Young's Modulus is to select several points of around the point, and create a linear line of best fit to find its slope. If there is a discontinuity in the at half its maximum stress, such as a major dip in stress levels, another point was chosen - above the half point - where there is a linear section of. Young's Modulus has units of GPa, and that strain was measured in % on the graph.

In order to calculate the Modulus Ratio, the following equation was used:

$$MR = E/\sigma_c, \qquad [3\text{-}3]$$

Where E is the Young's Modulus, and σ_c is the ultimate compressive stress.

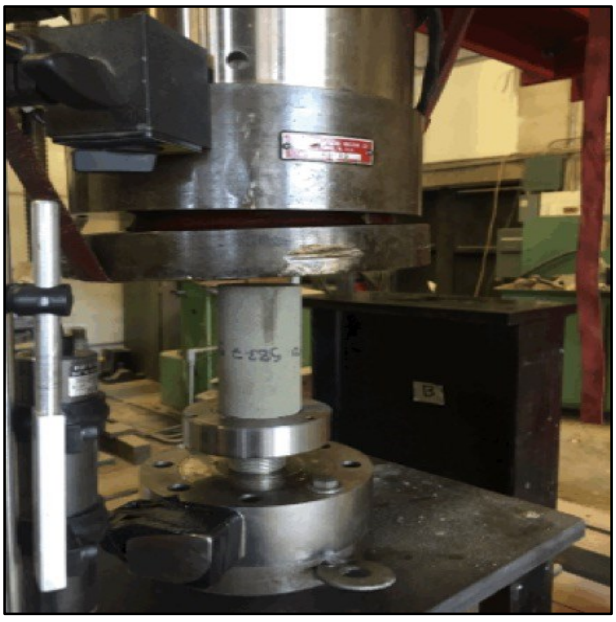

Figure 3.12 UCS test machine with a sandstone sample.

3.1.3 Rebound Test

In this study, the LHT is used for the following reasons: it is a non-destructive device that leaves little damage to the tested surface, which is good for many purposes such as measuring a thin layer and getting greater accuracy of its measurements. Furthermore, LHT can be completed in a matter of seconds. The important point of this device is that it has the ability to measure both soft and thin material due to its lower impact energy. Its only unfavourable point is its sensitivity to surface conditions (see subsection 2.4).

There is still no established testing procedure for using the LHT on rock materials. Therefore, the single impact method (12 impacts) on the core specimens (Daniels et al., 2012) was used on core specimens. The maximum and minimum readings were excluded and the average of the 10 remaining readings was used.

3.1.3.1 LHT and Schmidt Hammer Procedures

Before starting using the hardness test, the LHT should be calibrated with a standard test block. For the LHT loading, the concave area is held by the left hand and pressed down the body by the right hand while holding the loading key. The LHT is now ready to perform a test: one presses the release button at the top of the main unit to initiate the test. The sample and the LHT device must all be stable. The distance between any two indentations and the distances to the sample edge from the center of any indentation should meet the regulations of the LHT manual.

Table 3.1 Impact distance regulation (Equotip manual, 2010)

Distance between any two indentations (mm)	Indentation to the edge of tested sample (mm)
≥ 3	≥ 5

In this study, the most popular standard was chosen for the Schmidt Hammer application which is the American Society for Testing and Materials (ASTM). Applying 20 reading impacts on our lab sandstone specimens for a comparison purpose with LHT. USING the N-type of Schmidt Hammer that performs an impact energy of 2.207Nm. Discarding the Schmidt numbers that differing more than seven units from the average. And then averaged the remaining numbers. ASTM standard requires impacts be separated, to avoid overlap data, at least one plunger diameter. The ASTM Standard (D5731-95) was performed for application of Schmidt hammer. "The hammer was held vertically downward at right angles to the horizontal rock surface" (Selçuka & Yabalaka, 2014). The core specimen surfaces were smoothed to avoid an impact energy loss. 20 single readings were taken to obtain the average Schmidt number

3.1.3.2 Core Specimen

In this study, the LHT was performed to link the HLD to the UCS results for our core specimens. For that reason, the core specimens were prepared from different rock types (see sample preparation section). There is still no established testing procedure for using the LHT to predict UCS on rocks; therefore, the single impact method (12 impacts) described above was used, and the results are presented in the next chapter.

Additionally, this study investigated and quantified the optimum readings (impacts) that are required to get a valid LHT (see Number of Test section). Moreover, this study aims to examine the relationship between the sample size and the mean HLD to investigate the sample size effects (see Evaluation of Leeb Test Methodology section). For that reason, a number of core sandstone specimens were prepared, followed by an experimental study that was conducted on different sandstone sizes. All core specimens have been prepared with the same diameter of 54 mm (NX-size) with eight different lengths. For each length, the specimens were tested by the LHT, and the different core sample lengths after preparation were 9, 10, 22, 38, 76, 102, 152, and 190.5 mm, respectively.

3.1.3.3 Cubic Specimen

In this study, the LHT ("D" type) was used to examine the relationship between the sample size and the mean value of LH of cubic rock specimens. For that reason, the cubic specimens were prepared from different rock types. The averaged LH readings were plotted against the cubic sizes of rock specimens. Also, in this study, several cubic sandstone specimens were prepared (refer to the sample size section). Four cubic specimens with different lengths were prepared. For each length, the specimens were tested by the hardness tester. The different four cubic sample lengths after preparation were 25, 51, 102, and 203 mm, respectively.

3.2 Analysis Methods

This section discusses the various methods used to analyze the retrieved from the testing described above. Analysis and discussion of the results are covered in Chapter five.

3.2.1 Evaluation of Leeb Test Methodology

The appropriate number of impacts that are required to get a reasonable measure of the "Statistically representative" hardness of the sample rock, given the sensitivity to localized conditions, is a controversial issue amongst researchers. In order to address this issue and quantify the appropriate readings (impacts), this study was carried out using two approaches. First, an evaluation based on statistical theory was carried out, and, secondly, an evaluation based on sampling was carried out. Also, the scale effect on the specimen hardness has been addressed.

3.2.1.1 Number of Impacts Comprises a Test

As stated above, there were two types of tests carried out to quantify the appropriate number of impacts. The first approach in this study used a core sample (sandstone, granite,

dolostone and schist) of a L/D ratio of 2-2.5 with a total length of 121 mm. The average of 100 repeat measurements (readings) on different pots of the core sample is considered as the population mean (μ). The statistical measures of 100 readings on the core specimens, including the μ and σ, are presented in next chapter in Table 4.1. After that, the margin of error (***ME***) formula was used to determine the difference between the observed $\bar{X}$ and the μ when the experiment was repeated with the same testing condition for different sample sizes (e.g. 10 and 15). This method aids in finding out how many impacts one would need to get a $\bar{X}$ which is almost equal to the μ, based on 100 readings with a degree of confidence interval of 95%. The ideal sample mean can be quantified for sample sizes less than 100 by using ME. The relation between the μ and $\bar{X}$ can calculated using the following equation:

$$\mu = \bar{X} \pm 1.96 \left(\frac{\sigma}{\sqrt{n}}\right) \quad [4\text{-}1]$$

Where μ is the population mean, 1.96 is the critical Z value of the standard normal distribution at a 95% degree of confidence, σ is the standard deviation of the population, n is the sample size, and $\bar{X}$ is the sample mean. The formula to establish the ***ME*** at different sample sizes (e.g. at 10 and 15) is:

$$ME = 1.96 \left(\frac{\sigma}{\sqrt{n}}\right) \quad [4\text{-}2]$$

The second approach is based on sampling, relying on the Central Limit Theorem and the Law of Large Numbers. The key idea in the Central Limit Theorem is that when a population is repeatedly sampled, the calculated average value of the feature obtained by those specimens is equal to the true μ value. The Law of Large Numbers states that as a sample size grows, its mean will converge towards the mean of the whole population (Meyer and Krueger, 1997). Accordingly, this study was performed on a total of 100 readings (impacts) on a sandstone core sample. Once this population (100 readings) was captured, a subset number of readings (e.g., 10, 15, 20, 30) was randomly selected to ensure that all of the points were being well represented and took into consideration all different

aspects to avoid being biased by the performer, and the mean value was determined. This was done with subset sizes ranging from 1 to 100 readings.

Moreover, because of the high variability of $\bar{X}$ at low sample numbers, a total of five "realizations" of this randomized subset study were carried out. This allows one to visually assess how many impacts one would need to get a $\bar{X}$ which is almost equal to the μ, based on 100 readings (compared to the confidence interval). A graph was then plotted. It includes the average of the readings that were previously calculated on the vertical-axis against the number of tries, which was a 100 on the horizontal-axis. This method graphically examines the relationship between the mean hardness values of number of averaged and their arithmetic mean of the 100 readings (population mean). Moreover, this method helps to determine the minimum number of readings required to carry out a 'Valid' test based on the σ rules and to visually assess the error associated with limited sample size (e.g. 10 readings).

3.2.1.2 Rock Specimen (Sample) Size

It has been observed in several studies that there is a correlation between the scale effect on the specimen hardness, but little influence of sample size on this relation (e.g. Verwaal and Mulder, 1993; Asef, 1995; Kawasaki et al., 2000 and Lee et al., 2014). Others stated that there is no relation between the sample size and the HLD values (e.g. Yilmaz, 2013; Viles et al. 2011). Viles et al. (2011) studied the sample size effect on HLD values on sandstone block from Oribi Vulture site that had volumes that ranged between under 200 cm^3 to nearly 20 000 cm^3, and 30 hardness values were taken with the Equotip device.

They concluded that there is no relationship between the sample size and the HLD values. As a result of the mixed results and conclusions in the literature, it is clear that the effect of the sample size for a consistent HLD value determination has not been well investigated and not yet standardized by ISRM or ASTM. An understanding of the relationship between the hardness value of a sample, and the size/geometry of a sample (e.g. core volume), is necessary to determine the appropriate sample size that should be considered as a valid

measure. In order to investigate the relationship between the HLD values and the sample size, and then analyze the effect of sample size on HLD values that lead to evaluate this relationship between the HLD and the specimen size, an experimental study was conducted on different sandstone sizes, including both cubic and core sizes. All core specimens have been prepared with the same diameter of 54 mm (NX-size) and eight different lengths (see 3.1.3.1), In addition, four cubic specimens with different lengths were prepared (see 3.1.3.2). The results are presented in the next chapter. For each length, the specimens were tested by the hardness tester. The 12 single impacts on sample ends (Daniels et al., 2012) were used on all specimens. The maximum and minimum hardness reading were excluded, an average of remaining readings were used. The average value was recorded as the rebound Leeb number (HLD).

3.2.2 Leeb – UCS Correlation

This section describes the methods of Statistical Analysis that were performed on the results of UCS tests and HLD values. Included in this section is the comparison between the two proposed statistical models (Nonlinear and Regression), and an analysis of variance using two common tests (T-Test and F-Test). This section also examines the validity of the best-fit model.

3.2.2.1 Statistical Analysis of Data

Two statistical analysis models were performed in order to find the best correlation with the lowest S, which is a useful measure to assess the precision of the predictions. The first one is the least-squares regression model, and the second one is the nonlinear regression model. The curve was selected based on previous knowledge from the literature about the response curve's shape between UCS and HLD. These analyses were performed using Minitab software (Version 17.2014). Minitab uses a Gauss-Newton algorithm with maximum iterations of 200 and tolerance of 0.00001, to minimize the sum of squares of the residual error (Ryan et al., 2004). The S was used to assess how well the regression

model predicts the response between two models (see next chapter). The lower the value of S, the better the model predicts the response (UCS). In order to compare the two prediction models, the following statistical performance indexes were used: The S, the sum of squared errors of prediction (SSE) and the mean square of the error (MSE).

$$\boldsymbol{MSE = SSE/DF} \quad [4\text{-}3]$$

$$\boldsymbol{S = \sqrt{SSE/DF}} \quad [4\text{-}4]$$

Where DF= the number of degrees of freedom.

3.2.2.2. Regression

In order to develop relationships between UCS and HLD, regression analyses were used. Regression analysis is normally used to build a mathematical model that can be used to predict the dependent variable values based upon the Independent variable values. To perform the regression analyses, points were plotted in two dimensions in a scatterplot form. This format allows visualization of the prior to running a regression model. Different curve-fitting relationships, such as exponential, logarithmic, and power, can be used to analyze the relationship between the two variables, one dependent and the other independent. Once all possible regression curves fit and S values have been determined, the researcher decided which curve fit was better and most appropriate. Typically, the most appropriate curve is the one with the lowest S value (Meyer and Krueger, 1997). Based on the literature review, exponential relationships are expected between UCS and LHD. In addition, in the regression model, if a response (Y) and a predictor (X) relation does not satisfy the ordinary least squares regression and the residuals diverge as the X increases, then the needs to be adjusted to achieve a better fit. A common solution for this problem is to transform the response variable (Y). The transformation is simple when using the Box-Cox transformation function in Minitab. Therefore, this study used this function to get a better model for the UCS and HLD relationship. To test the significance of the least square

regression model, an analysis of the variance for the regression was used at 95% level of confidence (Ryan et al., 2004).

3.2.2.3 Nonlinear Regression

In this study, a nonlinear regression of the set was also performed. Using information from the literature about the response curve's shape and the behavior of the physical properties, an exponential growth curve was selected with the following expected function form for one parameter (UCS) and one predictor (HLD):

$$\boldsymbol{UCS = \theta 1\, HLD\, exp\, (\theta 2 \times\ HLD)} \qquad [4\text{-}5]$$

Where the θ represent fit parameters and HLD represent the predictor.

In the next sections (T – TEST and F – TEST), an F-test in regression compares the fit of different linear models. Unlike T-tests that can assess only one regression coefficient at a time, the F-test can assess multiple coefficients simultaneously.

3.2.2.4 T–TEST

In a T–Test, the coefficients in the least square regression represent the mean change in the response (UCS) related to the change in the predictor (HLD). The values of the y-intercept, the slope, and their P-values are the most useful in the analysis. If both of these values are less than the alpha level of 0.05, it indicates that the predictors are statistically significant. It also means that any changes in the UCS values are related to changes in the HLD. In this study, T-tests were used to test the overall significance for a regression model, to compare the fit of different models and to test specific regression terms (see next chapter).

3.2.2.5 F–TEST

In the Minitab software, Analysis of Variance (ANOVA) can determine the best fit of different models. ANOVA uses F-tests to statistically test the equality of means. The F-statistic is simply a ratio of two variances. Variances are a measure of dispersion, or how far the are scattered from the mean, and larger values represent greater dispersion (Ryan et al., 2004).

In this study, F-tests were used to test the overall significance for a regression model, to compare the fit of different models and to test specific regression terms (see next chapter). The hypotheses for the F-test of the overall significance are as follows:

- Null hypothesis: The fit of the intercept-only model and your model are equal.
- Alternative hypothesis: The fit of the intercept-only model is significantly reduced compared to your model.

If the P-value for the F-test of overall significance is less than the level of significance, one can reject the null-hypothesis and conclude that your model provides a better fit than the intercept-only model.

In the F-test, if the P-value is less than 0.05, then it can be said that there is a relationship between the two parameters. Also, if the P-values are close to zero, it is concluded that the models are valid according to the F-test (Ryan et al., 2004).

3.2.2.6 Validation of the Model

In the study, residual plots were checked in order to validate the model. In order to validate the model and to assess whether the residuals are consistent with random error and a constant variance, t needs to check a residual versus fitted values plot. If the residuals indicate that the model is systematically incorrect, it is possible to improve the model. The residuals plot should not be either systematically low or high. So, the residual plot should

be centered around zero throughout the range of fitted values. In other words, the model that we used is correct on average for fitted values. Furthermore, random errors are assumed to produce residual plots that are normally distributed. Therefore, the residual plot should have a constant spread throughout the range and fall in a symmetrical pattern.

CHAPTER 4 LABORATORY TESTING RESULTS

This chapter discusses the results of the laboratory experiments that were conducted on rock specimens to develop a better understanding of the methodology of LHT for rock and the HLD-UCS correlation. It also discusses the recommended LHT methodology developed as a result of the performed experiments.

4.1 Leeb Hardness Test Results

This section presents the results of LHT that were carried out on sandstone, granite, dolostone and schist. It also presents the results of a steel Reference (calibration) Hardness test block. The aim of these tests is to evaluate the number of readings that comprise an average test result and the sample size effect on the rebound hardness value. Moreover, this study aims to develop a database for UCS correlation. The evaluation of number of readings per test was divided into two subsections: one based on statistical theory and another based on a sampling approach. The following subsection shows the results of sample size effects on core and cubic specimens. The chapter ends with a presentation of the results of the scale effect for the mean HLD, normalized by the value of the standard length as a function of the core sample length and volume.

4.1.1 Number of Readings Averaged for a Test Result

The LHT methodology was evaluated to address the question of how many Leeb readings comprise an average test result. The appropriate number of impacts that are required to get a reasonable measure of the "Statistically representative" hardness of the sample rock, given the sensitivity to localized conditions, is a controversial issue amongst authors. In order to address this issue and quantify the appropriate readings (impacts), this study was carried out using two approaches mentioned in the previous chapter: the first evaluation is

based on statistical theory, and the second approach is based on semi-empiricist theory "sampling". It is relying on the Central Limit Theorem and the Law of Large Numbers.

4.1.1.1 Results of Evaluation Based on Statistical Theory

The first approach in this study, the evaluation of the Number of Readings, was based on statistical theory. The statistical measures of 100 readings on all tested specimens (sandstone, granite, dolostone, H-schist, V-schist and reference hardness block), including the μ and σ are presented in Tables 4.1.

The results using the tested specimens (sandstone, granite, dolostone, H-schist, V-schist and reference hardness block), for which we have 100 repeated measurements are shown in Table 4.2. This table illustrate that, by increasing the number of impact readings the associated margin of error decreases. In general, the LHT requires sampling effort to obtain a relatively good estimate of the true hardness of rocks.

Table 4.1 Statistical analysis of 100 impacts on tested rocks using LHT

Statistical measure	Test block	V-Schist	H-Schist	Dolostone	Granite	Sandstone
Standard deviation	2	56.5	92.5	18	43	21
Confidence Interval at 95%	±0.11	±9	±15	±9	±8	±4
Upper confidence limit	773	867	844	647	879	557
Lower confidence limit	764	584	447	564	863	548
Mean	770	759	710	594	879	552
Median	770	762	743	592	880	552

Table 4.2 Statistical details of the number of impacts that constitute a "valid" test on tested rocks (see 3. 2.1.1).

Tested rock	Number of impacts in subset		
	10	20	30
	Margin of error ($\pm$ $\boldsymbol{ME}$)		
Sandstone	13	9	8
Granite	27	19	15
Dolostone	11	8	6
H-Schist	57	40	32
V-Schist	35	25	20
Test block	1.24	0.88	0.72

4.1.1.2 Sample Size Evaluation Based on Sampling

The second approach that was used to evaluate the sample size effect is based on sampling, relying on the Central Limit Theorem and the Law of Large Numbers. The key idea in the Central Limit Theorem is that when a population is repeatedly sampled, the calculated average value of the feature obtained by those specimens is equal to the true μ value, and the Law of Large Numbers states that as a sample size grows, its mean will converge in probability towards the average of the whole population. Moreover, because of the high variability of the $\overline{\boldsymbol{X}}$ at low sample numbers, multiple "realizations" (a total of ten) of this randomized subset study were carried out.

Figure 4 Core specimens of sandstone, granite, dolostone, and schist were selected to evaluate the number of impacts required to validate a test

Graphs were plotted representing with the average of the readings that were previously calculated on the Y-axis against the number of tries, which was a 100 on the x-axis (Figures 4.1 to 4.6). This method graphically shows that by increasing the number of averaged, their arithmetic mean gets close to the 100 readings mean (population mean). As shown in Figure 4.7, one realization was picked for each presented rock, it is clear that there are minimal gains for extra tests beyond 10 in sandstone, granite and dolostone. This could be due to the uniformity of grain size in sandstone, granite durability and dolostone homogeneity. A reference hardness test block did not show any variation due to its consistency. Also, the Schist sample, for both H-Schist and V-Schist, showed less variation beyond 10. This could be due to the direction of schistosity plane.

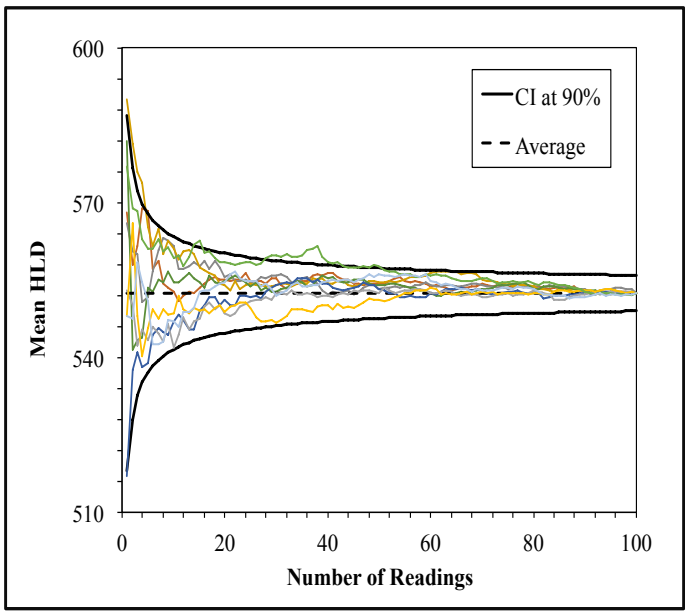

Figure 4.1. Number of Readings versus Leeb Hardness type D (HLD) value of Sandstone. The plot shows the confidence interval around the mean plus ten realizations (colored lines) of randomized subset means for subset sizes ranging from 1 to 100.

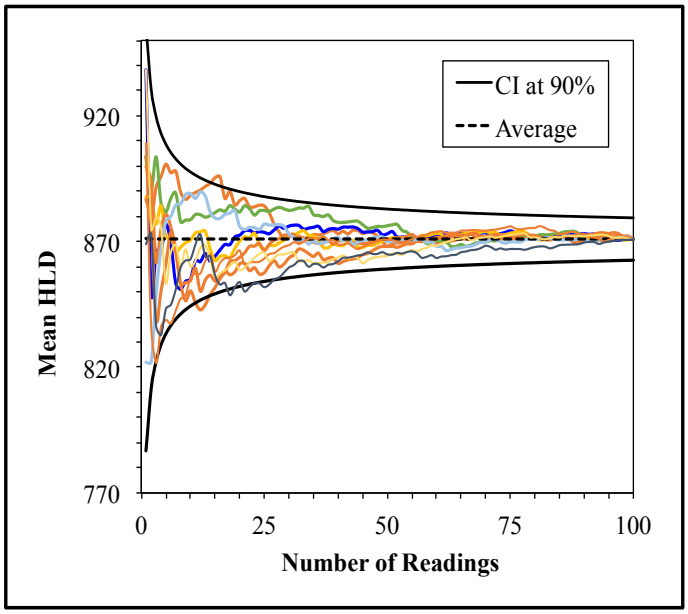

Figure 4.2 Impact Readings versus Leeb Hardness Type D (LHD) value of Granite. The plot shows the confidence interval around the mean plus ten realizations (colored lines) of randomized subset means for subset sizes ranging from 1 to 100.

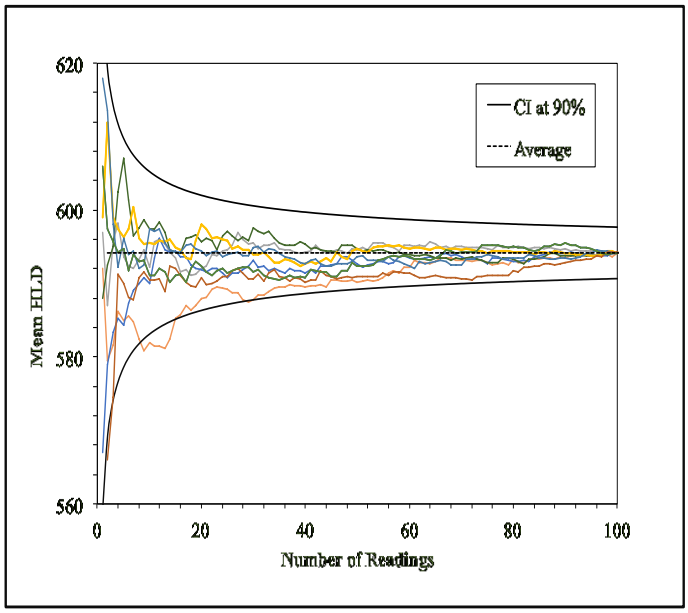

Figure 4.3 Impact Readings versus Leeb Hardness Type D (HLD) value of Dolostone. The plot shows the confidence interval around the mean plus ten realizations (colored lines) of randomized subset means for subset sizes ranging from 1 to 100.

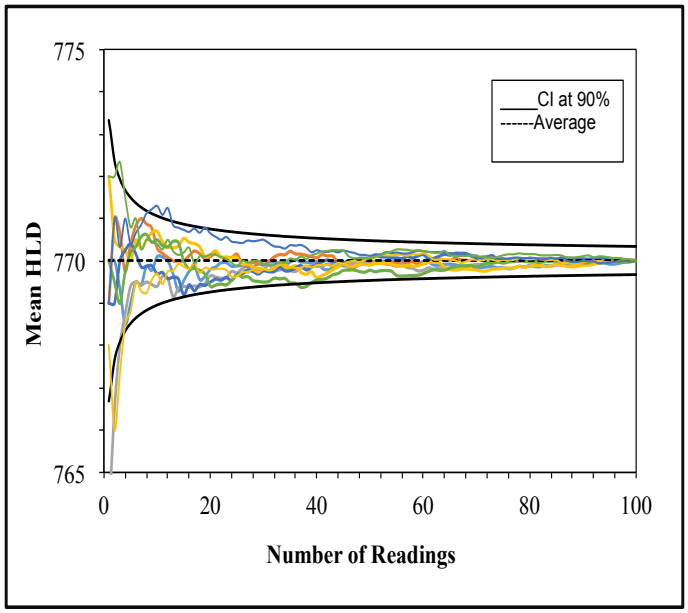

Figure 4.4 Number of Readings versus Leeb Hardness Type D (HLD) value of Reference Hardness test block.

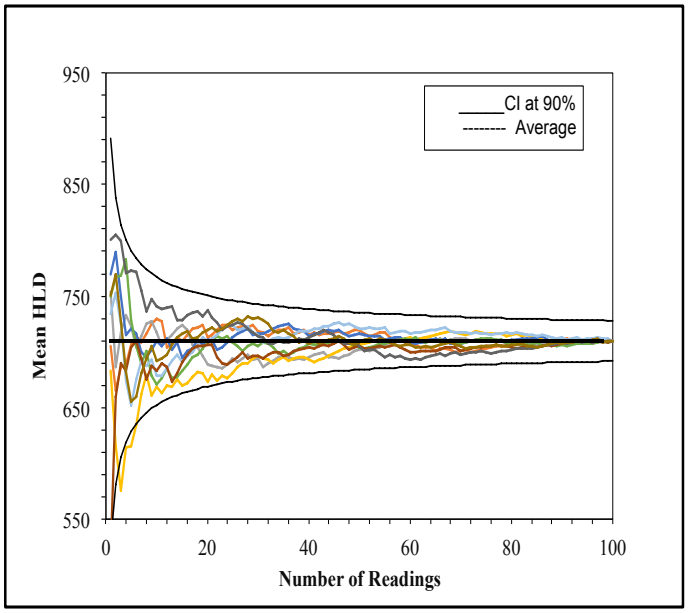

Figure 4.5 Number of Readings versus Leeb Hardness Type D (HLD) value of H-Schist. The plot shows the confidence interval around the mean plus ten realizations (colored lines) of randomized subset means for subset sizes ranging from 1 to 100.

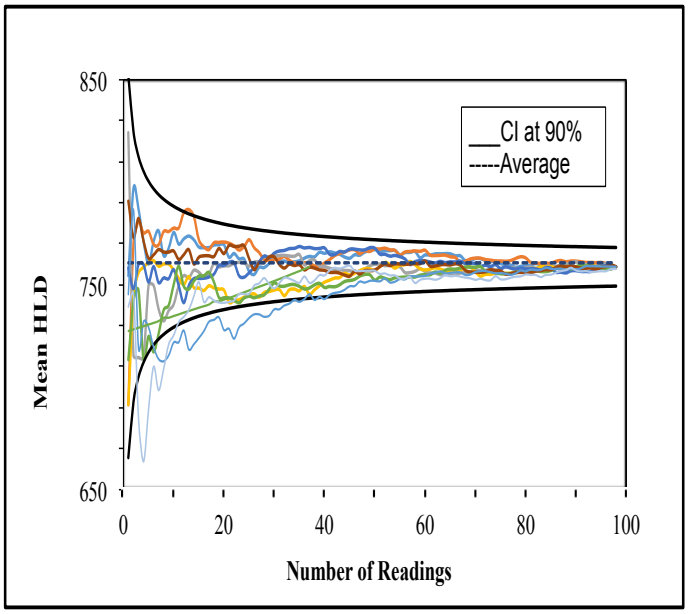

Figure 4.6 Number of Readings versus Leeb Hardness Type D (HLD) value of V-Schist. The plot shows the confidence interval around the mean plus ten realizations (colored lines) of randomized subset means for subset sizes ranging from 1 to 100.

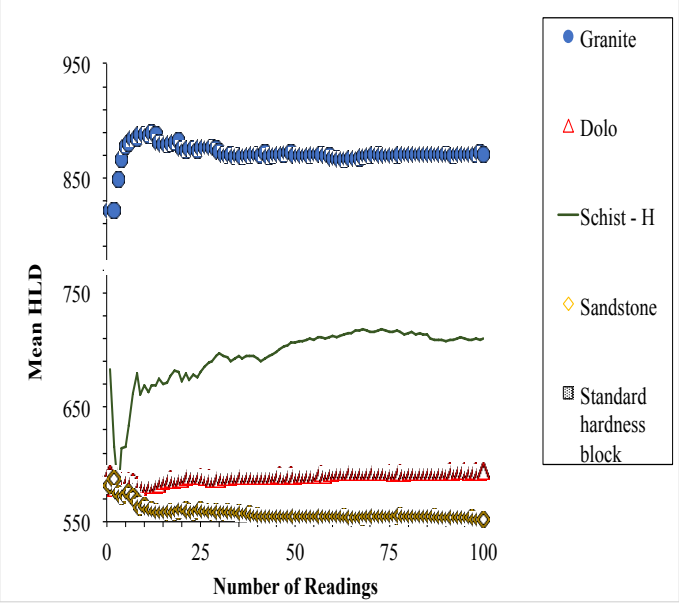

Figure 4.7 Number of readings versus Leeb hardness type D (HLD) values of granite, dolostone, H-Schist, V-Schist, sandstone and standard hardness block. One realization was picked for each tested rock.

The plots above show the steady increase of the five realizations (each one of them presents the different tested specimens) of randomized subset means for subset sizes ranging from 1 to 100, and inside the black box is the instability associated with limited sample size (e.g. 10 impacts).

4.1.2 Sample Size Effect Results

An understanding of the relationship between hardness value of the sample, and the size/geometry of the sample (e.g. core length) is necessary to determine the appropriate sample sizes that should be considered as a valid. Since there is no well-established procedure for the LHT in the rock engineering field, one of the main goals of this research was determining the sample size effect on HLD of a core sample of rock material. This could provide a very useful estimate of rock strength at the preliminary stage of engineering projects where limited core specimens are available in a project site. In practice, this case may face rock engineers very often in mining projects.

4.1.2.1 Results of Core and Cubic Size Effect

This section investigates the effect of sample size on HLD values and evaluates the correlation between the HLD and the specimen size. An experimental study was conducted on different sizes of Wallace sandstone, including cubic and core size, to quantify the sample size effect on HLD. In this experiment, 8 different sizes of core sandstone specimens were used. Table 4.3, illustrates the variation in HLD according to the core sample length of sandstone.

Table 4.3 Variation in HLD_L according to core sample length

HLD	Length (mm)	L/D ratio
325	9	0.17
386	10	0.19
489	21	0.39
506	38	0.70
522	76	1.41
533	102	1.89
538	152	2.81
551	190	3.52

All core specimens have been prepared with the same diameter of 54 mm (NX-size) and eight different lengths. In addition, four cubic specimens from the same sandstone block with different lengths were prepared (see section 3.1.3.1).

All hardness tests were conducted by using the LHT type "D". The results of these tests are presented in Table 4.14. Using the recommended hardness test methodology that was

proposed in this study, which is based on the investigated experiments, were conducted on core specimens to evaluate the number of readings (impacts) that comprise a valid test result. Of 12 single impacts, the highest and lowest HLD were excluded to avoid

observational errors, and the remain 10 got averaged and considered as the mean HLD of a core sample. The HLD values were then plotted against the size of core specimens. It is shown that the HLD values increase with the increasing of sample size until the HLD values become constant and the size sample no longer has any effect on HLD values. The HLD increases as sample length increases until reaching a minimum length to obtain consistent HLD value. It is noted that the HLD value for both core and cubic sizes increases non-linearly for the specimen length less than 10 cm, as shown in Figure 4.8. Thus, this is the minimum length of these specimens for valid HLD measurement. Figure 4.8 shows the results of the variation of the mean HLD as a function of the sample length. It shows an increase of the mean HLD as the length of the sample increases with a very good correlation with a positive power law. If the effect of sample size is neglected, the UCS will be underestimated. These finds support the observations in the previous studies of increasing HDL values with increasing the sample size until specific sample length (see section 2.5).

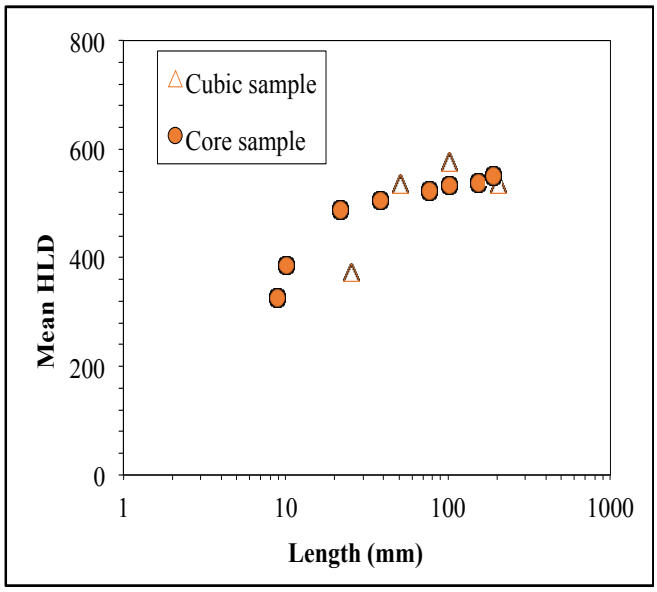

Figure 4.8 Non-linear increase of HLD with specimen length

Table 4.4. Leeb hardness values (HLD) for both cubic and core size.

Specimen Type	Dimension* (mm)	Specimen Volume (cm^3)	HLD
Core	9	20	325
Core	10	23	386

Specimen Type	Dimension* (mm)	Specimen Volume (cm^3)	HLD
Core	22	49	488
Core	38	87	506
Core	76	174.5	522
Core	102	233	533
Core	152	349	538
Core	190.5	436	551
Cube	25	16	373
Cube	51	131	534
Cube	102	1049	576
Cube	203	8390	535

*Length of 54 mm diameter core or cube side length

4.1.2.2 Results of Scale Effect for the Mean Normalized HLD

This subsection presents the results of the scale effect for the mean HLD normalized by the value of the standard length of 102 mm (101.6 mm, precisely) as a function of sample length that showed no effect of nonlinearly increasing on its hardness value. Here again, an increase in the value of the HLD as the length increases is observed. Figure 4.9 illustrates the influence of core sample length (HLD_L) related to standardized value (HLD_{102mm}). For specimen size correction of specimens less than L/D=1.5, the following formula is proposed:

$$HLD_L = 0.98\ L/D^{0.2} \times HLD_{102mm} \quad [5.1]$$

Table 4.13 shows the variation in HLD values according to the core sample length of sandstone and the L/D ratio.

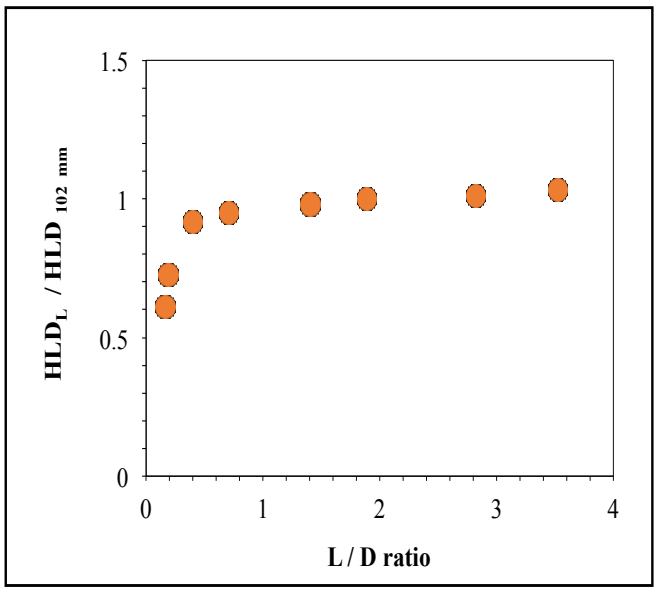

Figure 4.9 Influence of core sample size HLD_L related to HLD_{102mm}

In short, there is an observed nonlinear relationship between sample size and HLD below 1.5 L/D ratio and it was found to be constant above 1.5 L/D ratio. Small sample size could be corrected for, using the nonlinear relationship.

4.2 UCS TESTING RESULTS

This section contains the results of the UCS tests that were carried out on core specimens of different rock types, to corresponding HLD values, in which they used to evaluate the UCS and HLD correlation. The specimens include the following rocks: granite, dolomite, coal-sandstone, greywacke, limestone, and sandstone. The number of specimens that have been tested are as following: 10 schist, 3 granite, 3 dolostone, 4 coal sandstone, 3 greywacke, 3 limestone, 2 sandstones, 10 schist with horizontal foliation to load direction, and 6 Schist 2 Mafic dyke with vertical foliation to load direction. The total of 46 rock core specimens was tested at Dalhousie University. The UCS tests began in March 2015 and lasted until October 2015.

4.2.1 Schist Results

The UCS tests were performed on ten Schist specimens (Figure 4.10), after preparing the specimens according to the ASTM preparation procedure. The UCS test results ranged from 17 to 69 MPa. Young's Modulus (GPa) ranged from 4 to 11. The Poisson's ratio (ν), ranged from 0.2 to 0.3, as seen in Table 4.5. In Table 4.5, the mechanical properties of schist specimens are presented. In table 4.6, the geometric properties of schist sample are presented. The lithology description of the selected tested is given in Table 4.7. Table 4.7.1 shows the mechanical properties results of stress-strain curves of schist. Figure 4.11 shows some of the Stress–Strain curves of these core specimens. The rest of the stress-strain curves for schist rock were put in the Appendix B.

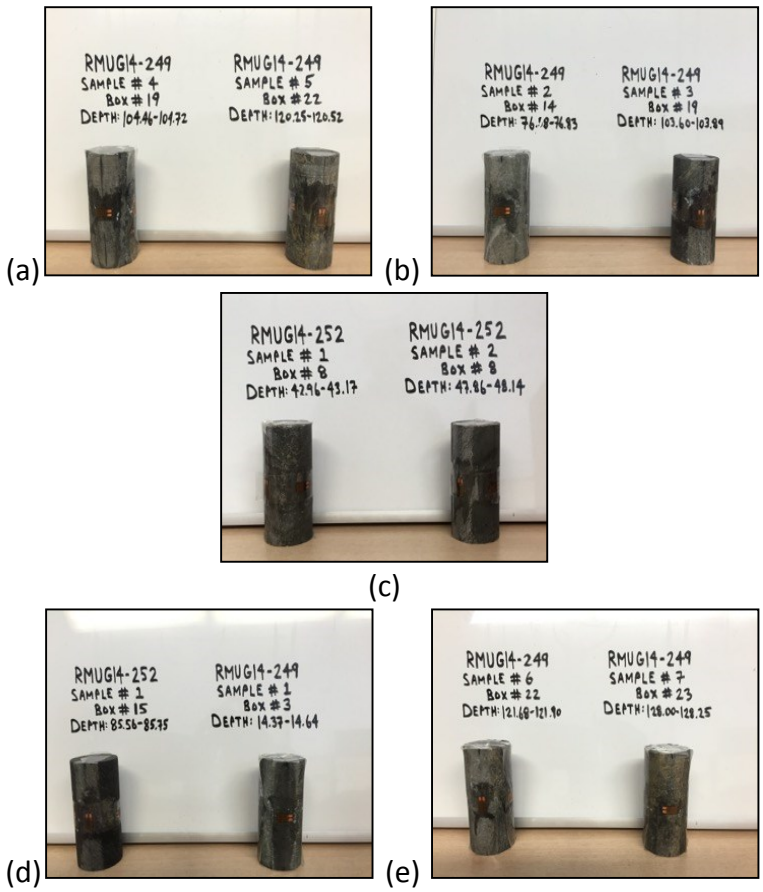

Figure 4.10 (a, b, c, d, e) Schist core specimens; the strain gauge pairs were installed at the opposite sides to measure the deformation caused by the UCS tests.

Table 4.5 Mechanical properties for schist specimens.

Hole #	UCS (MPa)	Force (kN)	Young's modulus (GPa)	Failure mode	Poisson's ratio, ν
RMUG14-252, Box-8, #1	43	44237	10	Structure	0.26
RMUG14-252, Box-8. #2	27	27374	5.5	Structure	0.24
RMUG14-252, Box-15, #1	17	17237	4.5	Structure	0.22
RMUG14-249, Box-3, #1	61	62806	5	Split	0.21
RMUG14-249, Box-14#2	38	39441	6.5	Split	0.22
RMUG14-249, Box-22, #5	69	70713	11	Split	0.20
RMUG14-249, Box-22, #6	27	28124	4	Structure	0.3
RMUG14-249, Box-23, #7	50	50927	7	Structure	0.21

Table 4.6 Geometric properties of schist specimens

Hole #	Length (Mm)	Dia (Mm)	L/D	Area (Mm2)	Weight (g)	Volume (Cm^3)
RMUG14-252, Box-8, 1	81	36	2	1027	243	83
RMUG14-252, Box-8, 2	80	36	2	1024	230	82
RMUG14-252, Box-15, 1	80	36	2	1026	233	82
RMUG14-249, Box-3, 1	80	36	2	1028	232	82
RMUG14-249, Box-14, 2	80	36	2	1029	229	83
RMUG14-249, Box-22, 5	80	36	2	1028	252	82
RMUG14-249, Box-22, 6	80	36	2	1027	248	83
RMUG14-249, Box-23, 7	80	36	2	1026	271	82

Table 4.7 Lithology for schist specimens.

Hole #	Lithology	Test type	Rock type	Foliation core Axis
RMUG14-252, Box-8. #2	Tzu- Sericite Schist	UCS	Schist	45
RMUG14-252, Box-15, #1	Tzu- Sericite Schist	UCS	Schist	45
RMUG14-249, Box-3, #1	Qtz- Sericite Schist	UCS	Schist	40
RMUG14-249, Box-22, #5	Qtz- Chlorite Schist	UCS	Weak-Moderate-Ore ZONE	45
RMUG14-249, Box-22, #6	Qtz- Chlorite Schist	UCS	Weak-Moderate-Ore ZONE	45
RMUG14-249, Box-23, #7	Qtz- Chlorite Schist	UCS	Weak-Moderate-Ore ZONE	35
RMUG14-252, Box-8, #1	Qtz- Chlorite Schist	UCS	Weak-Moderate-Ore ZONE	35

Table 4.7.1 Mechanical properties results of stress-strain curves of schist

Hole #	Sample number	Strain %	Area (mm2)	MR= E/UCS	Weight (g)	Axial strain %*10 at 50%	Lateral strain %*10 at 50%
RMUG14-252,Box-8	1	0.3	1027.37	232.24	243.33	0.4665	0.12
RMUG14-252,Box-8	2	0.2	1023.59	205.65	230.82	0.529	0.01
RMUG14-252,Box-15	1	0.2	1025.48	267.70	233.19	0.2555	0.02
RMUG14-249,Box-3	1	0.8	1027.56	81.80	232.16	0.506	0.10
RMUG14-249,Box-14	2	0.4	1028.88	169.56	229.18	0.651	0.06
RMUG14-249,Box-19	3	0.3	1027.75	207.18	224.11	0.2595	0.05
RMUG14-249,Box-19	4	0.1	1027.94	471.69	227.98	0.248	0.05
RMUG14-249,Box-22	5	0.2	1027.94	159.90	251.56	0.763	0.15
RMUG14-249,Box-22	6	0.4	1026.80	141.47	240.73	0.471	0.23
RMUG14-249,Box-23	7	0.3	1025.86	134.29	271.01	0.372	0.05

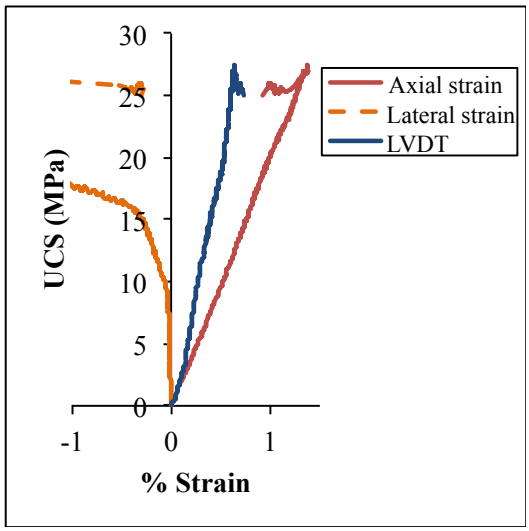

(a) RMUG 14-249, Box-22, sample 6

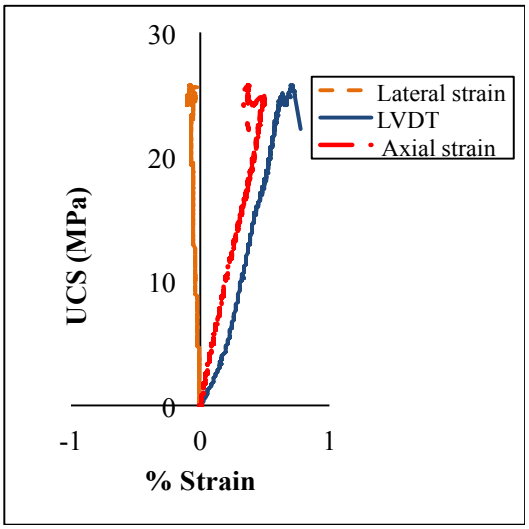

(b) RMUG14-249, Box-22, sample 5

Figure 4.11(a and b) Stress-Strain curves of schist specimens, using strain gauge and Linear Variable Differential Transformer (LVDT), which are transducers to measure the displacement for schist core specimens under UCS tests. LVDT is able to produce for small displacement.

*Note: The rest of the stress-strain curves for schist rock were put in the appendix.

Figure 4.12 Schist specimens with vertical schistosity (sv1, sv2, sv3, sv4, sv5)

Figure 4.13 Schist specimens with horizontal schistosity (sh4, sh5, sh6, sh7, sh8, sh9, sh10, sh11, sh12 and sh13)

Figure 4.14 Tested Schist specimens

4.2.2 Other Rocks

The UCS tests were carried out on a number of core specimens. The condition of these specimens before UCS testing is presented in a table with some comments (attached to Appendix 2). The description of Schist specimens after preparation is showed in a table (attached to Appendix 2). As a result of these tests, the UCS was ranged from 27 to 220 MPa. Some specimens showed shear failure mode, others showed an axial splitting. The Young's Modules were ranged from 5 to 21 MPa, (see Appendix 2). The geometric details of tested specimens are given in a table (attached to Appendix 2).

4.3 Chapter Summary

This chapter presented the results of laboratory experiments that were conducted on different rock types to develop methodology and correlation for UCS. The results of the laboratory experiments include the UCS tests and the LHT. These two tests help to develop a Leeb test methodology by evaluating the number of impacts that give a valid test, and examine the sample size effect on HLD for both core and cubic specimens of rock material. In addition, these tests help to develop correlation for UCS. The following correlations were presented: the correlation between the HLD and the specimen size, the correlation between the HLD and the specimen length, and the correlation between the HLD and the L/D ratio. Moreover, the plots of impact readings versus LHD values for tested specimens were presented with confidence intervals. This could provide a useful estimate of rock strength for engineering projects.

CHAPTER 5 ANALYSIS

Some scholars of rock engineering agree on the potential in studying and understanding the relationship between the UCS results and the Leeb hardness for intact rocks. Recently, many research studies, have demonstrated that the impact-rebound method has some correlation to UCS. However, there has been no universal correlation established for all rock types.

In order to increase confidence in an estimation parameter, it is important to analyze the same measurements that were conducted many times in different experiments. The greater the statistical strength (i.e. more measurements) the better the UCS estimate will be. Taking multiple measurements also allows one to better estimate the uncertainty in UCS measurements by checking how reproducible the measurements are. How precise UCS estimates of rock material are depends on the spread of the measurements (standard deviation) and the number (N) of repeated measurements that were taken. Therefore, statistical analysis is required to have a more sophisticated estimate of the uncertainty in the UCS measurement.

The main purpose of this study is to develop an understanding regarding the relationship between HLD and UCS. In order to develop such a relationship, one that can be used in the field, the evaluation of UCS-HLD correlation needed to be performed, and the results needed to be analyzed on a statistical basis. This provides a convenient means to obtain improved accuracy in field estimation of UCS. For that reason, this chapter contains a discussion of analysis. Included in this chapter are required statistical measurements on the database, which were collected from a thorough literature review and the results of laboratory tests. This is done in order to determine how well the regression line fits the; such values as (R^2) and the S are considered, and then the correlation of UCS-HLD is plotted to establish an equation relating the relationship between UCS and

HLD. In addition, the three main rock types are analyzed in subsections and the plot of UCS-HLD correlations are presented. This chapter ends with Leeb hardness analysis and comparison between HLD and Schmidt Hammer. The final section in this chapter reviews a conference paper studying sandstone (attached to the Appendix A). Statistical analysis (Regression, T-Test, F-Test and residual) has been used to develop the relationship between the mean value of hardness tests and their corresponding rock strengths to improve the LHT procedure. Then, the plots of UCS-HLD correlations were presented.

5.1 UCS–HLD CORRELATION

In order to quantitatively analyze and develop the relationship between HLD values and UCS, regression analyses were used. There are different curves, such as linear, logarithmic, power and polynomial, which can be used to study the correlation between the independent and dependent variables. The coefficient of determination (R^2), which is produced by the best-fit curve, is the measure of the variability proportion of one variable to the other variable (Sheskin, 2000). Once the regression best-fit curve and the value of R^2 have been determined, an examiner will then pick which best curve fits in the appropriate way. Usually, the most appropriate curve is the one with the relatively highest R^2 value. Based on the literature review, the exponential curve is expected between UCS, and HLD.

5.1.1 Database

A database was developed from the literature review (Table 5.1), BGC Engineering project files (provided by D Kinakin, pers. comm.) and the results of laboratory tests carried out as part of this study. The developed database and the results of laboratory tests were then verified. They cover a wide range of the UCS values of rock material from around the world. This will help to establish how accurately the UCS of rock material could be obtained by using a portable LHT.

Two statistical analysis models were performed in order to find the best correlation with the lowest S, which is a useful measure to assess the accuracy of the predictions. The first analysis is modeled by a power function; the second one is modeled by an exponential function. The curve was selected based on previous knowledge from the literature about the response curve's shape between UCS and HLD. The power model in Table 5.3 showed a slightly lower S with an R^2 of 0.70. These analyses were performed using the Minitab software (Ryan et al., 2004).

Figure 5.1 shows the relationship between HLD, and UCS for specimens tested both in the present study and collected from the literature. Such a large scatter of as seen in Figure 5.1 could be attributed to variation in Young's Modulus in specimens that have the same UCS value and rock conditions. In spite of the scatter in, there is a tendency for HLD to increase with increasing UCS. The points cover a wide range of UCS values, ranged from 3 MPa (green schist, Kawasaki et al., 2002) to 285 MPa that were observed in metavolcanic rocks. These values represent the wide practical range found in the field.

The HLD and UCS proposed correlation of previous studies were presented in Figure 5.2. The comparison between UCS-HLD improved database correlation and the correlation proposed by Verwaal & Mulder (1993) are presented in Figure 5.3. The proposed correlation in this study showed R^2 of 0.70 based on 311 UCS tests, while a proposed correlation suggested by Verwaal & Mulder (1993) showed R^2 of 0.77 based on only 27 UCS tests.

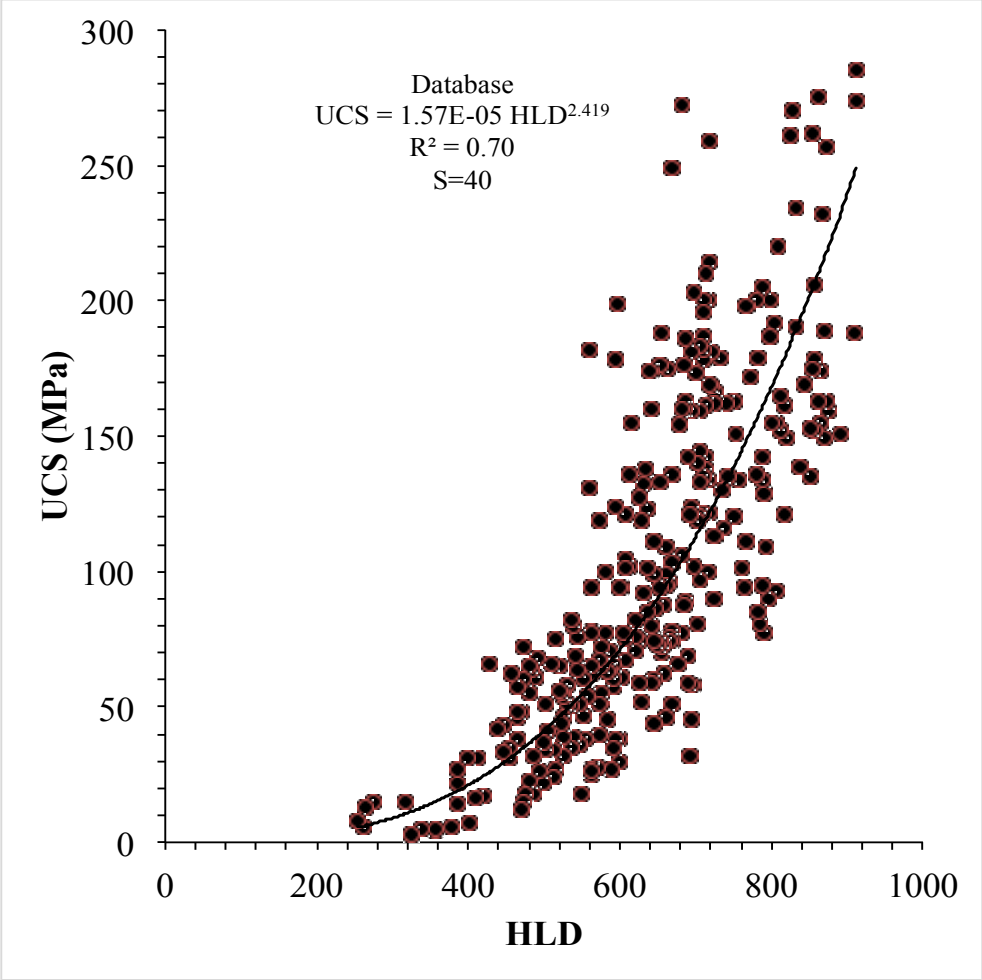

Figure 5.1 UCS-HLD correlation of the developed database.

Table 5.1 Description of rock specimens and number of tests from previous studies using the Leeb hardness test (LHT) that were used to develop the database

Source	Number of tests	Rock type
Verwaal and Mulder, 1993	27	Sandstone, limestone gypsum, dolostone, marble, granite, calcarenite
Hack et al 1993	15	Sandstone, granite, Limestone
Asef, M, 1995	63	gypsum, gypsum and silty clay, conglomerated, sandstone, dolomitic calcilutite, limestone muds-calcilutite, sandy clay, dolomitic breccia, limestone calcarenite layers, granodiorite, thinly bedded dolomite, calcilutite

Meulenkamp and Grima, 1999	32	mudstone, sandstone, limestone, granite, granodiorite
Kawasaki et al., 2002	31	greenschist, shale, sandstone, granite
Aoki and Matsukura, 2007	9	granite, gabrro, sandstone, andesite, Tuff, limestone
Lee et al, 2014	48	laminated Shale
Present study, 2016	31	schist, sandstone, granite, dolostone, limestone, graywake
BGC (confidential project files)	7	mafic volcanic, granite, felsic dyke
BGC (confidential project files)	10	porphyry, hornfels
BGC (confidential project files)	6	diorite
BGC (confidential project files)	13	metavolcanics
BGC (confidential project files)	9	limestone
BGC (confidential project files)	3	sandy siltstone, siltstone
BGC (confidential project files)	7	intrusive, sandstone, porphyry, conglomerate

Table 5.2 Descriptive of test procedure and coefficient of determination (R^2) were used in previous UCS - HLD correlations.

Author	Years	Impact device	R^2	Test procedure
Verwaal and Mulder	1993	D	0.77	10 single impacts
Hack et al	1993	D	0.77	Multiple impacts
Meulenkamp and Grima	1999	C	0.81	NF*
Aoki and Matsukura	2007	D	0.77	10 single impacts
Viles et al	2010	D	NF	50 impact readings
Daniels et al	2012	NF*	0.77	10 out 12 single impacts
Yilmaz	2013	D	0.82	20 single impacts

Author	Years	Impact device	R^2	Test procedure
Coombes et al	2013	D	NF*	10 single impacts
Lee et al	2014	D	0.81	10 single impacts

*NF is information not found

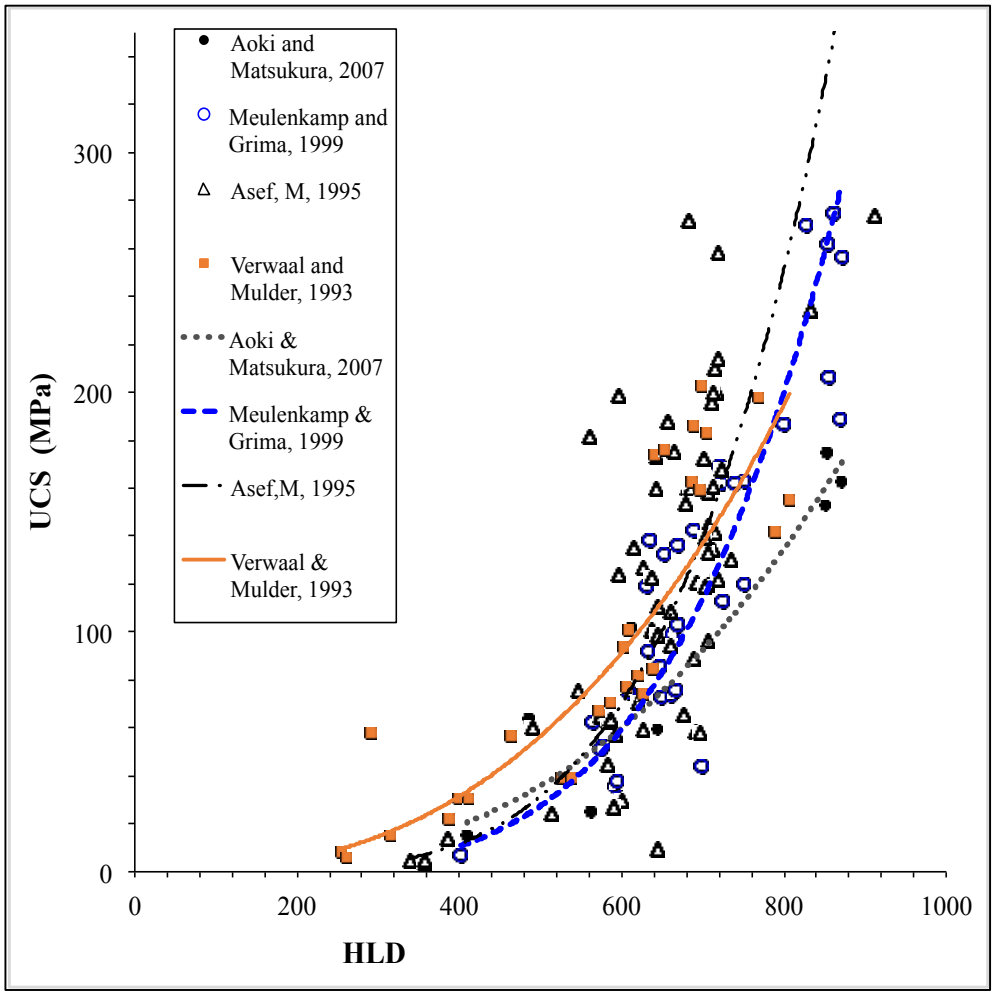

Figure 5.2 HLD and UCS proposed correlation from previous studies.

To test the models, an analysis of variance was conducted. Parameters for the analysis of variance for two models are given in Table 5.3. Since the power model had lower S, it is concluded that this model better represents the than exponential model.

In this study, an exponential model of the set was selected. Using information from the literature about the shape of the response curve and the behavior of the physical properties, an exponential growth curve was selected with the following expected function form for one parameter (UCS) and one predictor (HLD):

$$\mathbf{UCS} = \boldsymbol{\theta}_1 \times \boldsymbol{e}^{(\boldsymbol{\theta}_2 \times \mathbf{HLD})} \quad [5\text{-}1]$$

Where the θ_1 and θ_2 represent fit parameters and HLD represents the predictor. The trend expressed by the nonlinear model is described as:

$$\mathbf{UCS\ (MPa)} = \mathbf{3.1335\ EXP}^{\mathbf{0.0051\ HLD}} \quad [5\text{-}2]$$

The R^2 coefficient of 0.67 reflects the degree of scatter in the database. This shows UCS can be predicted with a reasonable degree of accuracy using the HLD. S was used to assess how well the regression model predicts the response between two models (Table 5.3). The lower the value of S, the better the model predicts the response (UCS). In order to compare the two prediction models, the following statistical performance indexes were used: The S, SSE, and MSE (see 3.2.2.1).

Comparing the exponential model to the power model, it is observed that the power model equation has the lowest S value which indicates the best fit. For the power model, S is calculated as 40, which indicates that the actual points are within a standard difference of 40 MPa (UCS) from the regression line which represents the predicted value (Table 5.3).

Table 5.3 Statistical analysis of two models were conducted on the database.

Statistical Model	Exponential	Power
Correlation Equation	UCS= 3.134 $Exp^{0.0051\ HL}$	UCS= 1.57E-005 $HL^{2.419}$
R^2	0.67	0.70
SSE	669989	500926
MSE	2154	1621
S	46	40

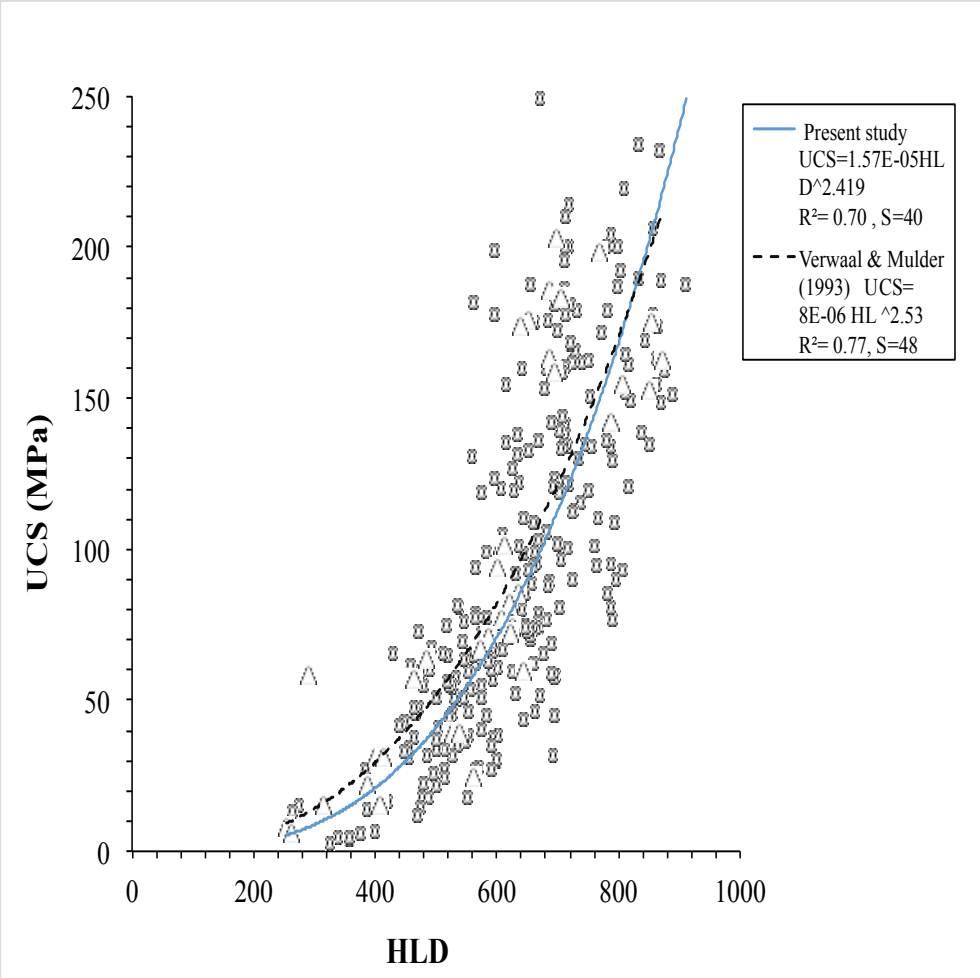

Figure 5.3 Comparison between UCS-HL database correlation and the Verwaal and Mulder (1993) results.

Table 5.4. Correlations by other authors

Source	Reported Best Fit Equation*	Number of Points in study	R^2 from author's dataset	S from pervious studies	S from presented dataset
Meulenkamp (1997)	$UCS=1.75 \times 10^{-9}$ $RHN^{3.8}$	194	0.806	46	40
Verwaal and Mulder (2000)	$UCS= 4.906 \times 10^{-7}$ $RHN^{2.974}$	28	--	48	40
Lee et al (2014)	$UCS= 2.3007e^{0.0057RHN}$	62	0.8235	58	40
Lee et al (2014)	$UCS= 2.1454e^{0.0058RHN}$	62	0.8093	59	40
Lee et al (2014)	$UCS= 3.7727e^{0.005RHN}$	62	0.7799	50	40
Yilmaz (2013)	UCS= 4.5847 ESH-142.22	18	0.674	-	-
Aoki and Matsukura (2008)[2]	$UCS= 8 \times 10^{-6}$ $RHN^{2.5}$	33	0.77	43	40
Aoki and Matsukura (2008)	$UCS= 0.079$ $e^{-0.039n}$ $RHN^{1.1}$	33	0.88	-	-
Meulenkamp and Grima (1999)[3]	UCS= 0.25RHN + 28.14(density) - 0.75(porosity) - 15.47(grain size) - 21.55(rock type)	33	0.9	-	-

[1] Terms used for Leeb Hardness (HLD) in original source study: Equotip Shore Hardness (ESH), Rebound Hardness Number (RHN), porosity (n).
[2] This equation was developed and reported by Aoki and Matsukura (2008) based partly on the set reported by Verwaal and Mulder (1993). As a result, this equation is sometimes referred to as the 1993 Verwaal and Mulder equation.
[3] This equation was developed using artificial neural network statistical methods where numerical values were used for the coefficients: density, porosity, grain size, and rock type.

Table 5.4 shows the S for these proposed equations that are high for the reliable UCS estimates for engineering projects. The reliabilities of these equations were assessed on the basis of S. S is used widely in comparisons between statistical models and its measurement is similar to σ. When the value of S approaches zero, the predicted values from the correlation equation are closer to the estimated values.

5.1.2 Three Rock Types

This section further develops a LHT procedure that can be used for field evaluation of UCS, to correlate UCS with HLD, which is the main point of this study, thereby providing a convenient means to obtain improved accuracy in the field estimation of UCS. This section contains a discussion of the analysis that was conducted on the three main rock types (igneous, metamorphic and sedimentary), collected from literature review and the results of laboratory tests which cover a wide range of the UCS values of rock material around the world, to establish how accurately the UCS of three rock types could be obtained by using a portable HLT.

Figure 5.4 demonstrates a comparison of HLD measured between three rock types. Even though these rock specimens are from the same designation of rocks (igneous), there is considerable scatter between the UCS values for each specimen. This could be attributed to variation in cementing material and mineral hardness. The shapes of the UCS-HLD curves are similar in each rock types, as shown in Figure 5.5.

Igneous specimens have HLD ranging from 409 to 911 HL with a UCS of 16 (Tuff, a porous rock, Aoki and Matsukura, 2007) to 275 MPa, (granodiorite, Meulenkamp and Grima, 1999). Sedimentary rocks have HLD that range from 255 to 833 HL, with UCS values of 4 (gypsum and salty clay) to 220 MPa, (greywacke). Metamorphic specimens have HLD ranging from 265 to 912 HL with UCS values of 3 for greenschist, as determined in Kawasaki et al (2002), and 285 MPa, (metavolcanics).

Figure 5.5 presents the correlation equations of all three rock types, with R^2 values. In general, there is an increase in UCS with increasing HLD, despite the fact that the specimens used to develop the relationship are differentiated by formation sites and weathering. The best-fit regression lines were plotted for the UCS-HLD correlation of all rock types, and are presented in figure 5.6. The R^2 value for the sedimentary rock is 0.71, and 0.83 for the metamorphic rocks. For igneous rocks, however, the R^2 value (0.56) is not

high. As seen in Figure 5.7, there are scattered around the best-fit curve; therefore, it could be said that the R^2 value is unreliable (see Table 5.5).

It was observed that there was one anomalous UCS value, (285 MPa), which is the sample of metavolcanics. In general, igneous rocks have a high UCS value relative to other rock types.

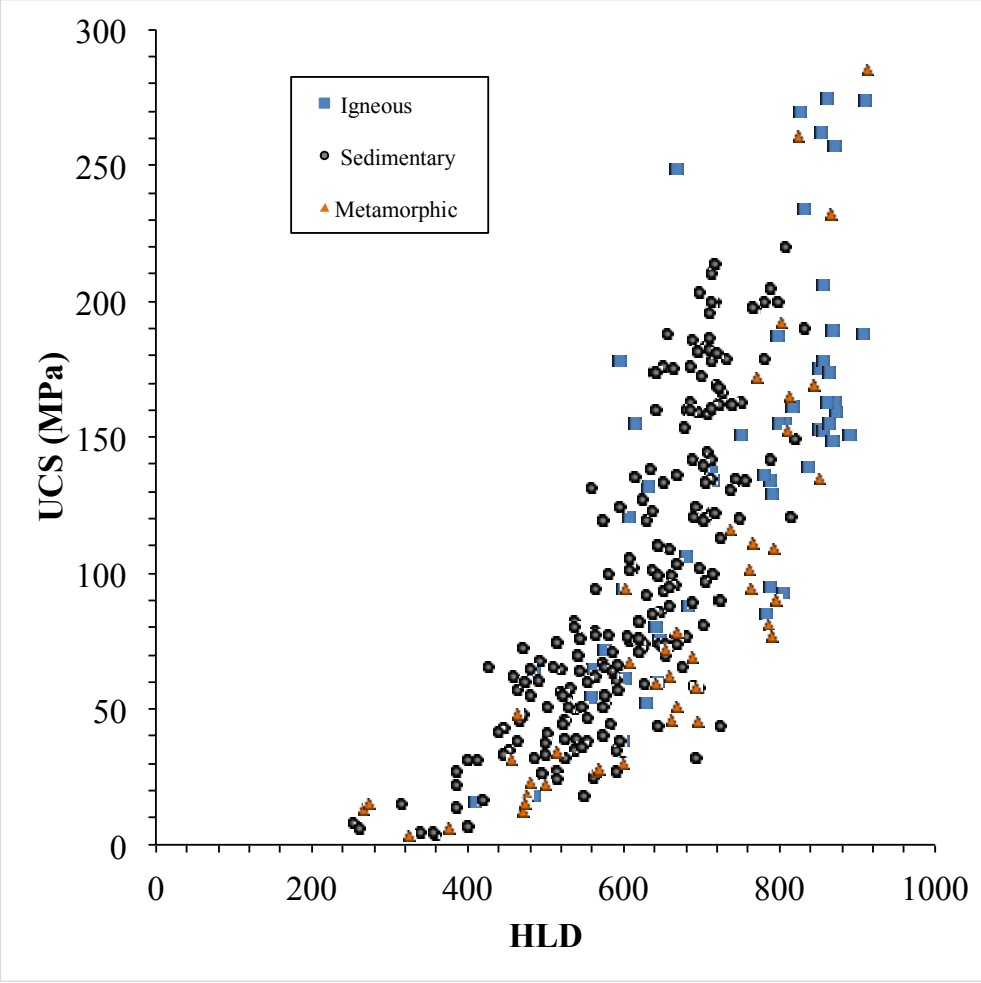

Figure 5.4 Comparison of three rock types (igneous, metamorphic, sedimentary)

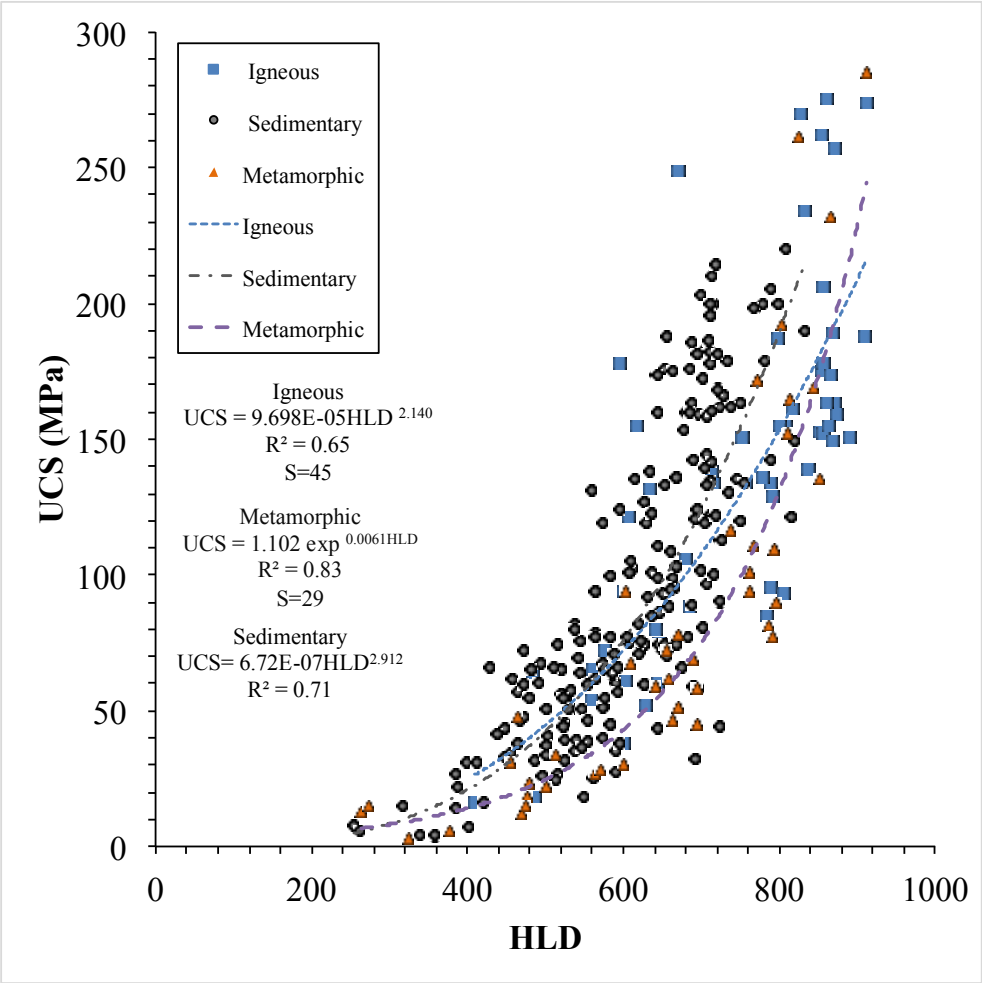
Igneous
Sedimentary
Metamorphic
Igneous
Sedimentary
Metamorphic
Igneous
UCS = 9.698E-05HLD 2.140
R² = 0.65
S=45
Metamorphic
UCS = 1.102 exp 0.0061HLD
R² = 0.83
S=29
Sedimentary
UCS= 6.72E-07HLD2.912
R² = 0.71
UCS (MPa)
HLD
0
50
100
150
200
250
300
0
200
400
600
800
1000

a)

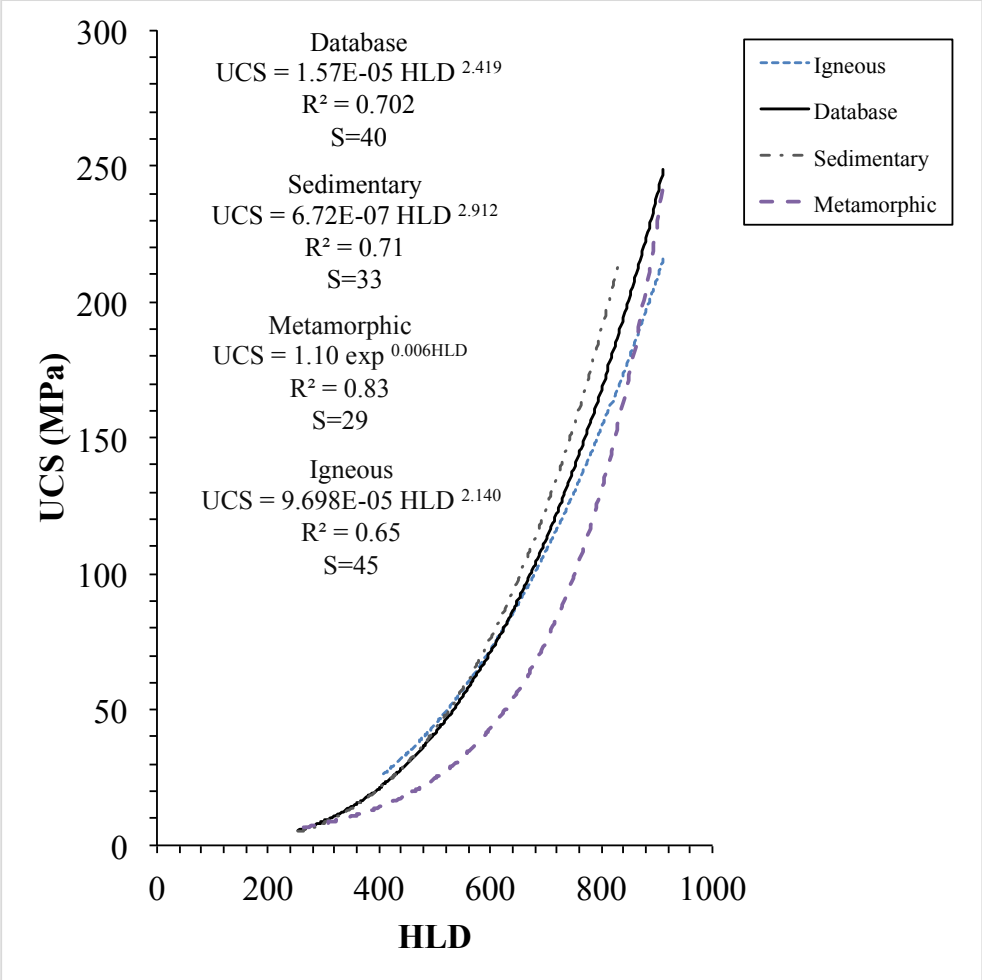

b)

Figure 5.5 (a, b) Three rock types proposed correlations compared with the proposed database correlation.

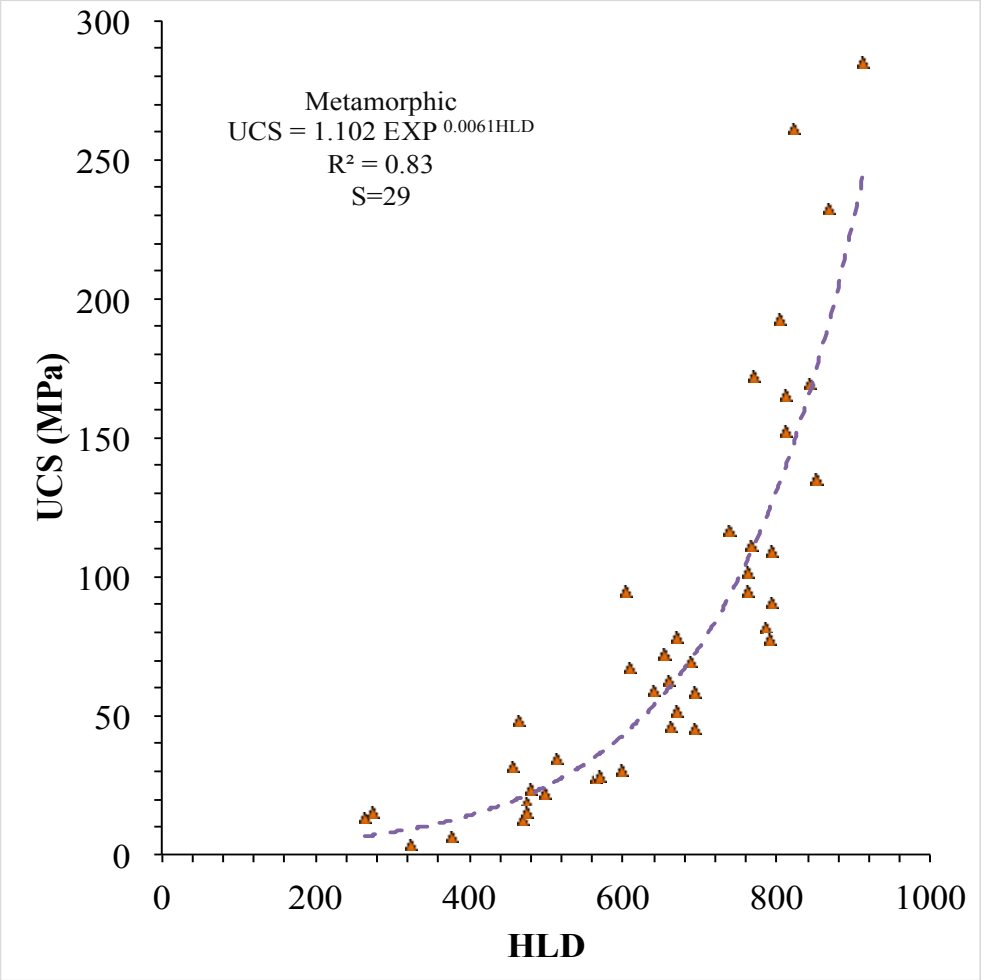

Figure 5.6 Metamorphic rocks proposed correlation

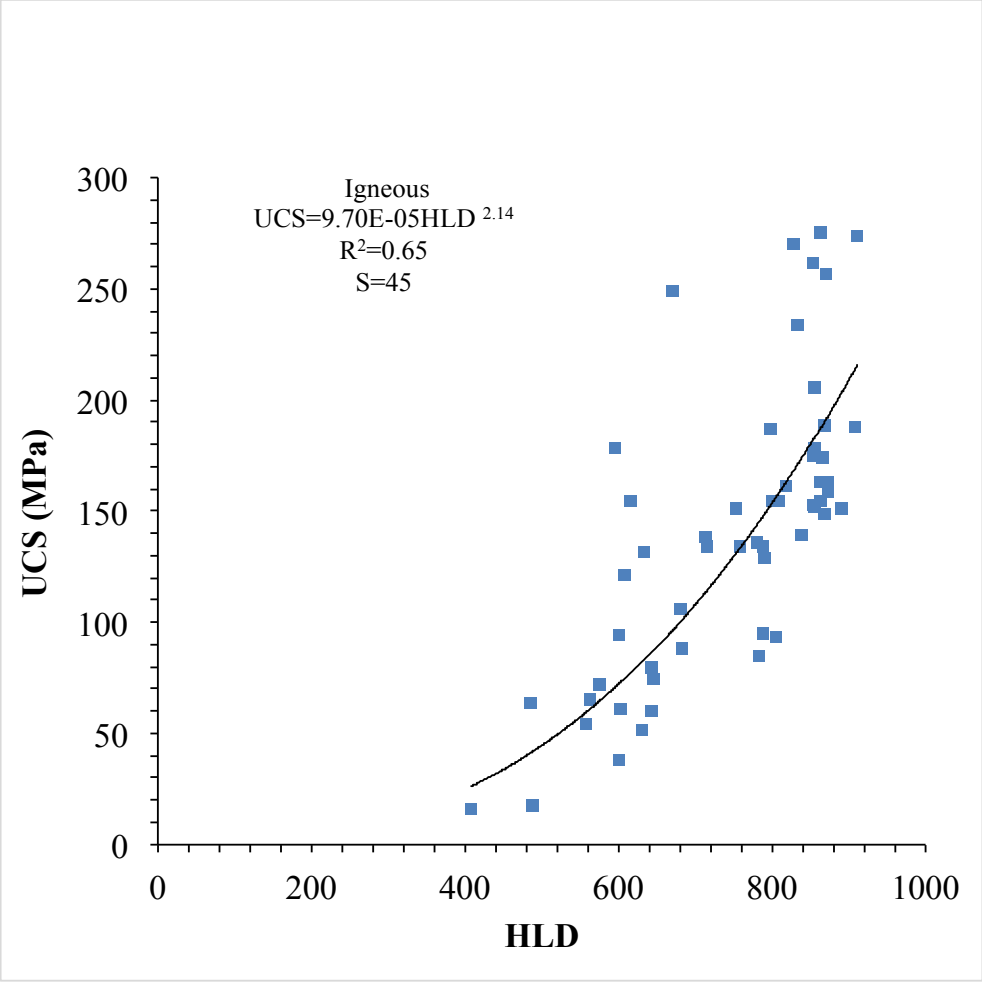

Figure 5.7 Igneous rocks proposed correlation

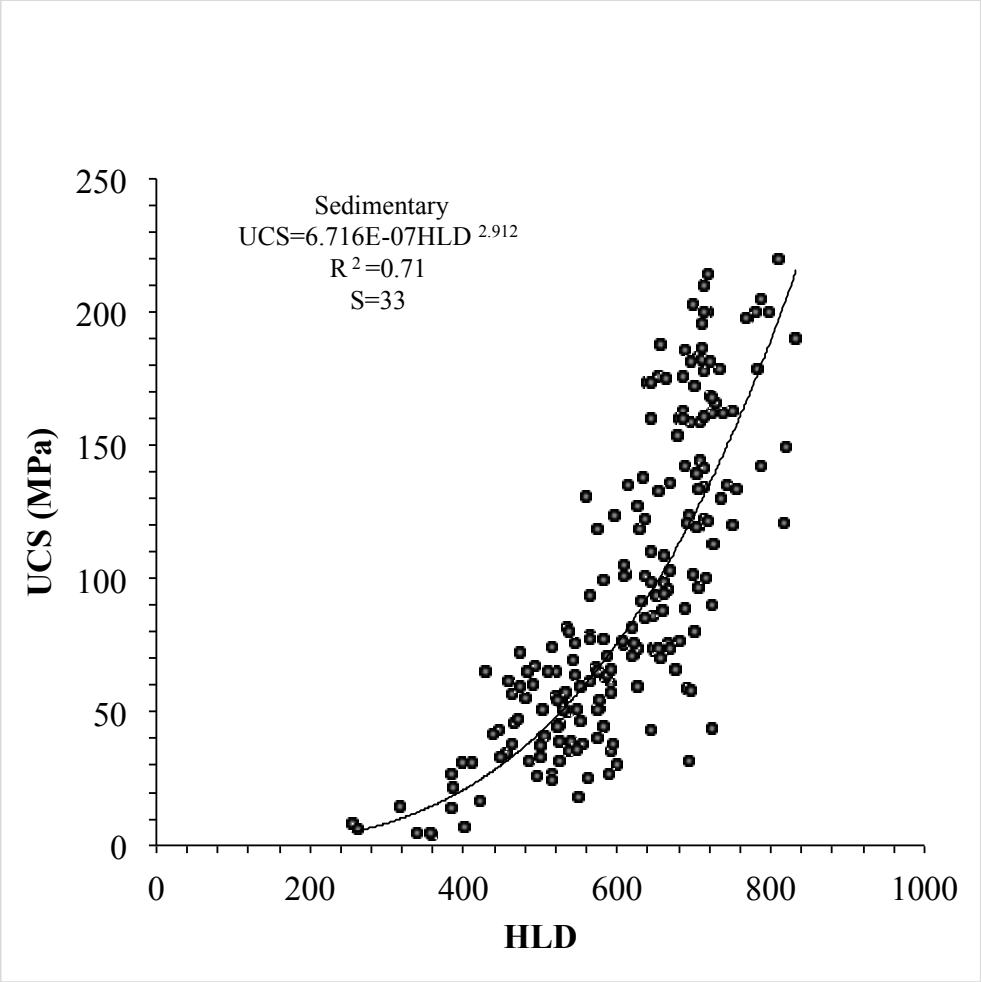

Figure 5.8 Sedimentary rocks proposed correlation

Table 5.5 Proposed correlation equations with coefficient of determination (R^2) in present study.

Rock Type	Recommended Equations	R^2
Presented database	UCS= 1.57E-05 HLD $^{2.419}$	0.70
Rock Classification		
Sedimentary	UCS= 6.72E-07 * HLD$^{2.91}$	0.71
Metamorphic	UCS= 1.102 EXP $^{0.0061HLD}$	0.83
Igneous	UCS= 9.70E-05 HLD $^{2.14}$	0.65
Specific Rock		
Sandstone	UCS= 9E-07 HLD $^{2.839}$	0.75
Limestone	UCS= 8E-07 HLD $^{2.896}$	0.50
Schist	UCS= 6E-06 HLD $^{2.479}$	0.73

Table 5.6 Leeb Hardness (HLD) and UCS correlation parameters.

Set	R^2	Equation Coefficients	
		a	b
All rock types	0.70	0.3	3
Sandstone	0.75	0.9	2.84
Sedimentary Rocks*	0.71	0.1	3.18
Metamorphic Rocks	0.79	0.3	2.98
Igneous Rocks	0.65	3	2.64

*Including sandstone

Table 5.7 presents the statistical analysis for HLD values of the 3 rock types, including from the proposed database. It can be seen that the metamorphic rocks showed a higher σ compared to the other rock types. This could be due to the existence of foliation in metamorphic rocks. Metamorphic rock texture could be foliated or nonfoliated; nonfoliated ones are usually uniform in texture, and contain only one mineral.

Table 5.7 Statistical analysis for LHD of three main rock types including proposed database.

Rock type	Sedimentary	Metamorphic	Igneous	Database
Mean	610	645	745	639
Standard deviations	110.5	167	127	132
Confidence interval at95%	15	50	34	15
Number of sample	209	43	55	311

5.2 Leeb Hardness Analysis

As evidenced by this study, HLD shows a reasonable correlation with UCS. Table 5.8 provides a classification of HLD that was generated for classifying the HLD values based on analyzing the presented study database. It provides a useful basis for classifying HLD and

for giving a clear relation to a rock's character. Table 5.9 illustrates the proposed uncertainty by the mean of the confidence limits for HLD value. These tables could be used to describe rocks, and thus they could contribute to classifying the HLD and provide a basic information of hardness of different rocks, thereby allowing them to be easily compared with other types of rock. In addition, they could help to appropriately obtained from the field for design purposes.

Table 5.8 ISRM Suggested Method – Equivalent Leeb Hardness (HLD)

		HLD range by rock type				
Grade	UCS (MPa)	All types	Sandstone	Sedimentary	Metamorphic	Igneous
R0	0.25 – 1	94 – 149	83 – 134	103 – 159	97 – 154	73 – 124
R1	1 – 5	149 – 255	134 – 237	159 – 264	154 – 265	124 – 227
R2	5 – 25	255 – 437	237 – 418	264 – 437	265 – 455	227 – 418
R3	25 – 50	437 – 550	418 – 533	437 – 544	455 – 574	418 – 544
R4	50 – 100	550 – 693	533 – 681	544 – 676	574 – 724	544 – 707
R5	100 – 250	693 – 941	681 – 940	676 – 902	724 – 985	707 – 1000
R6	>250	>941	>940	>902	>985	>1000

Table 5.9 Uncertainty of Leeb Hardness values for different rock types

	95%	90%	80%	STD	Number of sample
Rock type	±	±	±		
Schist	61	52	40	159	27
Limestone	22	19	14	79	52
Metamorphic	51	43	33	167	43
Sedimentary	15	13	10	110	209
Igneous	34	29	22	126	55

5.3 Comparison between HLD and Schmidt Hammer

The rock strength estimation by non-destructive hardness test methods is of great interest to mining and civil engineers' projects. The LHT and Schmidt hammer are the most commonly used methods for non-destructive testing of rock since the 1960s, due to their easy handling and cost effectiveness (Figure 5.9). They can be performed in either the laboratory or the field to provide preliminary of the material being investigated. The mechanism of the Schmidt hammer operation is quite simple (see 2.3.2). Despite the consistency of the Schmidt Hammer test, a number of factors affect measured values, which include calibration of the instrument, irregularities of a surface, weathering state, adjacent discontinuities, moisture content, size sample, edge effects, impacts destination, and orientation (Buyuksagis & Goktan, 2007).

The EHT has been found to be applicable to rocks in the range of 5–280 MPa (Grima & Babuška, 1999). Therefore, it is suitable for applications across a wider range of rock hardness than the Schmidt hammer (Aoki and Matsukura 2007). The principle of measurement for the LHT uses a slightly different approach (see 2.3.3).

Figure 5.9 Comparison between Leeb hardness tester (LHT) and Schmidt hammer, type R

Before examining the compatibility of the two hardness testers, a brief comparison was done (see Table 5.10). It is clear that the LHT is more convenient than the Schmidt hammer. As demonstrated in Figure 5.9, the LHT covers a wide range of UCS values. This is indicative of a better practical use of the LHT in fieldwork.

Table 5.10 Details on Leeb Hardness tester in comparison to Schmidt Hammer (type N).

Hardness Tester	Schmidt Hammer type N	Leeb Hardness Tester
Impact energy (Nm)	2.207	0.011
Length (cm)	30	15.5
Weight (kg)	1.52	0.166
Impact direction	90°	360°
Minimum thickness (mm)	100	5
UCS (MPa) range	10- 70	3-285
Impact plunger diameter (cm)	1.5	0.5

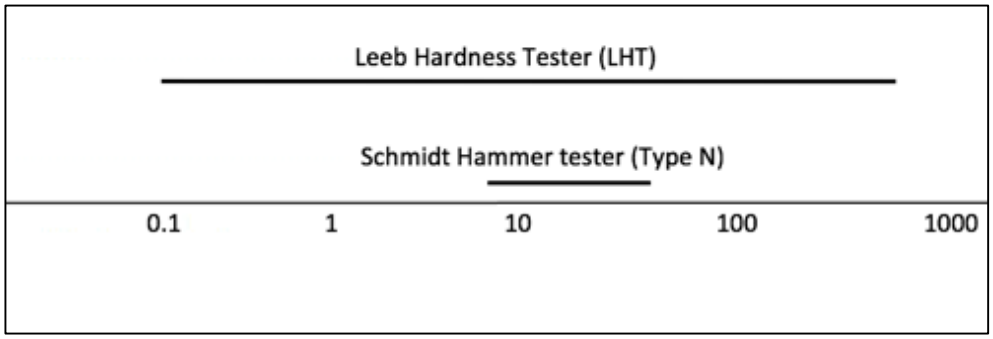

Figure 5.10 Measurement range of Leeb hardness tester (LHT) and Schmidt hammer type N (after Aoki& Matsukura, 2007).

To examine the compatibility of the two testers, an experimental performance investigation was performed in order to compare the prediction capabilities of both testers. In order to compare the capabilities of both devices, the block of sandstone was prepared to conduct the hardness test with a length of 35 cm., and a 23 cm. thickness. In addition, a core

sandstone sample was extracted from the block and then prepared to be tested by the UCS test to get its UCS value (Table 5.11). After having the UCS value, hardness tests were performed on the block sandstone in order to measure its rebound hardness by using the LHT and Schmidt hammer. The ASTM recommended hardness method (ASTM D5873) was used to calculate the Schmidt hammer number, which is an average of 10 readings, excluding more than 7 units offset.

Table 5.11 Details of core Sandstone sample.

Core Sandstone	
Properties	Value
Length (mm)	122
L/D ratio	2.3
Weight (g)	646
Load (kn)	139
Actual UCS (MPa)	61
Area (mm^2)	2289
Diameter (mm)	54

The hardness test results are presented in Table 4.14. A comparison study was conducted by using the values of rebound hardness with the proposed sandstone equations from previous studies and a general equation, as well. This allows for comparison between the estimated UCS and actual UCS of sandstone (60 MPa) according to proposed correlation equations using a Leeb Hardness value of 532 HLD, and a Schmidt hammer number value of 50 (Table 5.13 and 5.14). In Table 5.14, the lack of Schmidt hammer sensitivity leads to different predicted UCS values. The average of 20 impact readings (Table 5.12), for the Leeb hardness values was 531.55 HLD, while it was 50 for the Schmidt hammer number.

Table 5.12 Rebound Hardness values of Leeb Hardness Test (HLD) and Schmidt Hammer Test (R) on Sandstone Block.

HLD	R
566	44
487	46
530	48
535	50
523	52
554	48
523	50
544	54
556	46
524	50
488	48
530	52
570	50
526	54
481	50
530	52
560	48
528	54
530	52
546	52

Table 5.13 Comparison between estimated UCS and actual UCS of sandstone (60 MPa) using the proposed correlation equations in this study.

Estimated UCS (MPa)	UCS Equation with "HLD" value	Researcher	R	Lithology
49	UCS= 9E-07HLD $^{2.839}$	Present Study, 2016	0.72	Sandstone
57.5	UCS= 6.72E-07 * HLD$^{2.91}$	Present Study, 2016	0.7	Sedimentary
61.64	UCS= 1.57E-05HLD $^{2.419}$	Present Study, 2016	0.7	Varied
52	UCS= 8*10^{-6}*HLD $^{2.5}$	Aoki &Matsukura, 2008	0.77	Varied

Table 5.14. Comparison between estimated UCS and actual UCS of Sandstone (60 MPa) according to proposed correlation equations using Leeb Hardness value of 532 HLD, and Schmidt hammer number (R) of 50.2. The ASTM standard method was used to calculate the Schmidt hammer number.

Estimated UCS (MPa)	UCS Equation with "R" value	Researcher	R	Lithology
58.60	UCS =0.308R1.327	Sapporo et al (2013)	0.9	Sandstone, mudstone
104.4	UCS = 2R	Singh et al (1983)	0.72	Sandstone, mudstone
63.8	UCS=2.208e0.06R	Katz et al. (2000)	0.96	Sandstone, Limestone
49.5	UCS= 0.994R-0.383	Haramy&DeMarco, 1985	0.87	Sedimentary

5.4 Chapter Summary

This study has proposed to develop a correlation between the HLD and UCS by rock types, which could become a significant application for rock engineering practices. In order to propose a relationship that can be used in fieldwork, a field evaluation of the potential UCS-HLD correlation was performed, and a statistical analysis was conducted to analyze the results. This method provides a convenient means to obtain improved accuracy in the field estimation of UCS. Statistical measurements on the database were collected from the literature review and the results of laboratory tests to determine how well the regression line fits the database. Then, the UCS-HLD correlation was plotted to establish an equation relating UCS (MPa) and HLD. In addition, the three main rock types were analyzed and the plot of UCS-HLD correlations were presented.

Collected HLD values were classified based on three rock types, and a link between these classifications as well as rock strength grades established by ISRM has been proposed, the degree of uncertainty was also presented. The results of a comparison between two rebound hardness devices the LHT and Schmidt hammer were presented.

CHAPTER 6 CONCLUSION and RECOMMENDATION

Currently there are neither agreement on one prediction model that can predicate the UCS using LHT nor well-established procedure for LHT in the rock engineering field. Therefore, this study proposed a correlation of LHD with UCS to fill the gap of the limited precision and reliability of ISRM field estimate for estimating the strength of intact rocks or other indexing methods. Moreover, this study aimed to develop an understanding of the confidence associated with the number of impacts per test and the sample size effect on hardness values, and aimed to recommend a testing procedure based on the results. This could be used to appropriately obtain from the field for design purpose.

To get a reasonable measure of the representative hardness of a rock, the LHT methodology was examined by quantifying the sample size and the number of Leeb impacts. This was achieved by examining the number of impacts required for a valid test and the effect of sample size on the measured hardness value. The study proposed that there are minimal gains for extra tests beyond 10 impact readings to perform the LHT. In the study procedure, a trimmed mean was used where 12 readings were taken and the highest and lowest values were removed, and the remaining 10 impacts were averaged in a "test" result. This was observed to provide a more accurate basis for UCS determination. In addition, a nonlinear relationship between specimen size and HLD below 100 mm exists; however, results were relatively constant above 100 mm, indicating that this is the critical specimen length for the LHT. A small specimen size could be corrected for using the nonlinear relationship.

Moreover, this study provided the scale effect for the mean HLD, normalized by the value of the standard length of 102 mm, as a function of the specimen length. It has also been observed that there is an increase in the value of the HLD as the length increases. This study proposed a relationship for less than L/D=1.5 and the influence of core sample length (HLD_L) related to standardized value (HLD_{102mm}).

The statistical relationship between the HLD and UCS for different rock types was investigated. That was done by analyzing the points from our lab and other literature from

the mining industry partners. Building a database with a total of 311 points helped to establish how accurately the UCS of rock material could be obtained by using a portable LHT. Utilizing HLD-UCS database, this study has presented a nonlinear relation between HLD and UCS for improved accuracy in field estimation of UCS.

Analysis was conducted on the three main rock types (igneous, metamorphic and sedimentary), collected from a literature review and the results of our laboratory study. The results of a comparison between LHT and Schmidt Hammer show that even though these rock specimens are from the same designation of rocks (igneous), there is considerable scatter between the UCS values for each specimen. The shapes of the UCS-HLD curves were similar in each rock types. The best-fit regression lines were plotted for the UCS-HLD correlation of all rock type and the correlation equations of all three rock types were presented with suitable R^2 and S value.

Generally, there is an increase in UCS with increasing HLD, despite the fact that the specimens used to develop the relationship were differentiated by formation sites and weathering. The correlations of sedimentary and metamorphic rocks show lower S value and higher R^2 value than igneous rocks. Due to the durability of igneous rocks when subjected to a load, they showed high UCS values relative to other rock types.

An improved correlation between HLD and UCS for different rock types was found and its accuracy was assessed by the lowest S, which is a useful measure to assess the precision of the predictions of the results of correlation analysis. The value of S of the study was found to be lower than those that were calculated from other correlation equations, whereas S associated with the correlation model should be as small as possible. That means the reliability and accuracy of the HLD - UCS relationship of the proposed model in this study is high.

In summary, the results show that the LHT can be particularly useful for field estimation of UCS and offer a significant improvement over the field estimation methods outlined by

the ISRM (2007). The equations that relate HLD to UCS are simple, practical and accurate enough to apply in the field. This study will act as an improvement to the UCS-HLD correlations that were done by other authors.

For future Leeb hardness studies, including the effect of physical properties such as the effect of the following two efficiency components, 1. the bond between minerals or grains and 2. their strengths, the effect of a porosity degree, in addition, the effect of an inhomogeneity in hardness testing is recommended. For future research, the database would need to be expanded and improved (more rock types, larger range of UCS.) The LHT could also be considered for evaluation of anisotropic conditions with further research. Moreover, In the future, efforts could be made to develop a system where the LHT automatically preforms many tests over a specimen (e.g., core) with one push of the button. This would provide a systematic profile of readings.

Quantity the level of uncertainty associated with the HLD – UCS estimation could be done in future work. Especially, related to the ISRM method and the average of variability in the typical UCS.

REFERENCES

Akram, M., & Bakar, M. A. (2016). Correlation between uniaxial compressive strength and point load index for salt-range rocks. *Pakistan Journal of Engineering and Applied Sciences*.

Aoki, H., & Matsukura, Y. (2008). Estimating the unconfined compressive strength of intact rocks from Equotip hardness. Bulletin of Engineering Geology and the Environment, 67(1), 23–29.

Aoki, H., & Matsukura, Y. (2007). A new technique for non-destructive field measurement of rock-surface strength: an application of the Equotip hardness tester to weathering studies. Earth Surface Processes and Landforms, 32(12), 1759–1769.

Asef, M. R. (1995). Equotip as an index test for rock strength properties (Doctoral dissertation, M. Sc. Thesis, ITC Delft)

ASTM. D4543-08 (2008). Standard Practices for Preparing Rock Core as Cylindrical Test Specimens and verifying Conformance to Dimensional and Shape Tolerances. Astm, 1–9. article.

ASTM, a 956-12 (2012). Standard Test Method for Leeb Hardness Testing of Steel Products. Standards, 1–12.

ASTM, D3967-08 (2008). Standard Test Method for Splitting Tensile Strength of Intact Rock Core Specimens 1. ASTM International, West Conshohocken, PA, 20–23.

ASTM, D7012–14 (2014). Standard test method for compressive strength and elastic moduli of intact rock core specimens under varying states of stress and temperatures, ASTM International, West Conshohocken, Pa., doi, 10.

ASTM D5873-05 (2005). Standard Test Method for Determination of Rock Hardness by Rebound Hammer Method, ASTM International, West Conshohocken, PA, 2005.

Aydin, A., & Basu, A. (2005). The Schmidt hammer in rock material characterization. Engineering Geology, 81(1), 1–14.

Aydin, A. (2015). The ISRM Suggested Methods for Rock Characterization, Testing and Monitoring: 2007-2014. (R. Ulusay, Ed.). Cham: Springer International Publishing.

Basu, A., & Aydin, A. (2004). A method for normalization of Schmidt hammer rebound values. International Journal of Rock Mechanics and Mining Sciences, 41(7), 1211–1214.

Bell, F. G. (Ed.). (2013). Engineering in rock masses. Elsevier.

Bieniawski, Z. T. (1975). Estimating the strength of rock materials. Journal of the South African Institute of Mining and Metallurgy, March, 312–320.

Broch EM, Franklin JA (1972) The point load strength test. Int J Rock Mech Min Sci Geomech Abstr 9:669–697

BS 5930 (1981). Code of Practice for Site Investigations. British Standards Institution (BSI). London. 147 pp.

Burnett A.D. (1975). Engineering geology and site investigation - part 2: field studies. Ground engineering. July. pp. 29 - 32.

Buyuksagis, I. S., & Goktan, R. M. (2007). The effect of Schmidt hammer type on uniaxial compressive strength prediction of rock. International Journal of Rock Mechanics and Mining Sciences, 44(2), 299–307.

Cargill JS, Shakoor A. (1990). Evaluation of empirical methods for measuring the uniaxial compressive strength of rock. Int J Rock Mech Min Sci Geomech Abstr 1990;27(6):495–503.

Coombes, M. A., Feal-Pérez, A., Naylor, L. A., & Wilhelm, K. (2013). A non-destructive tool for detecting changes in the hardness of engineering materials: Application of the Equotip durometer in the coastal zone. Engineering Geology, 167, 14-19.

Corkum, a. G., & Martin, C. D. (2007). The mechanical behaviour of weak mudstone (Opalinus Clay) at low stresses. International Journal of Rock Mechanics and Mining Sciences, 44, 196–209.

D. Leeb. (1986). Definition of the hardness value "L" in the EQUOTIP dynamic measuring method?, VDI-Report No. 583, pp. 109-133

D. Leeb. (1990). Dynamische Härteprüfung, in Härteprüfung an Metallen und Kunststoffen, eds. W.W. Weiler, D.H. Leeb, K. Müller and D.M. Rupp., 2nd Edition, Expert Verlag, Ehningen bei Böblingen

Daniels, G., Mcphee, C., Sorrentino, Y., & McCurdy, P. (2012). Non-Destructive Strength Index Testing Applications for Sand Failure Evaluation. Proceedings of SPE Asia Pacific Oil and Gas Conference and Exhibition, (L), 1–12.

Demirdag, S., Yavuz, H., & Altindag, R. (2009). The effect of sample size on Schmidt rebound hardness value of rocks. International Journal of Rock Mechanics and Mining Sciences, 46(4), 725–730.

Dynamic, P., & Tester, H. (n.d.). Impact th-170 series portable dynamic hardness tester portable hardness tester, 170–173

Eassa, A., Staff, F., & Engineer, F. E. R. (2005). Practical Approach Towards Enhanced Accuracy.

Frank, S., & Schubert, H. (2002). Portable hardness testing- principles and applications. Journal of Nondestructive Testing, 7(10), 8

Gorski, B., Anderson, T., Rodgers, D., Rogers, D., Raven, K., Mccreath, D., & Lam, T. (2010). Supplementary Uniaxial Compressive Strength Testing of DGR-3 and DGR-4 Core.

Goudie, A. S. (2013). The Schmidt Hammer and Related Devices in Geomorphological Research. In Treatise on Geomorphology (Vol. 14, pp. 338–345).

Grima, M. A., & Babusï, R. (1999). Fuzzy Model for The Prediction of Unconfined Compressive Strength of Rock Specimens. International Journal of Rock Mechanics and Mining Sciences, 36, 339–349.

Guerra, E., de Lara, J., Malizia, A., & Díaz, P. (2009). Supporting user-oriented analysis for multi-view domain-specific visual languages. Information and Software Technology.

Hack, H., Hingira, J., & Verwaal, W. (1993). Determination of discontinuity wall strength by Equotip and ball rebound tests. International Journal of Rock Mechanics and Mining Sciences & Geomechanics Abstracts, 30(2), 151–155.

Hack, R., & Huisman, M. (2002). Estimating the intact rock strength of a rock mass by simple means. Engineering Geology for Developing Countries, (0), 1971–1977.

Hawkins AB (1998) Aspects of rock strength. Bull Eng Geol Env 57:17–30

Hawkins AB, Olver JAG (1986) Point load tests: correlation factor and contractual use. An example from the Corallian at Weymouth In: Hawkins AB (ed) Site Investigation Practice: Assessing BS 5930, Geological Society, London, pp 269–271

Hoek, E., & Martin, C. D. (2014). Fracture initiation and propagation in intact rock – A review. Journal of Rock Mechanics and Geotechnical Engineering, 6(4), 287–300. JOUR.

Houston, M., & Long, F. (2004). Correlations Between Different Its and Ucs Test Protocols for Foamed Bitumen Treated Materials, (September), 522–536.

Hoek E, Brown ET (1980) Underground excavations in rock. Inst Min Metal, London

Hucka, V. (1965). A rapid method of determining the strength of rocks in situ. In *International Journal of Rock Mechanics and Mining Sciences & Geomechanics Abstracts* (Vol. 2, No. 2, pp. 127IN3131-130IN6134). Pergamon.

Hudson, J. A. (1993). Comprehensive rock engineering: principles, practice, and projects. Book, Pergamon Press.

Hujer, W. H., Finkbeiner, T., & Persaud, M. (2014). Estimating Rock Strength From Non-Destructive Strength Testing (EQUOTIP) and Related Benefits.

Hujer, W. H., Finkbeiner, T., & Persaud, M. (2014). Estimating Rock Strength From Non-Destructive Strength Testing (EQUOTIP) and Related Benefits.

ISRM. International Society of Rock Mechanics Commission on Testing Methods, Suggested Method for Determining Point Load Strength, Int. J. Rock Mech. Min. Sci. and Geomech. Abstr. 22, 1985, pp.51-60.

ISRM. (1979). Suggested methods for determining the uniaxial compressive strength and deformability of rock materials. International Journal of Rock Mechanics & Mining Sciences, 16(December), 135–140.

Jonatan, P. (2015). UCS test Sample Preparation: A Guide. Department of Civil and Resource Engineering, Dalhousie University.

Kahraman, S. (2001). Evaluation of simple methods for assessing the uniaxial compressive strength of rock. Rock Mechanics, 38, 981–994.

Kahraman, S., Fener, M., & Gunaydin, O. (2004). Predicting the sawability of carbonate rocks using multiple curvilinear regression analysis. International Journal of Rock Mechanics and Mining Sciences, 41(7), 1123–1131.

Kallu, R., & Roghanchi, P. (2015). Correlations between direct and indirect strength test methods. International Journal of Mining Science and Technology, 25(3), 355–360.

Karakus, M., Kumral, M., & Kilic, O. (2005). Predicting elastic properties of intact rocks from index tests using multiple regression modelling. International Journal of Rock Mechanics and Mining Sciences, 42(2), 323-330.

Karaman, K., & Kesimal, A. (2014). Correlation of Schmidt Rebound Hardness with Uniaxial Compressive Strength and P-Wave Velocity of Rock Materials. Arab J Sci Eng, 40, 1897–1906.

Karpuz, C. (1990). A classification system for excavation of surface coal measures. Mining Science and Technology, 11(2), 157-163.

Katz, O., Reches, Z., & Roegiers, J. C. (2000). Evaluation of mechanical rock properties using a Schmidt Hammer. International Journal of Rock Mechanics and Mining Sciences, 37(4), 723–728.

Kawasaki, S., Tanimoto, C., Koizumi, K., & Ishikawa, M. (2002). An attempt to estimate mechanical properties of rocks using the Equotip hardness tester. Journal of the Japan Society of Engineering Geology, 43(4), 244-248.

Kawasaki, S., & Kaneko, K. (2004). Estimation method for weathering thickness of man-made weathering rocks by using the Equotip hardness tester. In Proc. ISRM Regional Symp. EUROROCK (pp. 491-494).

Kompatscher, M. (2004). Equotip-rebound hardness testing after D. Leeb. Proceedings, Conference on Hardness Measurements, 1975. Retrieved from http://www.imeko.org/publications/tc5-2004/IMEKO-TC5-2004-014.pdf

Landau, L. (1937). Method for Determining the Unconfined Compressive Strength of Intact Rock Core Specimens SC T 39. Zhurnal Eksperimental'noi I Teoreticheskoi Fiziki, 1–4. Retrieved from

Lee, J. S., Smallwood, L., & Morgan, E. (2014, A. (2014). New Application of Rebound Hardness Numbers to generate Logging of Unconfined Compressive Strength in Laminated Shale Formations. New Application of Rebound Hardness Numbers to Generate Logging of Unconfined Compressive Strength in Laminated Shale Formations.

Li, D., & Wong, L. N. Y. (2013). Point Load Test on Meta-Sedimentary Rocks and Correlation to UCS and BTS. Rock Mechanics and Rock Engineering, 46(4), 889–896.

Luppi, L., Rinaldi, M., Teruggi, L. B., Darby, S. E., & Nardi, L. (2009). Monitoring and numerical modelling of riverbank erosion processes: a case study along the Cecina River (central Italy), 1769, 1759–1769.

Meulenkamp, F., & Grima, M. A. (1999). Application of neural networks for the prediction of the unconfined compressive strength (UCS) from Equotip hardness. International Journal of Rock Mechanics and Mining Sciences, 36.

Mol, L. (2014). Measuring rock hardness in the field. British Society for Geomorphology Geomorphological Techniques, 32(1).

Momeni, E., Nazir, R., Armaghani, D. J., For, M., Amin, M., & Mohamad, E. T. (2015). Prediction of unconfined compressive strength of rocks : a review paper, 11, 43–50.

Palchik V, Hatzor YH (2004) The influence of porosity on tensile and compressive strength of porous chalks. Rock Mech Rock Eng 37(4):331–341

Proceq SA (1977a) Operating instructions concrete test hammer types N and NR. Zurich, Switzerland.

Proceq SA (1977b) Equotip operations instructions, 5th edn. PROCEQ SA Zurich, Switzerland

Pycnometer, W., Soil, T., & Limit, P. (2007). Standard Test Method for Unconfined Compressive Strength of Cohesive Soil 1, 3(Reapproved 2002), 1–6.

Rodríguez-Rellán, C., Valcarce, R. F., & Esnaola, E. B. (2011). Shooting out the slate: Working with flaked arrowheads made on thin-layered rocks. Journal of Archaeological Science, 38(8), 1939–1948.

Romana M (1999). Correlation between uniaxial compressive and point load (Franklin test) strengths for different rock classes. In: 9th ISRM Congress, 1999, vol 1, pp 673–676, Paris

Rusakov, N. G., & Mavrodi, P. I. (N.D.). Determination of The Strength Of Rock By The Impact Method.

Ryan, T. A., Joiner, B. L., & Ryan, B. F. (2004). Minitab™. John Wiley & Sons, Inc

Selçuk, L., & Yabalak, E. (2015). Evaluation of the ratio between uniaxial compressive strength and Schmidt hammer rebound number and its effectiveness in predicting rock strength. Nondestructive Testing and Evaluation, 30(1), 1–12.

Sheskin, D. J. (2000). Parametric and nonparametric statistical procedures. Boca Raton: CRC.

Sjoberg, J. (1997). Estimating rock mass strength using Hoek-Brown failure criterion and rock mass classification, 61.

Stefan, F. (2003). Mobile hardness testing. Insight, 45(9), 651

Szilágyi, K. (2012). Hardness studies on porous solids. In Conference of Junior Researchers in Civil Engineering (pp. 240–247).

Szilágyi, K. (2013). Rebound surface hardness and related properties of concete, 439.

Szwedzicki, T. (1998). Technical note Indentation Hardness Testing of Rock, 35(6), 825–829.

Thuro K, Plinninger RJ (2005) Scale effects in rock properties: Part 2. Point load test and point load strength index. EUROCK Swets and Zeitlinger, pp 175–180, Lisse

Torabi, S. R., Ataei, M., & Javanshir, M. (2011). Application of Schmidt rebound number for estimating rock strength under specific geological conditions. Journal of Mining and Environment, 1(2), 1–8.

Tsiambaos G, Sabatakakis N (2004) Considerations on strength of intact sedimentary rocks. Eng Geol 72:261–273

Van de Wall, I. A. R. G., & Ajalu Msc, J. S. (1997). Characterization of the geotechnical properties of rock material for construction purposes. International Journal of Rock Mechanics and Mining Sciences, 34(3–4), 319.e1-319.e12.

Verwaal, W., & Mulder, A. (1993). Estimating rock strength with the Equotip hardness tester. International Journal of Rock Mechanics and Mining Sciences & Geomechanics Abstracts, 30, 659–662. http://doi.org/10.1016/0148-9062(93)91226-9

Verwall, W., & Mulder, A. (2000). Rock and aggregate test procedures. Rock and aggregate laboratory manual, 13, 14.

Viles, H., Goudie, A., Grab, S., & Lalley, J. (2011). The use of the Schmidt Hammer and Equotip for rock hardness assessment in geomorphology and heritage science: A comparative analysis. Earth Surface Processes and Landforms, 36(July 2010), 320–333.

Yaşar, E., & Erdoğan, Y. (2004). Estimation of rock physicomechanical properties using hardness methods. Engineering Geology, 71(3–4), 281–288.

Yilmaz, N. G. (2013). The influence of testing procedures on uniaxial compressive strength prediction of carbonate rocks from Equotip hardness tester (EHT) and proposal of a new testing methodology: Hybrid dynamic hardness (HDH). Rock Mechanics and Rock Engineering, 46(1), 95–106.

Zhang, Q., Zhu, H., Zhang, L., & Ding, X. (2011). Study of scale effect on intact rock strength using particle flow modeling. International Journal of Rock Mechanics and Mining Sciences, 48(8), 1320–1328.

Appendix 1

CONFERENCE PAPER

Leeb Hardness Test for UCS estimation of Sandstone

Yassir Asiri, Andrew Corkum & Hany El Naggar
Department of Civil and Resource Engineering

ABSTRACT

An experimental exploration has been conducted to investigate the statistical relationship between Leeb Hardness ("D" type) values (HLD) and unconfined compressive strength values (UCS) for sandstone. Moreover, the Leeb test methodology was evaluated, such as sample size and the number of Leeb readings that comprise a valid test result. The laboratory testing was carried out on sandstone specimens and combined with other literature values to develop a database with a total of 45 test results. Statistical analysis was carried out on the database and the results of correlation analysis from tests are presented. A reasonable correlation was found to exist between LHD and UCS for sandstone. The results show that the Leeb Hardness test (LHT) can be particularly useful for field estimation of UCS. The method is fast, simple and equipment costs are low. The hardness testing cannot replace UCS tests but can complement these tests, especially if is needed immediately or other testing is not possible.

RÉSUMÉ

Une exploration expérimentale a été menée pour étudier la relation statistique entre Leeb Dureté (type « D ») des valeurs (HLD) et des valeurs de résistance à la compression uniaxiale (UCS) pour la roche. En outre, la méthodologie de test Leeb a été évaluée, comme la taille de l'échantillon et le nombre de lectures Leeb qui comprennent un résultat de test valide. Les tests de laboratoire ont été effectués sur des échantillons de grès et combiné avec d'autres valeurs de la littérature pour développer une base de données avec un total de 45 résultats. L'analyse statistique a été réalisée sur la base de données et les résultats de l'analyse de corrélation des essais sont présentés. Une corrélation raisonnable existe entre LHD et UCS pour le grès. Les résultats montrent que le test de dureté Leeb peut être particulièrement utile pour l'estimation du champ de UCS. La méthode est simple, rapide et les coûts d'équipement sont faibles. L'essai de dureté ne peut pas remplacer les tests UCS mais peut compléter ces tests, en particulier si les données sont nécessaires immédiatement ou autres tests n’est pas possible.

1 INTRODUCTION

The unconfined compressive strength (UCS) of rock is a very important parameter for rock classification, rock engineering design and numerical modeling. In addition, this property is essential for judgment about the rocks suitability for various construction purposes. However, determination of rock UCS is relatively time consuming and expensive for many projects. Consequently, the use of a portable, fast and cost effective index test that can reasonably estimate UCS would be desirable. Other index tests, such as the Schmidt hammer and Point Load Test are commonly used for this purpose. However, this work looked at the LHT, which is quick, inexpensive and nondestructive: particularly valuable at preliminary project stages.

The LHT method was introduced in 1975 by Dietmar Leeb at Proceq SA (Kompatscher, 2004). The LHT is a portable hardness tester originally for measuring the strength of metallic materials. Recently, it has been applied to various rocks for testing their hardness (e.g. Aoki and Matsukura, 2007; Viles et al., 2011), it can also be correlated with rock UCS according to Kawasaki et al., 2002; Aoki and Matsukura, 2007. Moreover, it is used to assess the weathering effects on hardness values (Kawasaki and Kaneko, 2004; Aoki and Matsukura, 2007; Viles et al., 2011). The LHT can be used in laboratory or the field at any angle (Viles et al., 2011), since the instrument uses automatic compensation for impact direction. It is suitable for applications to cover a wider range of most rock hardness compared with the Schmidt hammer (Aoki and Matsukura 2007).

The aim of this study is to investigate the statistical relationship between Leeb Hardness ("D" type) values (HLD) and UCS for sandstone, which is one of most uniform and consistent rocks. For this reason, the laboratory testing was carried out on sandstone and combined with other literature values to develop a database with a total of 45 test results. the LHT methodology was evaluated (sample size and the number of Leeb readings that comprise an average test result). Statistical analysis was carried out on the database and the results of correlation analysis from tests are presented. Reasonable correlations between LHD and UCS for sandstone were developed and their accuracy was assessed. The results show that the LHT can be particularly useful for field estimation of UCS and offer a significant improvement over the field estimation methods outlined by the ISRM (2007). The equations that relate HLD to UCS are simple, practical and accurate enough to apply.

The method is fast, simple and equipment costs are low. Although the empirically rock strength predicted from the in-direct LHT results contain some level of uncertainty, but are of significant value for preliminary design. Moreover, it could be used on core to provide a continuous profile of estimated UCS in a borehole log with minimal effort for UCS even beyond the preliminary engineering stage

2 Backgrounds

The LHT can determine the mechanical hardness without destruction of specimens, which in turn reduces cost and simplifies processes. It has been used widely in rock mechanics research due to its simplicity. In 1993, Verwaal and Mulder at Delft University of Technology, examined the possibility of predicting the UCS from HLD value. They presented the UCS versus HLD relationship and the influence of the surface roughness on the LHT measurement. Also, they stated that, provided the specimens have a thickness of greater than 50 mm, the sample thickness has slight effect on the LHT measurement. They ended with a simple equation for estimating UCS from the measurements of LHT. Additionally, Hack et al. (1993) used both LHT and ball rebound tests to describe the UCS of the discontinuity plane for mixed lithologies of various rock type specimens. They attempted to find the relationship between UCS and Equotip L-values or rebound values of the ball test and estimate the mechanical strength of the rock surface along a discontinuity using the Verwaal and Mulder equation.

In 1999 Meulenkamp and Grima used a neural network to predict the UCS from HLD and several other rock characteristics (porosity, density, grain size and rock type) as input. However, this is a complex approach and required many input parameters, each of which added complexity and additional uncertainty to the method. This removed the “simplicity” of the test and it restricted their approach to the availability and quality of the secondary inputs. Moreover, the proposed equation includes many variables, which in turn is not practical in field estimation. Finally, to the author’s knowledge, the neural network algorithm details were not published and made readily available.

Okawa et al. (1999) tested the effects of the measurement conditions on the rebound value and concluded that the rebound value depends partially on specimen support (i.e., physical constraint). In addition, multiple tests on the exact same location tend to increase the local

density, thus HLD increases with additional impacts at a given point. The roughness of the testing surface has no clear influence on the test result of rebound value. Kawasaki et al. (2002), studying unweathered rocks, proposed that the UCS could be estimated from LHT values by using the Leeb test to establish the strength of rocks in the field. They also, established the effects of the test conditions, including roughness, the size and the impact direction, using cylindrical specimens of rock types including sandstone, shale, granite, hornfels and schist, collected from different locations in Japan. They reported that the specimen thickness has slight influence on the LHT measurement in specimens more than 50 mm thick. In 2007, Aoki and Matsukura used type "D" hardness tester to study rock hardness from nine locations, eight in Japan and one in an Indonesia. They proposed an equation relating UCS to Leeb hardness and porosity:

$$\mathbf{UCS} = \mathbf{0.079e^{-0.039n}\, L^{1.1}} \qquad [1]$$

where "n" is the porosity and "L" is the Leeb hardness value.

Recently, Daniels, et al. (2012) studied the strength of sandstone. They indicated that the original Verwaal and Mulder (1993) correlation could overestimate rock strength of weak sandstone. Yilmaz (2013) considered only one rock group (carbonate rocks) to determine the suitability of different rebound testing procedures with the LHT for UCS estimations and came up with different regression models. He used a new testing methodology, hybrid dynamic hardness (HDH), which depends on a combination of the surface rebound hardness and compaction ratio (the ratio between HLD and the peak hardness value earned after ten repeated impacts at same spot) of a rock material. They pointed out that the predicted UCS is more accurately when density is available. Moreover, He reported that, for the range of specimen sizes, no clear evidence of size effect in the hardness values.

3 Comparisons between Leeb Hardness Test and Schmidt Hammer

Both the LHT and Schmidt hammer are rebound measuring devices. The Schmidt hammer follows the traditional static tests where the test uniformly loaded, while the LHT follows the dynamic testing methods that apply an impulsive load. The Schmidt hammer is the traditional method that is based on clear physical indentation. It measures the distance of rebound after a plunger hits the material surface. In contrast, the LHT (Figure 1) is a lighter,

smaller and non-destructiveness device that leaves a little damage with an indentation of just ~0.5 mm, which is good for a thin layer. LHT is also faster, a test takes a mere “2” seconds. Thus for practical purposes, speed, size and weight of the LHT make it easier to deal with in the field.

Figure 1. Leeb Hardness Tester. The lightweight and compact size of the device make it convenient for fieldwork.

The Schmidt Hammer has certain limitations in its application. It is not applicable to extremely weak rocks, nonhomogeneous rocks like conglomerates, and Breccia. It has high impact energy. Therefore, its result is influenced by the layer characteristics beneath the tested surface. This makes the Schmidt hammer more difficult to measure soft rocks than the LHT. Viles et al. (2011) points out that the impact energy of the LHT-D type is nearly 1/200 of the Schmidt Hammer Tester N-type, and 1/66 of the Schmidt Hammer L-type. By using LHT, less damage is caused to the tested surface. As a result, the LHT has ability to measure soft and thin material due to its lower impact energy, which is not possible with the Schmidt Hammer (Aoki and Matsukura, 2007a). Hack and Huisman (2002) reported that the material to a fairly large depth behind the tested surface influences the Schmidt hammer values. As a result, if a discontinuity exists within the influence zone, the Schmidt hammer values could be affected. They suggested that, the LHT or other rebound impact devices might be more suitable in this situation.

Moisture can influence Schmidt Hammer results, but does not significantly influence the LHT readings. Aoki and Matsukura (2007) examined this by preforming the tests on a sample when wet and when dry. For evaluating of moisture effect, Haramy and DeMarco

(1985), reported that Schmidt's is affected by water content of the surface in addition to the roughness of the surface area, rock strength, cleavage and pores as well. The LHT device is sensitive to surface conditions, so it cannot be used successfully on friable or rough surfaces of rocks.

The LHT has the ability to repeat the impact test on the same sample even on the same spot without breaking the sample, which is not always possible with Schmidt hammer (Aoki and Matsukura, 2007a). This allows the LHT to be used on small specimens or on those of limited thickness. In the laboratory both devices require the specimens to be well clamped in order to avoid any movement.

The Schmidt Hammer is less sensitive to localized conditions at the impact location making reading more consistent and representing the average rock properties. The LHT is more precise (smaller area) and therefore is affected by local mineralogy and geometry. Doing multiple Leeb readings and averaging them for a single "test" reading can alleviate this. LHT has certain advantages such as the smaller diameter of its tip (3 mm), which means greater accuracy of its measurement, also the automatic correction of the angle, which minimizes the variations in measurements produced by the gravity force. In addition, the LHT can be used either in laboratory or the field, because of portability, simplicity, low cost, its speed and non-destructiveness. Also, it positions at any angle and either straight or curved surface while Schmidt's direction is restricted.

4 STUDY METHODOLOGY

This section describes the methodology used to conduct the LHT and UCS tests.

4.1 Leeb Hardness Tester: Theory and methodology

In the LHT the rock hardness is known as the material response to an Impacting devices. This better reflects the elasticity of the material than a direct measurement of the material's strength. The theory behind the method is based upon the dynamic impact principle, the height of the rebound of a small tungsten carbide ball (diameter of 3 mm) on a material surface. This depends on the elasticity of the surface and energy loss by plastic deformation, all related to the mechanical strength of a material (Aoki and Matsukura, 2008). The ball rebounds faster from harder spacemen than it does from softer ones. The impact ball is shot against the material surface and when the ball rebounds through the coil, it induces a current in the coil. Measured voltage of this electric current is proportional to the rebound velocity. The hardness value is the ratio of rebound velocity to impact velocity, is quoted in the Leeb hardness unit HL (Leeb hardness) and also known as L-value. The HLD denotes testing with the D device, which can be described as

$$\mathbf{L} = \frac{\mathbf{V\ rebound}}{\mathbf{V\ impact}}\mathbf{X1000} \qquad [2]$$

In this study, the EHT ("D" type) was used to predict the UCS for five sandstone core specimens. There is still no established testing procedure for using the LHT to predict UCS on rocks. Therefore, the single impact method (12 impacts) on the core specimens (Daniels et al., 2012) was used on core specimens. The maximum and minimum reading was excluded and the average of 10 remaining readings was used. The averaged HLD readings were correlated with UCS-test, the results show that the LHT can be particularly useful for estimated the UCS with some level of uncertainty. Moreover, to get a reasonable measure of the "Statistically representative" hardness of a sample rock, the LHT methodology was examined by quantifying sample size and the number of Leeb readings.

4.2 Unconfined Compressive Strength Test

The UCS can be determined both directly and indirectly. In the direct test (UCS) peak strength is the stress at which the sample fails under unconfined compressive load. In this study, according to the suggested procedure by ASTM (2010), five core specimens (54 mm diameter and 121 mm high) were prepared from Wallace sandstone block, which is quarried from Wallace Quarries in Nova Scotia province of Canada. Using a 100-ton compression-testing machine with the load rate of 0.3 - 0.5 mm/min was applied for test with duration of 7 – 13 minutes. The UCS ranged from 80.48 MPa to 219.7 MPa, combining with "40" specimens from previous studies (Hack et al 1993, Verwaal & Mulder, 1993; Asef, M, 1995; Meulenkamp & Grima, 1999; Kawasaki et al., 2002; and Aoki and Matsukura, 2007), that ranged from 15 MPa to 198 MPa. These points cover a wide range of UCS values that represent the practical range found in the field.

5 RESULTS AND DISCUSSION

5.1 How many "Readings" constitute a "Valid" Test?

The appropriate number of impacts that are required to get a reasonable measure of the "Statistically representative" hardness of the sample rock, given the sensitivity to localized conditions, is a controversial issue amongst authors. In order to address this issue and quantify the appropriate readings (impacts), this study was carried out in two approaches. First an evaluation based on statistical theory was carried out and an evaluation based on sampling was carried out.

The first approach in this study used a sandstone core sample of a L/D ratio of 2-2.5 with a total length of 121mm. It has been assumed that the average of 100 repeat measurements (readings) on different spots of sandstone sample considers as the μ. The statistical measures of a 100 readings on sandstone, including the μ and standard deviation are presented in Table 1. After that, margin of error (**ME**) formula was used to determine the difference between the observed $\overline{\mathbf{X}}$ and the μ when the experiment was repeated on the same testing condition, for different sample sizes (e.g. 10 and 15). This helps to find out how

many impacts we would need to get a $\bar{\mathbf{X}}$ which is almost equal to the population mean, based on 100 readings with a degree of confidence interval of 95%.

We can quantity the precise of our $\bar{\mathbf{X}}$, for sample sizes less than 100, by using ME. The relation between population mean and $\bar{\mathbf{X}}$ can calculate using:

$$\boldsymbol{\mu = \bar{X} \pm \ 1.96 \left(\frac{\sigma}{\sqrt{n}} \right)} \quad [3]$$

where μ is the population mean,1.96 is the critical Z value of the standard normal distribution at a 95% degree of confidence, σ is the standard deviation of the population, n is the sample size and $\bar{\mathbf{X}}$ is the sample mean. The formula to establish the margin of error at different sample sizes (e.g. at 10 and 15) is:

$$\boldsymbol{ME = 1.96 \left(\frac{\sigma}{\sqrt{n}} \right)} \quad [4]$$

The results using the sandstone sample, for which we have 100 repeated measurements are shown in Table 2. Table 2 illustrates that, in general, LHT require much more sampling effort to obtain a good estimate of the true hardness on rocks.

The second approach is based on sampling, relying on the Central Limit Theorem and the Law of Large Numbers. The key idea in the Central Limit Theorem is that when a population is repeatedly sampled, the calculated average value of the feature obtained by those specimens is equal to the true population mean value, and the Law of Large Numbers states that as a sample size grows, its mean will converge in probability towards the average of the whole population. Accordingly, this study was performed on a total of 100 readings (impacts) on a sandstone core sample of a L/D ratio of 2-2.5 with a total length of 121mm. Once this population set (100 readings) was captured, a subset number of readings (e.g., 10, 15, 20, 30) were randomly selected, to ensure that all of the points are being well represented taking into consideration all different aspects to avoid being biased by the performer, and the mean value was determined. This was done on with subset sizes ranging

from 1 to 100 readings. Moreover, because of the high variability of $\overline{\mathbf{X}}$ at low sample numbers, a total of five "realizations" of this randomized subset study were carried out.

This helps to visually assess how many impacts we would need to get a $\overline{\mathbf{X}}$ which is almost equal to the population mean, based on 100 readings with a degree compared to the confidence interval. A graph was then plotted representing the with the average of readings that was previously calculated on the Y-axis against the number of tries, which was a 100 on the X- axis (Figure 2). This method graphically shows that by increasing the number of averaged, their arithmetic mean gets close to the 100 readings mean (population mean). Moreover, this graph helps determine the minimum number of readings required to carry out a 'Valid' test based on the standard deviation rules and visually assess the error associated with limited sample size (e.g. 10 readings). As shown in Figure 2, it is clear that there are minimal gains for extra tests beyond 10 in sandstone.

5.2 Evaluation of Sample Size and Scale Effects

It has been observed in several studies that there is a correlation between the scale effects on the specimen hardness (e.g. Aoki and Matsukura, 2007; Lee, Smallwood and Morgan, 2014). An understanding of the relationship between hardness value of the sample, and the size/geometry of the sample (e.g. core length) is necessary to determine the appropriate sample sizes that should be considered as a valid. To try and investigate the effect of sample size on HLD values and to evaluate this correlation between the HLD and the specimen size, an experimental study was conducted on different sandstone sizes, including cubic and core size. All core specimens have been prepared with the same diameter of 54 mm (NX-size) and eight different lengths. In addition, four cubic specimens with different lengths were prepared. The results presented in Figure 3 indicate that the points show an initially highly non-linear trend of increasing HLD with sample length and then become nearly level. Table 3 shows the HLD for both cubic and core size.

For each volume, the specimens were tested by the hardness tester, the different core sample volume after preparation were 20.4, 23.3, 49.4, 87.3, 174.5, 232.7, 349, and 436.3 cm^3, respectively. And four cubic sample with different volumes of 131.1, 16.4, 131.1, 1048.8, and 8390.2 cm^3, respectively. The 12 single impacts on sample ends (Daniels et

al., 2012) were used on all specimens. The maximum and minimum hardness reading were excluded, an average of remaining readings were used. The average value was recorded as the rebound Leeb number (HLD). The HLD increases as sample volume increases until reaching a minimum volume to obtain consistent HLD value. It is noted that the HLD value for both core and cubic size increase non-linearly until the curve becomes nearly flat at the volume of 100 cm^3 as shown in Figure 3. Thus, this is the minimum volume of these specimens for valid HLD measurement. Figure 3 shows the results of the variation of the mean HLD as a function on the sample volume. It shows an increasing of the mean HLD as the volume of the sample increase with a very good correlation with a positive power law.

Figure 4 shows the scale effect for the mean HLD normalized by the value of the standard length of 102 mm (actually, 101.6 mm) as a function of the sample length. Here again, an increase in the value of the HLD as the length increase is observed. Figure 4 illustrate the Influence of core sample length (HLD_L) related to standardized value (HLD_{102mm}) by the relationship for less than L/D=1.5:

$$HLD_L = 0.35\ L^{0.28} \times HLD_{102mm} \qquad [5]$$

Table 4 shows the variation in HLD values according to core sample length of sandstone and L/D ratio.

5.3 Relationship between Leeb hardness and unconfined compressive strength and Statistical Analysis of

Two statistical analysis models were performed in order to find the best correlation with the lowest S, which is a useful measure to assess the precision of the predictions. The first one is the least-squares regression model; the second one is the nonlinear regression model. The curve was selected based on previous knowledge from the literature about the response curve's shape between UCS and HLD. The nonlinear method in Figure 5 showed a slightly lower S. These analyses were performed using Minitab (Version 17.2014) software.

Figure 5. Relationships between HLD and UCS for different sandstone units broken out by grain size.

Figure 5 shows the relationship between HLD, and UCS for specimens tested both in the present study and collected from the literature. A cluster of greywacke is located in the upper end of the fit line and shows high strength. This could be due to poorly sorted angular grains set in a matrix of fine clay in greywacke specimens. Such a large scatter of as seen in Figure 5 could be attributed to variation in cementing material. In spite of the scatter in, there is a tendency for HLD to increase with increasing UCS. The points cover a wide range of UCS values, ranged from 15 MPa to 219.7 MPa, representing the practical range found in the field.

5.3.1 least square regression analysis

The UCS and the HLD relation in a regression analysis does not satisfy the ordinary least squares regression and the residuals get diverge as the HLD increase, thus, the needs to be adjusted to achieve a better fit. A common solution for this problem is to transform the response variable (UCS). The transformation is simple by using the Box-Cox transformation function in Minitab. To test the significance of the least square regression model, analysis of variance for the regression was utilized at 95% level of confidence. For the f-test, if P-value is less than 0.05 then there is a real relation between the two parameters. Parameters for the analysis of variance for the least square regression equations are given in Table 5. Since the P-values are zero, therefore it is concluded that the models are valid according to f-test (Ryan et al., 2004)

The coefficients in the least square regression (Table 6); represent the mean change in the response (UCS) related to the change in the predictor (HLD). In Table 6 the y intercept was found to be 1.013 and the slope was found to be 0.00518. These had P-values of 0.003 and 0.000, respectively. Both of these are less than the alpha level of 0.05 indicating that the predictors are statistically significant. It means that, any changes in the UCS values are related to changes in the HLD. Least square regression Equation:

$$\text{UCS (MPa)} = \exp(1.013 + 0.00518\ \text{HLD}) \qquad [6]$$

5.3.2 Nonlinear regression analysis

In this study, a nonlinear regression of the set was also performed. Using information from the literature about the response curve's shape and the behavior of the physical properties, an exponential growth curve was selected with the following expected function form for one parameter (UCS) and one predictor (HLD):

$$Y = \text{Theta1} \times \exp(\text{Theta2} \times X) \quad [7]$$

Where the thetas represent fit parameters and X represent the predictor. The trend expressed by the nonlinear model is described as:

$$\text{UCS(MPa)} = 2.548 \times \exp(0.00537 \times \text{HLD}) \quad [8]$$

The R^2 coefficient of 0.72 reflects the degree of scatter in the datapoints. This shows that UCS can be predicted with a reasonable degree of accuracy using the LHT.

Minitab uses a Gauss-Newton algorithm with maximum iterations of 200 and tolerance of 0.00001, to minimize the sum of squares of the residual error (Ryan et al., 2004). The S was used to assess how well the regression model predicts the response between two models (Table 8). The lower the value of S, the better the model predicts the response (UCS).

5.4 Equation comparison

In order to compare the two prediction models, the following statistical performance indexes were used: The S, SSE and MSE.

Comparing with the least square regression model, the nonlinear equation has the lowest S value, which indicates the best fit. For nonlinear model, S is calculated as 29.3 this indicates that the actual points are within a standard difference of 29.3 MPa (UCS) from the regression line which represents the predicted value (Table 7).

$$MSE = SSE/DF \quad [9]$$

$$S = \sqrt{SSE/DF} \quad [10]$$

Where: DF= the number of degrees of freedom

In order to validate the model and to assess whether the residuals are consistent with random error and a constant variance, t needs to check a residual versus fitted values plot. In Figure 7, the residual plot indicates a good fit and reasonable with randomly scattered of the residuals around zero.

6 CONCLUSION

Currently there is no well-established procedure for LHT in the rock engineering field. We have developed an understanding of the confidence associated with the number of readings per test and provided a recommended testing procedure. We have examined the number of specimens required for a valid test and determined that a minimum of 10 tests should be performed. In our procedure 12 readings and disregarding the highest and lowest provides and even more accurate basis for UCS determination. In addition, we have found a nonlinear relation between sample size and HLD below 100 cm^3 and we found it to be a constant above 100 cm^3. Small sample size could be corrected for, using the nonlinear relationship. Utilizing our HLD-UCS database for sandstone, we have presented a nonlinear relation between HLD and UCS for improved accuracy in field estimation of UCS. We are currently continuing to research other rock types.

Acknowledgements

The writers would like to acknowledge the Saudi Bureau in Canada for providing funding for this research and Derek Kinakin of BGC Engineering Inc. for his valued suggestions as well as Jesse Keane and Alexander Mckenney for laboratory assistance and writing assistance, respectively.

REFERENCES

Aoki, H., & Matsukura, Y. (2007). A new technique for non-destructive field measurement of rock-surface strength: An application of the Equotip hardness tester to weathering studies. Earth Surface Processes and Landforms, 32, 1759–1769. doi:10.1002/esp.1492

Aoki, H., & Matsukura, Y. (2008). Estimating the unconfined compressive strength of intact rocks from Equotip hardness. Bulletin of Engineering Geology and the Environment, 67(1), 23–29.

Asef, M.R. 1995. Eqoutip as an index test for rock strength properties. M.Sc. Thesis, ITC Delft.

ASTM D7012-10. (2010). Standard Test Method for Compressive Strength and Elastic Moduli of Intact Rock Core Specimens under Varying States of Stress and Temperatures. ASTM International, West Conshohocken, PA, pp.1–9. doi:10.1520/D7012-10.1.

BGC engineering Inc. (2012). Technical Report. Unpublished raw .

Daniels, G., Mcphee, C., Sorrentino, Y., & McCurdy, P. (2012). Non-Destructive Strength Index Testing Applications for Sand Failure Evaluation. Proceedings of SPE Asia Pacific Oil and Gas Conference and Exhibition, (L), 1–12. doi:10.2118/158326-MS

Hack, H., Hingira, J., & Verwaal, W. (1993). Determination of discontinuity wall strength by Equotip and ball rebound tests. International Journal of Rock Mechanics and Mining Sciences & Geomechanics Abstracts, 30(2), 151–155. doi:10.1016/0148-9062(93)90707-K.

Haramy, K. Y., & DeMarco, M. J. (1985, January). Use of the Schmidt hammer for rock and coal testing. In The 26th US Symposium on Rock Mechanics (USRMS). American Rock Mechanics Association.

ISRM (2007). The complete ISRM suggested methods for rock characterization, testing and monitoring: 1974-2006. International Society for Rock Mechanics, Commission on Testing Methods, 2007.

Kawasaki S, Tanimoto C, Koizumi K, Ishikawa M. 2002. An attempt to estimate mechanical properties of rocks using the Equotip Hard- ness tester. Journal of Japan Society of Engineering Geology 43: 244–248 (in Japanese with English abstract).

Kawasaki S, Kaneko K. 2004. Estimation method for weathering thick- ness of man-made weathering rocks by using the Equotip hardness Tester. Proceedings of the ISRM Regional Symposium EUROROCK 2004 and 53rd Geomechanics Colloquy; Salzburg 491–494.

Lee, J. S., Smallwood, L., & Morgan, E. (2014, August). New Application of Rebound Hardness Numbers to Generate Logging of Unconfined Compressive Strength in Laminated Shale Formations. In 48th US Rock Mechanics/Geomechanics Symposium. American Rock Mechanics Association.

Leeb, D.H. 1978. New dynamic method for hardness testing of metallic materials. VDI-Report. 308:123-128.

Meulenkamp, F., & Grima, M. A. (1999). Application of neural networks for the prediction of the uncon ® ned compressive strength (UCS) from Equotip hardness. International Journal of Rock Mechanics and Mining Sciences, 36.

Verwaal, W., & Mulder, A. (1993). Estimating rock strength with the Equotip hardness tester. International Journal of Rock Mechanics and Mining Sciences & Geomechanics Abstracts, 30, 659–662. doi:10.1016/0148-9062(93)91226-9

Viles, H., Goudie, A., Grab, S., & Lalley, J. (2011). The use of the Schmidt Hammer and Equotip for rock hardness assessment in geomorphology and heritage science: A comparative analysis. Earth Surface Processes and Landforms, 36(July 2010), 320–333. doi:10.1002/esp.2040

Yilmaz, N. G. (2013). The influence of testing procedures on uniaxial compressive strength prediction of carbonate rocks from Equotip hardness tester (EHT) and proposal of a new testing methodology: Hybrid dynamic hardness (HDH). Rock Mechanics and Rock Engineering, 46(1), 95–106. doi:10.1007/s00603-012-0261-y

Appendix 2

The HLD of 100 impact readings on different rock types used in the sampling approach for evaluation the number of impact comprises LHT

Granite	Dolostone	H-Schist	Sandstone	Standard hardness block	V-Schist
822	592	683.0	582	772	755
822	580	615.5	587	771	771
849	582	575.7	574	770	712
867	586	614.0	572	770	758
878	585	615.0	573	770	771
880	586	634.2	575	771	718
885	585	662.0	573	770	758
885	583	679.4	568	771	797
889	581	660.4	563	771	743
889	582	668.7	564	771	767
887	581	663.1	560	770	801
890	582	669.6	561	770	722
888	581	669.0	559	770	691
882	583	674.9	558	770	670
879	585	669.8	559	771	717
879	586	671.4	558	770	790
881	587	676.9	559	770	740
881	586	681.4	559	770	845
882	587	681.3	559	770	773
876	588	672.7	561	770	749
875	588	679.1	560	770	621
876	589	674.0	559	770	834
876	590	678.1	559	770	824
875	589	676.6	559	770	797
877	589	681.0	560	770	841
877	589	685.9	560	770	759
877	589	689.1	559	770	838
877	588	690.1	559	770	703
876	587	694.2	559	770	716
873	588	696.7	559	770	826
872	588	694.4	559	770	769

Granite	Dolostone	H-Schist	Sandstone	Standard hardness block	V-Schist
870	588	693.4	559	770	770
871	589	689.8	558	770	778
869	589	692.7	558	770	775
870	590	694.9	558	770	754
869	590	692.1	557	770	800
870	590	694.5	557	770	731
870	590	695.1	557	770	766
871	590	694.8	556	770	867
872	590	692.5	555	770	852
870	590	690.5	555	770	704
872	590	693.0	555	770	768
869	590	694.4	555	770	791
870	590	695.8	554	770	732
871	591	698.7	555	770	738
871	590	701.0	554	770	721
872	590	702.7	555	770	797
872	590	704.3	555	770	741
872	591	706.1	555	770	745
870	590	706.1	554	770	805
870	590	707.5	554	770	808
870	590	708.1	554	770	754
871	590	709.1	554	770	761
870	590	710.2	555	770	713
871	591	709.2	555	770	773
871	591	711.0	554	770	584
871	592	711.7	555	770	671
870	591	710.6	554	770	718
870	592	711.6	555	770	770
868	592	712.9	555	770	783
868	593	710.6	555	770	793
866	593	711.9	555	770	756
867	593	713.4	554	770	729
867	593	714.2	554	770	641
867	593	714.6	554	770	669
868	593	716.5	554	770	828
868	593	716.9	554	770	790
869	593	718.5	554	770	748
870	593	717.0	554	770	738
870	593	716.2	555	770	679
871	593	715.5	555	770	650

Granite	Dolostone	H-Schist	Sandstone	Standard hardness block	V-Schist
871	593	716.8	555	770	830
870	593	718.5	554	770	797
869	593	716.9	554	770	723
870	593	716.1	554	770	824
870	593	715.8	555	770	757
870	593	716.7	555	770	849
871	593	716.2	555	770	716
871	593	714.0	555	770	779
871	593	714.9	555	770	759
871	593	715.8	555	770	755
871	593	714.0	555	770	753
871	593	714.7	555	770	778
871	594	713.3	555	770	790
871	593	713.6	555	770	819
871	593	710.5	554	770	749
871	594	708.6	554	770	750
871	593	708.9	554	770	840
871	594	708.9	554	770	810
871	593	707.5	554	770	612
870	594	708.4	554	770	766
870	594	708.9	554	770	798
871	594	709.7	553	770	705
871	594	710.6	553	770	607
871	594	710.3	553	770	786
871	594	708.3	553	770	763
871	594	709.2	553	770	824
872	594	709.8	553	770	850
872	594	709.2	553	770	766
871	594	709.7	552	770	798

Comments on some UCS test specimens that were tested in this study.

ID	Comments
SH4	Horizontal vein near top of sample.
SH5	Schistosity at top of sample, with approximately horizontal veins in the center.
SH6	Slight angled veins at top and bottom.
SH7	No dominant mode.
SH8	Small slightly angled veins in center, traces of pyrite on ends of sample.
SH12	Sample failed immediately upon pre-loading. No acquired
SV6	It has fractures/ a crack along its side
C1	Holds concretion and microdefect laminated mud& silt sandstone with ripple mark.
C3	Holds concretion and microdefect laminated mud& silt sandstone with ripple mark.
C4	Holds concretion and microdefect laminated mud& silt sandstone with ripple mark.

Description of Schist specimens after preparing

ID	Schistosity	Damage
SH 4	Nice horizontal veins at top. Small inclusions elsewhere, no clear pattern.	Perfect top, small chips from saw on bottom edge with a small dip on the bottom surface.
SH 5	Slight angled in middle, smaller vein at top of sample.	Perfect top, small chips from saw on bottom edge.
SH 6	Very little, small inclusions, slight angled vein near bottom.	Small saw marks on top and bottom edges.
SH 7	Two veins create eye shaped patterning center.	Both ends in excellent shape.
SH 8	Horizontal vein on top, no other significant pattern.	Tiny dip on top surface, with few shallow saw marks on bottom edge.
SH 9	Few inclusions, no pattern.	No damage.
SH 10	Blotch of pyrite in center, several veins dispersing on an angle from	Small saw teeth marks on top edge.
SH 11	Nice horizontal vein at the top, small striations along column.	No damage.
SH 12	Three small, horizontal striations.	No damage.
SV 2	Vertical grain, but no visible pyrite inclusions.	Small chips along top and bottom edge.

ID	Schistosity	Damage
SV 3	Vertical grain, but no visible pyrite inclusions.	Small chips along top and bottom edge.
SV 4	Vertical grain, with a few visible pyrite inclusions.	Small chips along top and bottom edge.
SV 5	Vertical grain, but no visible pyrite inclusions.	Small chips along top and bottom edge.

Mechanical properties results of UCS test on different core specimens.
*SH - shear; AS - axial splitting; SC - structurally controlled. SH-Specimens cut to have horizontal schistosity. SV-Specimens cut to have vertical schistosity

TI	Stress rate (mm/min)	Duration (Min)	UCS (MPa)	Young's Modulus (GPa)	Failure mode	Structure orientation
SH4	0.25	13.34	78.4	18	SH	90
SH5	0.25	11:05	71.5	21	SH	90
SH 6	0.25	8	27.3	6	SH	90
SH 7	0.25	10.39	47.7	15	SH	90
SH 8	0.25	12.14	51.4	13	SH	90
SH 9	0.25	14.42	57.6	17	SH	90
SH 10	0.25	11.03	46.2	11	SH	90
SH11	0.25	12:42	66.8	17	SH	90
SH13	0.25	12:05	58.8	18	SH	-
S.S1	0.5	7:00	82	17	SH	-
S.S2	0.24	13	80	17	SH	-
SV1	0.3	9:00	101	13	SC	0
SV2	0.25	6:38	111	15	SC	0
SV3	0.3	6:44	81	13	SC	0
SV4	0.3	7:06	94	11	SC	0
SV5	0.3	6:42	77	11	SC	0
SV6	0.4	6:03	47	5	SC	0
G1	0.4	5:00	93	14	SH	-
G2	0.4	5:56	85	12	AS	-
G3	0.4	5:26	129	16	SH	-
D1	0.4	5:22	131	14	SH	-
D2	0.4	5:00	66	10	AS	-
D3	0.4	5:52	119	18	SH	-
L1	0.3	5:36	70	21		
L2	0.3	5:48	40	6		
L3	0.3	5:45	100	15		
W1	0.3	7:48	220	13		
W2	0.3	7:53	205	17		
W3	0.3	7:30	190	11		
C1	0.3	4:17	81	17	SH	90
C3	0.2	9:24	66	ND	Spalling	90
C4	0.2	8	134	18	Burst	90

Geometric details of tested specimens that were used in this study lab program.

Sample. No	Weight (g)	Height (mm)	Diameter (mm)	Area (mm^2)
SH4	695	110	53.87	2278
SH5	693	113	53.87	2278
SH6	707	111	53.93	2283
SH7	832	117	53.96	2286
SH8	739	117	53.96	2286
SH9	773	122	53.87	2278
SH10	796	123	53.87	2278
SH11	718	113	53.82	2274
SH12	790	125	53.96	2286
SH13	798	120	53.93	2283
S.S1	645	121	53.92	2282
S.S2	635	118	53.89	2280
SV1	688	111	53.91	2281
SV2	689	111	53.93	2283
SV3	688	111	53.93	2283
SV4	689	111	53.97	2287
SV5	689	111	53.96	2286
SV6	689	111	53.96	2286
G1	742	121	53.97	2287
G2	741	121	53.93	2283
G3	744	120	53.93	2283
D1	716	120.5	53.94	2284
D2	724	120.5	53.92	2282
D3	723	120.5	53.94	2284
L1	758	124	53.93	2283
L2	730	121	53.975	2287
L3	697	113	53.93	2284
W1	746	121	53.925	2283
W2	752	121	53.92	2282
W3	749	121	53.9	2281
C1	779	124	53.91	2281
C3	790	124	53.94	2284

Sample. No	Weight (g)	Height (mm)	Diameter (mm)	Area (mm^2)
C4	798	124	53.93	2283

Selected sample presented in the sandstone conference paper.

HLD	Actual UCS (MPa)	Nonlinear UCS (MPa)	Least square	Grain size	Source
631	91.7	75.75 ± 11	72.70 ± 8	Fine	Meulenkamp & Grima, 1999
714	91.7	118.20 ± 10	111.7 ± 13	Fine, slightly weathered	Asef, M, 1995
620	82	71.328 ±11	68.59 ± 7	Fine	Verwaal & Mulder, 1993
606	77	66.124 ±11	63.76 ± 7	Fine	Verwaal & Mulder, 1993
659	36.8	87.814 ±10	83.83 ± 9	Fine	Asef, M, 1995
677	35.4	96.627 ±10	91.93 ± 10	Fine	Asef, M, 1995
412	31	23.354 ±8.	23.36 ± 5	Fine	Verwaal & Mulder, 1993
315	15	13.883 ±6	14.14 ± 4	Calcareous	Verwaal & Mulder, 1993
595	38	62.329 ±11	60.22 ± 7	Conglomerate	Meulenkamp & Grima, 1999
591	35.4	61.102 ±11	59.08 ± 7	Conglomerate	Meulenkamp & Grima, 1999
809	219.651	196.914 ±19	182.73 ± 31	Greywacke	Present study
787	204.575	175.338 ±15	163.37 ± 25	Greywacke	Present study
833	189.889	223.535 ±26	206.51 ± 38	Greywacke	Present study
770	198	159.346 ±13	148.97 ± 21	Massive Micaceous	Verwaal and Mulder, 1993
788	142	175.809 ±16	163.79 ± 25	Micaceous, medium grained	Verwaal & Mulder, 1993
667	75.9	91.966 ±10	87.65 ± 9.2	Medium	Meulenkamp & Grima, 1999
649	72.7	83.265 ±11	79.64 ± 8.3	Medium	Meulenkamp & Grima, 1999
627	59.4	73.863 ±11	70.94 ± 7	Medium	Asef, M, 1995
576	52.3	56.31 ±11	54.60 ± 7	Medium	Meulenkamp & Grima, 1999

574	51	55.678 ±11	54.01 ± 7	Medium	Meulenkamp & Grima, 1999
642	39.9	80.191 ±11	76.8 ± 8	Medium	Asef, M, 1995
798	200	185.514 ±17	172.5 1 ± 28	–	Kawasaki et al., 2002
780	200	168.413 ±14	157.1 4 ± 24	–	Kawasaki et al., 2002
767	198	157.051 ±13	146.9 0 ± 21	–	Kawasaki et al., 2002
732	179	130.128 ±10	122.5 2 ± 15	–	Kawasaki et al., 2002
782	179	170.232 ±14	158.7 8 ± 24	–	Kawasaki et al., 2002
712	178	116.869 ±10	110.4 5 ± 12	–	Kawasaki et al., 2002
728	166	127.361 ±10	120.0 1 ± 15	–	Kawasaki et al., 2002
819	149.24	208.197 ±22	192.8 2 ± 34	–	Hack et al 1993
744	135	138.794 ±11	130.3 9 ± 17	–	Kawasaki et al., 2002
756	134.056	148.331 ±11	139.0 ± 19	–	Hack et al 1993
726	113	126 ±10	118.8 ± 14	–	Kawasaki et al., 2002
612	101.5	68.363 ±11	65.84 ± 7	–	Aoki and Matsukura, 2007
658	88.4	87.437 ±11	83.48 ± 9	–	BGC
536	81.6	45.396 ±10.67	44.35 ± 7	–	Present study
538	80.48	45.936 ±10.7	44.86 ± 7	–	Present study
545	75.9	47.671 ±10.8	46.5 ± 7	–	Asef, M, 1995
646	74	81.977 ±10.8	78.45 ± 8	–	Kawasaki et al., 2002
654	74	85.578 ±10.7	81.77 ± 8	–	Kawasaki et al., 2002
666	74	91.277 ±10.5	87.02 ± 9	–	Kawasaki et al., 2002
668	74	92.263 ±10	87.93 ± 9	–	Kawasaki et al., 2002
622	72.2	72.137 ±11	69.34 ± 7	–	Aoki and Matsukura, 2007
482	51.9	33.909 ±10	33.47 ± 6	–	Asef, M, 1995

591	37	60.905 ±11	58.90 ± 7	–	Asef, M, 1995
450	14.5	28.522 ±9	28.33 ± 6	Red, weathered, porous.	Asef, M, 1995

Geometric description of UCS tested Schist used in presented lab program

Sample #	Hole #	Depth (m)	Length . avg	Dia. avg	L/ D	Area (mm^2)	Weight (g)	Volume (cm^3)
1	RMUG14-252,Box-8	42.96-43.17	80.54	36.18	2.23	1027.37	243.33	82.74
2	RMUG14-252,Box-8	47.86-48.14	79.81	36.11	2.21	1023.59	230.82	81.70
1	RMUG14-252,Box-15	85.56-85.75	80.36	36.14	2.22	1025.48	233.19	82.41
1	RMUG14-249,Box-3	14.37-14.64	79.83	36.18	2.21	1027.56	232.16	82.03
2	RMUG14-249,Box-14	76.58-76.83	80.26	36.20	2.22	1028.88	229.18	82.57
3	RMUG14-249,Box-19	103.6-103.89	78.96	36.18	2.18	1027.75	224.11	81.15
4	RMUG14-249,Box-19	104.46-104.72	80.03	36.19	2.21	1027.94	227.98	82.27
5	RMUG14-249,Box-22	120.25-120.52	80.19	36.19	2.22	1027.94	251.56	82.43
6	RMUG14-249,Box-22	121.68-121.9	80.39	36.17	2.22	1026.80	240.73	82.55
7	RMUG14-249,Box-23	128.0-128.25	80.37	36.15	2.22	1025.86	271.01	82.45

Raw Leeb hardness for the four cubic sandstone

#	HLD			
Size (in)	8	4	2	1
Weight (g)	-	2583	288	48
Side (mm)	203.20	101.60	50.80	25.40
Volume cm3	8390.18	1048.77	131.10	16.39
No	HLD			
1	501	547	491	331
2	518	550	502	340
3	526	558	523	351
4	529	558	523	353
5	531	565	528	362
6	533	571	529	363
7	534	578	539	365
8	537	587	541	381
9	543	587	545	387
10	543	596	556	400
11	551	605	558	418
12	556	606	579	423
Mean	534.5	575.5	534.4	372
STD	9.50	18.12	16.93	24.18
CI	3.00	5.73	5.35	7.65
Min	501	547	491	331
Max	556	606	579	423

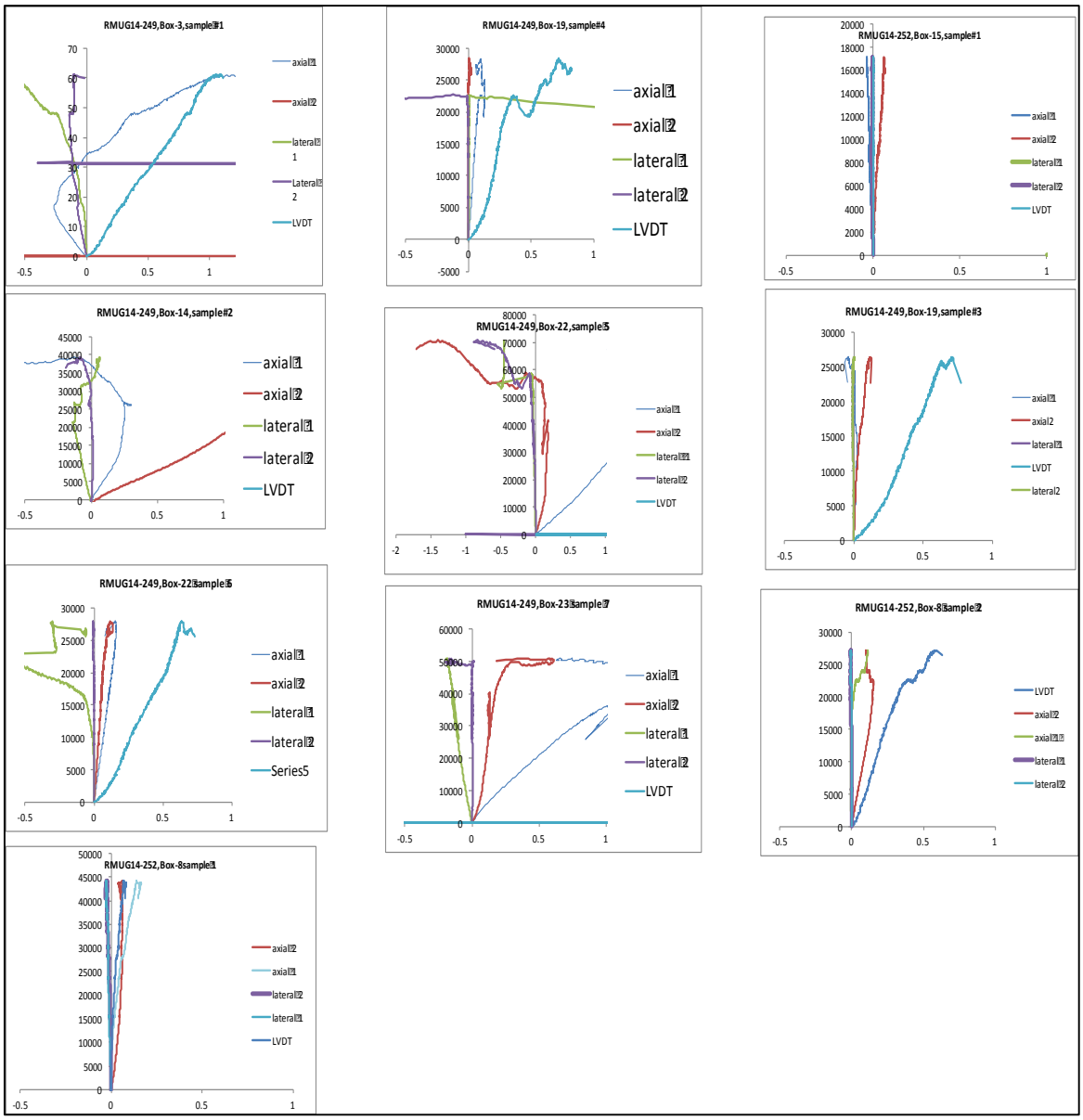

Figure 4.11 Stress - Strain curves of schist specimens, using strain gauge and Linear Variable Differential Transformer (LVDT), which are transducers to measure the displacement for schist core specimens under UCS tests.

UCS test results for some rock specimens used in present lab program

Dalhousie Rock Mechanics Testing	
Test type	UCS
Rock type	Schist (SH4)
Test duration (min)	13:34
Young's Modulus	18.05
Poisson's	0.2334077
UCS (MPa)	78.63216209
Date of Test	10/06/2015 8:56:30 AM

ID	Duration (sec)	μ strain	Force (N)	LVDT	LVDT	Stress (MPa)
1	0.2	0	-450	7.032	6.197	-0.197437063
2	0.4	0	-487	7.035	6.197	-0.213670777
3	0.6	0	-468	7.035	6.199	-0.205334545
4	0.8	0	-450	7.035	6.199	-0.197437063
5	1	0	-431	7.04	6.202	-0.189100831
6	1.2	0	-450	7.035	6.199	-0.197437063
7	1.4	0	-431	7.037	6.202	-0.189100831
8	1.6	0	-450	7.035	6.202	-0.197437063
9	1.8	0	-468	7.037	6.202	-0.205334545
10	2	0	-450	7.04	6.199	-0.197437063
3823	764.6	1406	159001	8.009	6.965	69.76153423
3824	764.8	1405	158777	8.006	6.965	69.66325445
3825	765	1406	158645	8.009	6.965	69.60533958
3826	765.2	1405	158421	8.006	6.962	69.5070598
3827	765.4	1405	158421	8.006	6.962	69.5070598
3828	765.6	1406	158852	8.006	6.967	69.69616063
3829	765.8	1407	159301	8.009	6.965	69.89315894
3830	766	1408	159414	8.006	6.965	69.94273758
3831	766.2	1408	159489	8.011	6.965	69.97564376
3832	766.4	1407	159320	8.009	6.965	69.90149517
3833	766.6	1408	159282	8.011	6.962	69.88482271
3834	766.8	1407	159226	8.011	6.965	69.86025276
3835	767	1408	159133	8.011	6.965	69.8194491
3836	767.2	1408	159076	8.011	6.962	69.79444041
3837	767.4	1408	159526	8.014	6.967	69.99187747
3838	767.6	1409	159957	8.011	6.967	70.1809783

Dalhousie Rock Mechanics Testing	
Test type	UCS

Rock type	G1
Test duration (min)	5.5
Young's Modulus	13.576
Poisson's	-
UCS (MPa)	93
Date of Test	Wed 09 Feb 2005 00:25:12

Time (min)	Position (mm)	Strain	Load (N)	Stress (MPa)
0	0	0	0	0
0.00167	0	0	-6	-0.0026309
0.00333	0	0	-7	-0.0030694
0.005	0	0	-6	-0.0026309
0.00667	0	0	-6	-0.0026309
0.00833	0	0	-7	-0.0030694
0.01	0	0	-5	-0.0021924
0.01167	0	0	-2	-0.000877
0.01333	0	0	0	0
0.015	0	0	0	0
0.01667	0.0063	5.2234E-05	5	0.00219242
0.01833	0.0063	5.2234E-05	3	0.00131545
0.02	0.0063	5.2234E-05	2	0.00087697
0.02167	0.0063	5.2234E-05	2	0.00087697
0.02333	0.0063	5.2234E-05	-5	-0.0021924
0.025	0.0063	5.2234E-05	-9	-0.0039463
0.02667	0.0063	5.2234E-05	-7	-0.0030694
0.02833	0.0063	5.2234E-05	-8	-0.0035079
0.03	0.0063	5.2234E-05	-3	-0.0013154
0.03167	0.0063	5.2234E-05	-2	-0.000877
0.03333	0.0063	5.2234E-05	-2	-0.000877
0.035	0.0127	0.0001053	3	0.00131545
0.03667	0.0127	0.0001053	8	0.00350786
0.03833	0.0127	0.0001053	9	0.00394635
0.04	0.0127	0.0001053	5	0.00219242
0.04167	0.0127	0.0001053	5	0.00219242
0.04333	0.0127	0.0001053	6	0.0026309
0.045	0.0127	0.0001053	5	0.00219242
0.04667	0.0127	0.0001053	6	0.0026309
0.04833	0.0127	0.0001053	15	0.00657725
0.05	0.019	0.00015753	21	0.00920814
0.05167	0.019	0.00015753	21	0.00920814

Time (min)	Position (mm)	Strain	Load (N)	Stress (MPa)
0.05333	0.019	0.00015753	16	0.00701573
0.055	0.019	0.00015753	11	0.00482331
0.05667	0.019	0.00015753	7	0.00306938
0.05833	0.019	0.00015753	3	0.00131545
0.06	0.019	0.00015753	1	0.00043848
0.06167	0.019	0.00015753	0	0
0.06333	0.019	0.00015753	4	0.00175393
0.065	0.019	0.00015753	6	0.0026309
0.06667	0.0254	0.0002106	18	0.00789269
0.06833	0.0254	0.0002106	19	0.00833118
0.07	0.0254	0.0002106	19	0.00833118
0.07167	0.0254	0.0002106	18	0.00789269
0.07333	0.0254	0.0002106	10	0.00438483
0.075	0.0254	0.0002106	12	0.0052618
0.07667	0.0254	0.0002106	16	0.00701573
0.07833	0.0254	0.0002106	14	0.00613876
0.08	0.0254	0.0002106	18	0.00789269
0.08167	0.0317	0.00026283	25	0.01096208
0.08333	0.0317	0.00026283	23	0.01008511
0.085	0.0317	0.00026283	18	0.00789269
0.08667	0.0317	0.00026283	12	0.0052618
0.08833	0.0317	0.00026283	11	0.00482331
0.09	0.0317	0.00026283	7	0.00306938
0.09167	0.0317	0.00026283	8	0.00350786
0.09333	0.0317	0.00026283	10	0.00438483
0.095	0.0317	0.00026283	8	0.00350786
4.79833	1.9177	0.01590001	210965	92.5045773
4.8	1.9177	0.01590001	211278	92.6418225
4.80167	1.9177	0.01590001	211152	92.5865736
4.80333	1.9177	0.01590001	210895	92.4738835
4.805	1.9177	0.01590001	210699	92.3879408
4.80667	1.9177	0.01590001	210628	92.3568085
4.80833	1.9177	0.01590001	210732	92.4024107
4.81	1.9177	0.01590001	211093	92.5607031
4.81167	1.9177	0.01590001	211824	92.8812342
4.81333	1.9241	0.01595307	212635	93.236844
4.815	1.9241	0.01595307	212662	93.248683
4.81667	1.9241	0.01595307	212267	93.0754822
4.81833	1.9241	0.01595307	211756	92.8514174
4.82	1.9241	0.01595307	211277	92.641384
4.82167	1.9241	0.01595307	210877	92.4659908

Time (min)	Position (mm)	Strain	Load (N)	Stress (MPa)
4.82333	1.9241	0.01595307	210546	92.3208529
4.825	1.9241	0.01595307	210245	92.1888695
4.82667	1.9241	0.01595307	210026	92.0928417
4.82833	1.9241	0.01595307	210137	92.1415133
4.83	1.9304	0.01600531	210482	92.29279
4.83167	1.9304	0.01600531	210180	92.1603681
4.83333	1.9304	0.01600531	209510	91.8665844
4.835	1.9304	0.01600531	208792	91.5517536
4.83667	1.9304	0.01600531	208174	91.2807711
4.83833	1.9304	0.01600531	207731	91.0865231
4.84	1.9304	0.01600531	207504	90.9869874
4.84167	1.9304	0.01600531	207509	90.9891798
4.84333	1.9304	0.01600531	207886	91.1544879
4.845	1.9368	0.01605837	208619	91.475896
4.84667	1.9368	0.01605837	209009	91.6469044
4.84833	1.9368	0.01605837	208767	91.5407915
4.85	1.9368	0.01605837	208309	91.3399663
4.85167	1.9368	0.01605837	207855	91.140895
4.85333	1.9368	0.01605837	207494	90.9826026
4.855	1.9368	0.01605837	207296	90.8957829
4.85667	1.9368	0.01605837	207280	90.8887672
4.85833	1.9368	0.01605837	207484	90.9782178
4.86	1.9368	0.01605837	208046	91.2246452
4.86167	1.9431	0.0161106	208636	91.4833502
4.86333	1.9431	0.0161106	207648	91.050129
4.865	1.9431	0.0161106	206435	90.518249
4.86667	1.9431	0.0161106	205285	90.0139935
4.86833	1.9431	0.0161106	204234	89.5531478
4.87	1.9431	0.0161106	203341	89.1615825
4.87167	1.9431	0.0161106	202650	88.8585907
4.87333	1.9431	0.0161106	202169	88.6476803
4.875	1.9495	0.01616367	202044	88.59287
4.87667	1.9495	0.01616367	201591	88.3942371
4.87833	1.9495	0.01616367	196279	86.0650152
4.88	1.9495	0.01616367	189813	83.2297837
4.88167	1.9495	0.01616367	184414	80.8624137
4.88333	1.9495	0.01616367	179490	78.7033232
4.885	1.9495	0.01616367	174768	76.6328062
4.88667	1.9495	0.01616367	170426	74.7289128
4.88833	1.9495	0.01616367	165842	72.7189065
4.89	1.9558	0.0162159	160376	70.3221581

Time (min)	Position (mm)	Strain	Load (N)	Stress (MPa)
4.89167	2.2225	0.01842716	119740	52.5039608
4.89333	2.1209	0.01758478	63727	27.9432095
4.895	2.0002	0.01658403	34336	15.0557541

Dalhousie Rock Mechanics Testing	
Test type	UCS
Rock type	Dolostone (D1)
Test duration (min)	5.22
Young's Modulus	13.576
MR	0.0453
UCS (MPa)	131
Date of Test	Wed 09 Feb 2005 00:54:31

Time (min)	Position (mm)	μ strain	Load (N)	Stress (MPa)
0	0	0	0	0
0.00167	0	0	-5	-0.0021892
0.00333	0	0	-2	-0.0008757
0.005	0.0127	0.00010539	-4	-0.0017513
0.00667	0.0127	0.00010539	-2	-0.0008757
0.00833	0	0	3	0.0013135
0.01	0.0127	0.00010539	1	0.00043783
0.01167	0.0127	0.00010539	-3	-0.0013135
0.01333	0.0127	0.00010539	0	0
0.015	0.0127	0.00010539	4	0.00175133
0.01667	0.0127	0.00010539	-1	-0.0004378
0.01833	0.0127	0.00010539	-2	-0.0008757
0.02	0.0127	0.00010539	-2	-0.0008757
0.02167	0.0127	0.00010539	-6	-0.002627
0.02333	0.0127	0.00010539	-2	-0.0008757
0.025	0.0127	0.00010539	0	0
0.02667	0.0127	0.00010539	2	0.00087567
0.02833	0.0127	0.00010539	4	0.00175133
0.03	0.0191	0.00015849	5	0.00218916
0.03167	0.0191	0.00015849	2	0.00087567
0.03333	0.0191	0.00015849	2	0.00087567
0.035	0.0191	0.00015849	1	0.00043783
0.03667	0.0191	0.00015849	-1	-0.0004378
0.03833	0.0191	0.00015849	-7	-0.0030648
0.04	0.0191	0.00015849	-5	-0.0021892
0.04167	0.0191	0.00015849	-2	-0.0008757

Time (min)	Position (mm)	μ strain	Load (N)	Stress (MPa)
0.04333	0.0191	0.00015849	-4	-0.0017513
0.045	0.0191	0.00015849	-2	-0.0008757
0.04667	0.0191	0.00015849	-2	-0.0008757
0.04833	0.0254	0.00021077	7	0.00306483
0.05	0.0254	0.00021077	9	0.0039405
5.32667	2.1336	0.01770475	296355	129.753989
5.32833	2.1336	0.01770475	296037	129.614758
5.33	2.1336	0.01770475	295883	129.547332
5.33167	2.1336	0.01770475	296000	129.598558
5.33333	2.1336	0.01770475	296471	129.804778
5.335	2.1336	0.01770475	297253	130.147163
5.33667	2.1399	0.01775703	298288	130.60032
5.33833	2.1399	0.01775703	298770	130.811356
5.34	2.1399	0.01775703	298649	130.758378
5.34167	2.1399	0.01775703	298333	130.620023
5.34333	2.1399	0.01775703	298019	130.482543
5.345	2.1399	0.01775703	297813	130.392349
5.34667	2.1399	0.01775703	297778	130.377025
5.34833	2.1399	0.01775703	298033	130.488673
5.35	2.1463	0.01781014	298607	130.739989
5.35167	2.1463	0.01781014	299048	130.933073
5.35333	2.1463	0.01781014	298700	130.780707
5.355	2.1463	0.01781014	297996	130.472473
5.35667	2.1463	0.01781014	297287	130.162049
5.35833	2.1463	0.01781014	296750	129.926933
5.36	2.1463	0.01781014	296204	129.687876
5.36167	2.1463	0.01781014	294889	129.112126
5.36333	2.1463	0.01781014	293394	128.457566
5.365	2.1527	0.01786325	292045	127.866929
5.36667	2.2035	0.01828479	290035	126.986885
5.36833	2.4447	0.02028628	180012	78.8151881
5.37	2.3876	0.01981246	96516	42.2578866
5.37167	2.2352	0.01854784	51871	22.7108338

Details of database that were used in this study

No	Source	HLD	UCS (MPa)	Rock type
1	Kawasaki et al., 2002	324	3	Greenschist
2	Asef, M, 1995	358	4	gypsum and silty clay
3	Asef, M, 1995	357	5	gypsum and silty clay
4	Asef, M, 1995	339	5	gypsum
5	Verwaal and Mulder, 1993	377	6	Calcarenite
6	Kawasaki et al., 2002	262	6	Greenschist
7	Meulenkamp and Grima, 1999	401	7	mudstone
8	Verwaal and Mulder, 1993	255	8	Gypsum
9	Kawasaki et al., 2002	470	12	Greenschist
10	Kawasaki et al., 2002	265	13	Greenschist
11	Asef, M, 1995	385	14	conclomerated
12	NW Zone PFS	474	15	Metavolcanics
13	Kawasaki et al., 2002	316	15	Greenschist
14	Verwaal and Mulder, 1993	274	15	Sandstone
15	Aoki and Matsukura, 2007	409	16	Tuff
16	Lee et al2014	420	17	Laminated Shale
17	NW Zone PFS	550	18	Metavolcanics
18	Cobre Del Mayo	487	18	Porphyry
19	Kawasaki et al., 2002	476	18	Shale
20	Verwaal and Mulder, 1993	500	22	Limestone
21	Cobre Del Mayo	387	22	Hornfels
22	Cobre Del Mayo	480	23	Hornfels
23	Asef, M, 1995	514	24	conclomerated
24	Aoki and Matsukura, 2007	562	25	Limestone
25	Lee et al2014	562	26	Laminated Shale
26	Kawasaki et al., 2002	495	26	Shale
27	Lee et al2014	590	27	Laminated Shale
28	Lee et al2014	564	27	Laminated Shale
29	Kawasaki et al., 2002	515	27	Greenschist
30	Asef, M, 1995	385	27	sandstone
31	Yassir, 2016	570	28	Qtz-chlorite Schist
32	Cobre Del Mayo	600	30	Hornfels
33	Asef, M, 1995	600	30	dolomitic calcilutite
34	Verwaal and Mulder, 1993	456	31	Limestone
35	Verwaal and Mulder, 1993	412	31	Sandstone
36	Cobre Del Mayo	400	31	Hornfels
37	Lee et al2014	693	32	Laminated Shale
38	Lee et al2014	526	32	Laminated Shale
39	Kawasaki et al., 2002	486	32	Shale
40	Lee et al2014	448	33	Laminated Shale
41	Lee et al2014	514	34	Laminated Shale
42	Kawasaki et al., 2002	501	34	Greenschist

43	Lee et al2014	591	35	Laminated Shale
44	Coal Valley	537	35	Siltstone
45	Meulenkamp and Grima, 1999	455	35	sandstone
46	Lee et al2014	548	36	Laminated Shale
47	Lee et al2014	500	37	Laminated Shale
48	Lee et al2014	601	38	Laminated Shale
49	Meulenkamp and Grima, 1999	595	38	sandstone
50	Yassir, 2016	555	38	Mafic Dyke
51	Lee et al2014	464	38	Laminated Shale
52	Verwaal and Mulder, 1993	539	39	Dolomite
53	Verwaal and Mulder, 1993	526	39	Limestone
54	Yassir, 2016	574	40	limestone
55	Lee et al2014	504	41	Laminated Shale
56	Lee et al2014	439	42	Laminated Shale
57	Lee et al2014	447	43	Laminated Shale
58	Coal Valley	644	44	Siltstone
59	Lee et al2014	523	44	Laminated Shale
60	Asef, M, 1995	695	45	conglomerates
61	Kawasaki et al., 2002	583	45	Greenschist
62	Lee et al2014	662	46	Laminated Shale
63	Lee et al2014	526	46	Laminated Shale
64	yassir2016	466	46	schist-H
65	Lee et al2014	553	47	Laminated Shale
66	Lee et al2014	471	48	Laminated Shale
67	yassir2016	464	48	schist-H
68	Lee et al2014	536	50	Laminated Shale
69	Lee et al2014	670	51	Laminated Shale
70	Lee et al2014	574	51	Laminated Shale
71	Lee et al2014	547	51	Laminated Shale
72	Meulenkamp and Grima, 1999	531	51	sandstone
73	yassir2016	531	51	schist-H
74	Lee et al2014	502	51	Laminated Shale
75	Cobre Del Mayo	630	52	Porphyry
76	Meulenkamp and Grima, 1999	576	52	sandstone
77	Cobre Del Mayo	558	54	Porphyry
78	Lee et al2014	527	54	Laminated Shale
79	Lee et al2014	576	55	Laminated Shale
80	Lee et al2014	526	55	Laminated Shale
81	Lee et al2014	523	55	Laminated Shale
82	Lee et al2014	480	55	Laminated Shale
83	Lee et al2014	520	56	Laminated Shale

84	Verwaal and Mulder, 1993	593	57	Limestone
85	Asef, M, 1995	464	57	dolomitic breccia
86	Yassir, 2016	697	58	schist-H
87	Lee et al2014	694	58	Laminated Shale
88	Asef, M, 1995	532	58	limestone muds-calcilutite
89	Asef, M, 1995	690	59	limestone
90	Yassir, 2016	642	59	schist-H
91	Asef, M, 1995	627	59	sandstone
92	Lee et al2014	644	60	Laminated Shale
93	Lee et al2014	591	60	Laminated Shale
94	Aoki and Matsukura, 2007	553	60	Tuff
95	Coal Valley	473	60	Sandy siltstone
96	Asef, M, 1995	602	61	sandstone
97	Yassir, 2016	490	61	Mafic Dyke
98	Lee et al2014	659	62	Laminated Shale
99	Meulenkamp and Grima, 1999	564	62	limestone
100	NW Zone PFS	458	62	Metavolcanics
101	Asef, M, 1995	585	63	sandy clay
102	Lee et al2014	586	64	Laminated Shale
103	Aoki and Matsukura, 2007	545	64	Andesite
104	Asef, M, 1995	485	64	limestone muds-calcilutite
105	Brucejack	575	65	Intrusive
106	Lee et al2014	562	65	Laminated Shale
107	Lee et al2014	520	65	Laminated Shale
108	Asef, M, 1995	482	65	limestone
109	Lee et al2014	676	66	Laminated Shale
110	Lee et al2014	593	66	Laminated Shale
111	Asef, M, 1995	511	66	dolomitic limestone
112	Yassir, 2016	428	66	dolomites
113	Yassir, 2016	609	67	schist-H
114	Verwaal and Mulder, 1993	573	67	Dolomite

115	Lee et al2014	493	68	Laminated Shale
116	Yassir, 2016	689	69	Qtz-chlorite Schist
117	Lee et al2014	542	69	Laminated Shale
118	Yassir, 2016	655	70	limestone
119	Asef, M, 1995	620	71	calcilutite
120	Verwaal and Mulder, 1993	587	71	Limestone
121	Yassir, 2016	655	72	schist-H
122	Brucejack	622	72	Intrusive
123	Aoki and Matsukura, 2007	576	72	Sandstone
124	Lee et al2014	472	72	Laminated Shale
125	Meulenkamp and Grima, 1999	659	73	sandstone
126	Meulenkamp and Grima, 1999	649	73	limestone
127	Verwaal and Mulder, 1993	668	74	Limestone
128	Kawasaki et al., 2002	666	74	Sandstone
129	Kawasaki et al., 2002	654	74	Sandstone
130	Kawasaki et al., 2002	646	74	Sandstone
131	Kawasaki et al., 2002	627	74	Sandstone
132	RoxGold	646	75	Mafiv Volcanic
133	Lee et al2014	608	75	Laminated Shale
134	Meulenkamp and Grima, 1999	516	75	dolomite
135	Miller-Braeside	667	76	Limestone
136	Asef, M, 1995	621	76	sandstone
137	Meulenkamp and Grima, 1999	545	76	sandstone
138	Yassir, 2016	790	77	schist-V

139	Verwaal and Mulder, 1993	682	77	sandstone
140	Kawasaki et al., 2002	606	77	Shale
141	Lee et al2014	582	77	Laminated Shale
142	Lee et al2014	564	77	Laminated Shale
143	yassir2016	669	78	schist-H
144	Lee et al2014	564	78	Laminated Shale
145	Brucejack	642	80	Intrusive
146	Yassir, 2016	538	80	sandstone
147	Miller-Braeside	786	81	Limestone
148	Yassir, 2016	702	81	schist-V
149	Yassir, 2016	620	82	sandstone
150	Verwaal and Mulder, 1993	536	82	Sandstone
151	Verwaal and Mulder, 1993	783	85	Limestone
152	Yassir, 2016	637	85	granite
153	Meulenkamp and Grima, 1999	647	86	dolomite
154	RoxGold	684	88	Mafic Volcanic
155	Brucejack	658	88	Sandstone
156	Asef, M, 1995	688	89	dolomitic calcilutite
157	Kawasaki et al., 2002	795	90	Shale
158	Miller-Braeside	724	90	Limestone
159	NW Zone PFS	723	90	Metavolcanics
160	Meulenkamp and Grima, 1999	631	92	sandstone
161	Yassir, 2016	806	93	granite
162	Miller-Braeside	763	94	Limestone

163	Brucejack	652	94	Conglomerate
164	Brucejack	603	94	Porphyry
165	Verwaal and Mulder, 1993	601	94	Marble
166	Yassir, 2016	564	94	schist-V
167	Asef, M, 1995	788	95	dolomitic limestone
168	RoxGold	660	95	Granite
169	Miller-Braeside	666	96	Limestone
170	Asef, M, 1995	706	97	limestone
171	Asef, M, 1995	662	99	limeston breccia and conglomerate
172	Meulenkamp and Grima, 1999	644	99	limestone
173	Miller-Braeside	716	100	Limestone
174	Yassir, 2016	582	100	limestone
175	Verwaal and Mulder, 1993	762	101	Limestone
176	Asef, M, 1995	636	101	dolomitic breccia
177	Yassir, 2016	608	101	schist-V
178	Aoki and Matsukura, 2007	699	102	Sandstone
179	Miller-Braeside	612	102	Limestone
180	Meulenkamp and Grima, 1999	668	103	limestone
181	Miller-Braeside	609	105	Limestone
182	Brucejack	681	106	Porphyry
183	Asef, M, 1995	793	109	limestone
184	Cobre Del Mayo	660	109	Hornfels
185	Asef, M, 1995	767	111	dolomitic calcilutite
186	yassir2016	644	111	schist-V

187	Meulenkamp and Grima, 1999	726	113	limestone
188	Kawasaki et al., 2002	724	113	Sandstone
189	Kawasaki et al., 2002	738	116	Greenschist
190	yassir2016	703	119	dolomites
191	Asef, M, 1995	629	119	limestone
192	Meulenkamp and Grima, 1999	574	119	limestone
193	Asef, M, 1995	750	120	limestone
194	Meulenkamp and Grima, 1999	706	120	dolornitic lmst
195	KGHM Ajax	816	121	Diorite
196	Asef, M, 1995	692	121	limestone
197	Kawasaki et al., 2002	607	121	Shale
198	Asef, M, 1995	718	122	dolomitic calcilutite
199	Asef, M, 1995	712	122	calcarenite
200	Asef, M, 1995	636	123	dolomitic breccia
201	Asef, M, 1995	694	124	limestone and dolomite
202	Miller-Braeside	596	124	Limestone
203	Asef, M, 1995	626	127	limestone and dolomite
204	yassir2016	790	129	granite
205	Asef, M, 1995	736	130	limestone muds-calcilutite
206	yassir2016	560	131	dolomites
207	KGHM Ajax	633	132	Diorite
208	Meulenkamp and Grima, 1999	706	133	limestone
209	Asef, M, 1995	653	133	limestone muds-calcilutite
210	Hack et al 1993	788	134	Sandstone

211	Cobre Del Mayo	757	134	Porphyry
212	Cobre Del Mayo	756	134	Porphyry
213	RoxGold	716	134	Granite
214	Asef, M, 1995	851	135	limestone
215	NW Zone PFS	744	135	Metavolcanics
216	Kawasaki et al., 2002	712	135	Sandstone
217	Asef, M, 1995	780	136	limestone and dolomite
218	KGHM Ajax	668	136	Volcanics
219	Meulenkamp and Grima, 1999	614	136	limestone
220	Meulenkamp and Grima, 1999	713	138	limestone
221	Hack et al 1993	634	138	granite
222	Hack et al 1993	838	139	granite
223	Asef, M, 1995	703	140	limestone muds-calcilutite
224	Asef, M, 1995	788	142	dolomitic limestone
225	Verwaal and Mulder, 1993	714	142	Sandstone
226	Meulenkamp and Grima, 1999	689	142	limestone
227	Asef, M, 1995	707	144	dolomitic limestone
228	Kawasaki et al., 2002	869	149	Granite
229	Hack et al 1993	819	149	Sandstone
230	Hack et al 1993	890	151	granite
231	RoxGold	753	151	Granite
232	NW Zone PFS	856	152	Metavolcanics
233	Kawasaki et al., 2002	811	152	Granite
234	Aoki and Matsukura, 2007	852	153	Gabrro

235	Asef, M, 1995	678	154	dolomitic breccia
236	KGHM Ajax	863	155	Volcanics
237	Hack et al 1993	807	155	granite
238	Verwaal and Mulder, 1993	801	155	granite
239	Kawasaki et al., 2002	616	155	Granite
240	Asef, M, 1995	874	159	limestone
241	Verwaal and Mulder, 1993	707	159	Limestone
242	RoxGold	696	159	Granite
243	Asef, M, 1995	685	160	limestone
244	Asef, M, 1995	681	160	limestone-calcarenite layers
245	Asef, M, 1995	643	160	limestone muds-calcilutite
246	Asef, M, 1995	818	161	limestone muds-calcilutite
247	Hack et al 1993	713	161	granite
248	Meulenkamp and Grima, 1999	739	162	limestone
249	Meulenkamp and Grima, 1999	723	162	limestone
250	Aoki and Matsukura, 2007	872	163	Granite
251	Meulenkamp and Grima, 1999	862	163	limestone
252	Verwaal and Mulder, 1993	751	163	Limestone
253	Hack et al 1993	687	163	granite
254	NW Zone PFS	812	165	Metavolcanics
255	Kawasaki et al., 2002	728	166	Sandstone
256	Asef, M, 1995	722	168	dolomitic breccia
257	Meulenkamp and Grima, 1999	844	169	limestone
258	NW Zone PFS	720	169	Metavolcanics

259	NW Zone PFS	771	172	Metavolcanics
260	Asef, M, 1995	701	173	limestone muds-calcilutite
261	Asef, M, 1995	865	174	limestone
262	Hack et al 1993	643	174	granite
263	Verwaal and Mulder, 1993	640	174	Limestone
264	Aoki and Matsukura, 2007	853	175	Granite
265	Asef, M, 1995	664	175	limestone muds-calcilutite
266	Hack et al 1993	685	176	Limestone
267	Verwaal and Mulder, 1993	653	176	Limestone
268	Hack et al 1993	856	178	granite
269	KGHM Ajax	712	178	Volcanics
270	Kawasaki et al., 2002	596	178	Sandstone
271	Kawasaki et al., 2002	782	179	Sandstone
272	Kawasaki et al., 2002	732	179	Sandstone
273	Hack et al 1993	721	181	Limestone
274	Hack et al 1993	695	181	Limestone
275	Asef, M, 1995	711	182	dolomitic limestone
276	Hack et al 1993	561	182	Limestone
277	Verwaal and Mulder, 1993	705	183	Limestone
278	Verwaal and Mulder, 1993	688	186	Limestone
279	Hack et al 1993	798	187	Limestone
280	Meulenkamp and Grima, 1999	710	187	granite
281	Asef, M, 1995	909	188	limestone muds-calcilutite
282	RoxGold	656	188	Felsic Dyke

283	Meulenkamp and Grima, 1999	869	189	granite
284	yassir2016	833	190	sandstone graywake
285	NW Zone PFS	804	192	Metavolcanics
286	Asef, M, 1995	711	196	limestone
287	Kawasaki et al., 2002	770	198	Sandstone
288	Verwaal and Mulder, 1993	767	198	Sandstone
289	Asef, M, 1995	597	199	dolomitic limestone
290	Asef, M, 1995	798	200	dolomites
291	Asef, M, 1995	780	200	limestone
292	Kawasaki et al., 2002	717	200	Sandstone
293	Kawasaki et al., 2002	712	200	Sandstone
294	Verwaal and Mulder, 1993	698	203	Limestone
295	yassir2016	788	205	sandstone graywake
296	Meulenkamp and Grima, 1999	856	206	granite
297	Asef, M, 1995	714	210	dolomitic limestone
298	Asef, M, 1995	718	214	dolomites
299	yassir2016	809	220	sandstone graywake
300	NW Zone PFS	867	232	Metavolcanics
301	Asef, M, 1995	833	234	granodiorite
302	KGHM Ajax	670	249	Volcanics
303	Meulenkamp and Grima, 1999	871	257	granodiorite
304	Asef, M, 1995	718	259	limestone muds-calcilutite
305	NW Zone PFS	824	261	Metavolcanics
306	Meulenkamp and Grima, 1999	854	262	granite

307	Meulenkamp and Grima, 1999	827	270	granodiorite
308	Asef, M, 1995	682	272	thinly bedded dolomite
309	Asef, M, 1995	911	274	granodiorite
310	Meulenkamp and Grima, 1999	862	275	granodiorite
311	NW Zone PFS	912	285	Metavolcanics

Sandstone datapoints (UCS - HLD correlation)

HLD	UCS (MPa)	Fits	CI lower	CI upper
809	220	197	177	217
788	205	175	160	191
798	200	186	168	203
780	200	168	154	183
770	198	159	146	172
767	198	157	145	170
833	190	224	197	250
782	179	170	156	185
732	179	130	120	140
712	178	117	107	127
728	166	127	117	138
819	149	208	186	231
788	142	176	160	191
744	135	139	128	150
756	134	148	137	160
726	113	126	116	136
612	102	68	57	79
631	92	76	65	87
714	92	118	108	128
658	88	87	77	98
620	82	71	60	82
536	82	45	35	56
538	80	46	35	57
606	77	66	55	77
667	76	92	82	102
545	76	48	37	58
668	74	92	82	103
666	74	91	81	102
654	74	86	75	96
646	74	82	71	93
649	73	83	73	94
622	72	72	61	83
627	59	74	63	85
576	52	56	45	67
482	52	34	24	44
574	51	56	45	67
642	40	80	69	91
595	38	62	51	73
591	37	61	50	72

HLD	UCS (MPa)	Fits	CI lower	CI upper
659	37	88	77	98
591	35	61	50	72
677	35	97	86	107
412	31	23	15	32
316	15	14	7	20
450	15	29	19	38

Igneous datapoints (UCS - HLD correlation)

HLD	UCS (MPa)	Fits	CI lower	CI upper
827	270	170	156	184
854	262	182	166	199
871	257	190	171	209
869	189	189	171	208
862	275	186	168	203
856	206	183	166	200
798	187	158	144	171
409	16	38	19	56
644	60	100	82	118
872	163	191	172	209
853	175	182	165	198
485	64	54	34	74
852	153	181	165	198
807	155	161	148	175
487	18	55	35	75
558	54	73	53	93
630	52	95	77	113
716	134	125	110	140
757	134	141	127	154
684	88	113	97	130
874	159	191	172	211
788	95	153	140	166
788	134	153	140	166
909	188	208	184	233
890	151	199	178	220
646	75	100	82	118
642	80	99	81	117
576	72	78	59	98
681	106	112	96	129

HLD	UCS (MPa)	Fits	CI lower	CI upper
562	65	74	54	94
601	94	86	67	105
670	249	108	92	125
607	121	88	69	107
633	132	96	78	114
780	136	150	137	163
616	155	91	72	109
596	178	84	65	104
856	152	183	166	200
863	155	186	169	204
869	149	189	171	208
856	178	183	166	200
865	174	187	169	205
862	163	186	168	203
753	151	139	126	153
801	155	159	146	172
818	161	166	152	180
713	138	124	109	139
838	139	175	160	190
833	234	173	158	188
911	274	209	184	234
806	93	161	148	174
783	85	151	138	164
790	129	154	141	167
602	61	86	67	105
601	38	86	67	105

Sedimentary datapoints (UCS - HLD correlation)

HLD	UCS (MPa)	Fits	CI lower	CI upper
720	169	141	134	147
751	163	159	151	168
723	162	143	136	149
724	113	143	136	150
662	99	110	105	115
647	86	103	98	108
659	73	109	104	114
649	73	104	99	109
564	62	69	63	75

HLD	UCS (MPa)	Fits	CI lower	CI upper
576	52	74	68	79
574	51	73	67	79
591	35	79	74	85
739	162	152	144	160
689	142	124	119	129
634	138	97	92	102
668	136	113	108	118
653	133	106	101	111
750	120	159	150	167
629	119	95	90	100
668	103	113	108	118
631	92	96	91	101
667	76	113	108	118
608	75	86	81	91
595	38	81	75	86
401	7	26	20	31
622	72	92	87	97
612	102	88	82	93
562	25	68	63	74
255	8	7	4	9
262	6	7	5	10
316	15	13	9	16
387	22	23	18	28
400	31	25	20	31
412	31	28	22	33
464	57	39	33	45
526	39	56	50	62
539	39	61	55	67
573	67	72	67	78
587	71	78	72	83
606	77	85	80	91
608	101	86	81	91
620	82	91	86	96
627	74	94	89	99
637	85	99	94	104
640	174	100	95	105
653	176	106	101	111
687	163	123	118	128
688	186	123	118	129

HLD	UCS (MPa)	Fits	CI lower	CI upper
696	159	128	122	133
698	203	129	123	134
705	183	132	127	138
770	198	171	161	182
788	142	183	171	195
564	94	69	63	75
658	88	108	103	113
537	35	60	54	66
591	60	79	74	85
644	44	102	97	107
693	32	126	121	131
724	44	143	136	150
682	77	120	115	126
723	90	143	136	149
816	121	203	187	218
699	102	129	124	135
609	105	86	81	92
724	90	143	136	150
652	94	106	101	111
702	81	131	125	137
582	100	76	70	81
666	96	112	107	117
621	76	92	86	97
694	124	127	121	132
646	74	103	98	108
654	74	106	101	111
666	74	112	107	117
668	74	113	108	118
726	113	144	137	151
744	135	155	147	163
728	166	145	138	152
712	178	136	130	143
732	179	148	141	155
782	179	179	168	191
798	200	190	177	203
780	200	178	167	189
767	198	169	159	179
550	18	64	58	70
685	176	122	117	127

HLD	UCS (MPa)	Fits	CI lower	CI upper
695	181	127	122	133
711	182	136	130	142
721	181	141	135	148
710	187	135	129	141
756	134	162	153	171
819	149	205	189	221
536	50	60	54	66
531	51	58	52	64
526	46	56	50	62
555	38	66	60	72
523	44	56	49	62
526	32	56	50	62
547	51	63	57	69
520	65	55	49	61
516	75	53	47	59
504	41	50	44	56
480	55	43	37	49
527	54	57	51	63
515	27	53	47	59
520	56	55	49	61
553	47	65	59	71
511	66	52	46	58
526	55	56	50	62
548	36	64	58	70
582	77	76	70	81
564	78	69	63	75
531	51	58	52	64
576	55	74	68	79
545	64	63	57	69
553	60	65	59	71
466	46	40	34	46
455	35	37	31	43
471	48	41	35	47
532	58	58	52	64
493	68	47	41	53
486	32	45	39	51
472	72	41	35	47
482	65	44	38	50
458	62	38	32	44

HLD	UCS (MPa)	Fits	CI lower	CI upper
448	33	35	30	41
420	17	29	24	35
447	43	35	29	41
385	27	23	18	28
439	42	33	28	39
473	60	41	35	47
428	66	31	25	37
464	38	39	33	45
495	26	47	41	53
564	77	69	63	75
542	69	62	56	68
500	37	49	43	55
523	55	56	49	62
502	51	49	43	55
501	34	49	43	55
714	210	137	131	144
722	168	142	135	149
692	121	125	120	131
712	122	136	130	143
711	196	136	130	142
575	65	73	67	79
643	174	101	96	106
660	95	109	104	114
636	101	98	93	103
593	57	80	75	86
707	159	134	128	140
385	14	23	18	28
514	24	53	47	59
627	59	94	89	99
545	76	63	57	69
707	144	134	128	140
717	200	139	133	146
714	142	137	131	144
676	66	117	112	122
706	120	133	127	139
718	214	140	133	146
712	200	136	130	143
583	45	76	71	82
712	135	136	130	143

HLD	UCS (MPa)	Fits	CI lower	CI upper
681	160	120	115	125
643	160	101	96	106
703	119	131	126	137
690	59	124	119	130
706	97	133	127	139
644	99	102	97	107
585	63	77	71	83
614	136	89	83	94
596	124	81	76	87
626	127	94	89	99
660	109	109	104	114
718	122	140	133	146
358	4	18	14	23
339	5	16	12	20
490	61	46	40	52
688	89	123	118	129
600	30	83	77	88
644	111	102	97	107
656	188	107	102	112
706	133	133	127	139
736	130	150	143	158
685	160	122	117	127
664	175	111	106	116
620	71	91	86	96
703	140	131	126	137
697	58	128	123	134
701	173	130	125	136
713	161	137	131	143
590	27	79	73	84
586	64	77	72	83
636	123	98	93	103
678	154	118	113	123
357	5	18	14	23
536	82	60	54	66
538	80	60	54	66
655	70	107	102	112
574	40	73	67	79
716	100	139	132	145
560	131	68	62	74

HLD	UCS (MPa)	Fits	CI lower	CI upper
593	66	80	75	86
574	119	73	67	79
809	220	198	183	212
788	205	183	171	195
833	190	215	198	233

Metamorphic datapoints (UCS - HLD correlation)

HLD	UCS (MPa)	Fits	CI lower	CI upper
603	94	43	32	53
265	13	5	2	9
274	15	6	2	9
324	3	8	3	12
377	6	11	5	16
470	12	19	11	27
514	34	25	16	33
564	27	34	24	43
695	45	74	63	86
738	116	96	85	108
669	78	63	52	75
655	72	58	47	70
464	48	18	11	26
670	51	64	52	76
694	58	74	62	86
662	46	61	49	72
609	67	44	33	55
642	59	54	43	65
762	101	112	100	123
767	111	115	103	126
786	81	129	117	141
763	94	112	101	124
790	77	132	120	144
570	28	35	25	45
689	69	72	60	83
771	172	118	106	129
476	18	20	12	27
811	152	150	137	163
659	62	60	48	71
795	90	136	124	148
844	169	183	166	200

HLD	UCS (MPa)	Fits	CI lower	CI upper
804	192	144	131	156
912	285	277	237	316
474	15	19	12	27
851	135	191	173	210
812	165	151	138	164
867	232	211	188	233
824	261	162	148	177
793	109	135	123	147
456	31	17	10	25
600	30	42	31	52
480	23	20	12	28
500	22	23	15	31

Statistical details of database (UCS - HLD correlation)

HLD	UCS (MPa)	Fits	CI lower	CI upper
912	285	228	212	244
911	274	228	212	243
909	188	226	211	242
890	151	215	201	229
874	159	206	193	218
872	163	205	192	217
871	257	204	192	216
869	189	203	191	215
869	149	203	191	215
867	232	202	190	214
865	174	201	189	213
863	155	200	188	211
862	275	199	188	211
862	163	199	188	211
856	178	196	185	207
856	152	196	185	207
856	206	196	185	207
854	262	195	184	206
853	175	194	183	205
852	153	194	183	204
851	135	193	182	204
844	169	189	179	199
838	139	186	176	196
833	190	183	174	193

HLD	UCS (MPa)	Fits	CI lower	CI upper
833	234	183	174	193
827	270	180	171	189
824	261	179	170	187
819	149	176	167	185
818	161	175	167	184
816	121	174	166	183
812	165	172	164	181
811	152	172	164	180
809	220	171	163	179
807	155	170	162	178
806	93	169	161	177
804	192	168	160	176
801	155	167	159	174
798	187	165	158	173
798	200	165	158	173
795	90	164	156	171
793	109	163	155	170
790	129	161	154	168
790	77	161	154	168
788	142	160	153	167
788	95	160	153	167
788	205	160	153	167
788	134	160	153	167
786	81	159	152	166
783	85	158	151	165
782	179	157	151	164
780	200	156	150	163
780	136	156	150	163
771	172	152	146	158
770	198	152	145	158
767	111	150	144	156
767	198	150	144	156
763	94	148	142	154
762	101	148	142	154
757	134	145	140	151
756	134	145	139	151
753	151	144	138	149
751	163	143	137	148
750	120	142	137	148

HLD	UCS (MPa)	Fits	CI lower	CI upper
744	135	139	134	145
739	162	137	132	143
738	116	137	131	142
736	130	136	130	141
732	179	134	129	139
728	166	132	127	138
726	113	131	126	137
724	113	131	125	136
724	90	131	125	136
723	162	130	125	135
723	90	130	125	135
722	168	130	125	135
721	181	129	124	134
720	169	129	124	134
718	259	128	123	133
718	214	128	123	133
718	122	128	123	133
717	200	128	122	133
716	100	127	122	132
716	134	127	122	132
714	210	126	121	131
714	142	126	121	131
713	161	126	121	131
713	138	126	121	131
712	122	125	120	130
712	200	125	120	130
712	178	125	120	130
712	135	125	120	130
711	182	125	120	130
711	196	125	120	130
710	187	125	119	130
707	144	123	118	128
707	159	123	118	128
706	120	123	118	128
706	133	123	118	128
706	97	123	118	128
705	183	122	117	127
703	140	122	117	127
703	119	122	117	127

HLD	UCS (MPa)	Fits	CI lower	CI upper
702	81	121	116	126
701	173	121	116	126
699	102	120	115	125
698	203	119	115	124
697	58	119	114	124
696	159	119	114	124
695	45	118	113	123
695	181	118	113	123
694	58	118	113	123
694	124	118	113	123
693	32	117	112	122
692	121	117	112	122
690	59	116	111	121
689	142	116	111	121
689	69	116	111	121
688	186	115	110	120
688	89	115	110	120
687	163	115	110	120
685	160	114	109	119
685	176	114	109	119
684	88	114	109	119
682	272	113	108	118
682	77	113	108	118
681	106	113	108	118
681	160	113	108	118
678	154	111	106	116
676	66	111	106	116
670	51	108	103	113
670	249	108	103	113
669	78	108	103	113
668	136	107	102	112
668	103	107	102	112
668	74	107	102	112
667	76	107	102	112
666	96	107	102	112
666	74	107	102	112
664	175	106	101	111
662	46	105	100	110
662	99	105	100	110

HLD	UCS (MPa)	Fits	CI lower	CI upper
660	109	104	99	109
660	95	104	99	109
659	73	104	99	109
659	62	104	99	109
658	88	104	99	109
656	188	103	98	108
655	70	102	97	108
655	72	102	97	108
654	74	102	97	107
653	176	102	97	107
653	133	102	97	107
652	94	101	96	106
649	73	100	95	105
647	86	99	94	105
646	75	99	94	104
646	74	99	94	104
644	99	98	93	103
644	60	98	93	103
644	111	98	93	103
644	44	98	93	103
643	174	98	93	103
643	160	98	93	103
642	80	98	92	103
642	59	98	92	103
640	174	97	92	102
637	85	96	91	101
636	123	95	90	101
636	101	95	90	101
634	138	95	89	100
633	132	94	89	100
631	92	94	88	99
630	52	93	88	98
629	119	93	88	98
627	74	92	87	97
627	59	92	87	97
626	127	92	87	97
622	72	90	85	96
621	76	90	85	95
620	82	90	84	95

HLD	UCS (MPa)	Fits	CI lower	CI upper
620	71	90	84	95
616	155	88	83	94
614	136	88	82	93
612	102	87	82	92
609	105	86	80	91
609	67	86	80	91
608	101	86	80	91
608	75	86	80	91
607	121	85	80	91
606	77	85	79	90
603	94	84	78	89
602	61	84	78	89
601	94	83	78	89
601	38	83	78	89
600	30	83	77	88
600	30	83	77	88
597	199	82	76	87
596	178	82	76	87
596	124	82	76	87
595	38	81	76	87
593	57	81	75	86
593	66	81	75	86
591	35	80	74	85
591	60	80	74	85
590	27	80	74	85
587	71	79	73	84
586	64	78	73	84
585	63	78	72	84
583	45	77	72	83
582	100	77	71	83
582	77	77	71	83
576	52	75	69	81
576	72	75	69	81
576	55	75	69	81
575	65	75	69	80
574	119	74	69	80
574	51	74	69	80
574	40	74	69	80
573	67	74	68	80

HLD	UCS (MPa)	Fits	CI lower	CI upper
570	28	73	68	79
564	62	71	66	77
564	78	71	66	77
564	77	71	66	77
564	27	71	66	77
564	94	71	66	77
562	25	71	65	76
562	65	71	65	76
562	26	71	65	76
561	182	70	65	76
560	131	70	64	76
558	54	70	64	75
555	38	69	63	74
553	60	68	62	74
553	47	68	62	74
550	18	67	61	73
548	36	67	61	72
547	51	66	61	72
545	76	66	60	71
545	64	66	60	71
542	69	65	59	71
539	39	64	58	70
538	80	64	58	69
537	35	63	58	69
536	82	63	57	69
536	50	63	57	69
532	58	62	56	68
531	51	62	56	67
531	51	62	56	67
527	54	61	55	66
526	55	60	54	66
526	46	60	54	66
526	39	60	54	66
526	32	60	54	66
523	55	59	54	65
523	44	59	54	65
520	65	59	53	64
520	56	59	53	64
516	75	58	52	63

HLD	UCS (MPa)	Fits	CI lower	CI upper
515	27	57	51	63
514	34	57	51	63
514	24	57	51	63
511	66	56	50	62
504	41	54	49	60
502	51	54	48	60
501	34	54	48	59
500	37	53	48	59
500	22	53	48	59
495	26	52	46	58
493	68	52	46	57
490	61	51	45	57
487	18	50	44	56
486	32	50	44	56
485	64	50	44	55
482	65	49	43	55
480	55	48	43	54
480	23	48	43	54
476	18	47	42	53
474	15	47	41	53
473	60	47	41	52
472	72	46	41	52
471	48	46	40	52
470	12	46	40	52
466	46	45	39	51
464	57	44	39	50
464	38	44	39	50
464	48	44	39	50
458	62	43	38	49
456	31	43	37	48
455	35	42	37	48
448	33	41	35	46
447	43	41	35	46
439	42	39	33	44
428	66	37	31	42
420	17	35	30	40
412	31	33	28	39
409	16	33	28	38
401	7	31	26	36

HLD	UCS (MPa)	Fits	CI lower	CI upper
400	31	31	26	36
387	22	29	24	34
385	14	28	23	33
385	27	28	23	33
377	6	27	22	32
358	4	24	19	28
357	5	24	19	28
339	5	21	17	25
324	3	19	15	23
316	15	18	14	22
274	15	12	9	16
265	13	11	8	15
262	6	11	8	14
255	8	10	8	13